Inactivation of Lgl1 in glioblastoma

Alexander Gont

A thesis submitted to the

Faculty of Graduate and Postdoctoral Studies

in partial fulfilment of the requirements for the

PhD degree in Biochemistry

Biochemistry, Immunology and Microbiology

Faculty of Medicine

University of Ottawa

Abstract

Glioblastoma is the most aggressive and invasive adult brain cancer. In glioblastoma, the loss of the tumour suppressor *PTEN* is the most common genetic alteration resulting in aberrant activation of the PI3-kinase pathway. In *Drosophila*, the loss of tumour suppressor *Lgl* results in massive overgrowth of brain tissue that is highly invasive when transplanted into wildtype hosts. Subsequent study of Lgl protein function revealed that it is important for maintenance of cell polarity and neuroblast differentiation through asymmetric cell divisions. It is unclear if inactivation of Lgl occurs in human brain cancers and what role it plays in glioblastoma malignancy. Firstly, this study demonstrated that the loss of *PTEN* leads to inactivation of Lgl1 via phosphorylation by atypical protein kinase C iota (PKCι). In primary glioblastoma cultures, preventing Lgl1 inactivation by either PTEN expression, PKCι knockdown or expression of non-phosphorylatable Lgl (Lgl3SA) promoted differentiation. In a follow-up study, the effect of active Lgl1 in glioblastoma invasion was investigated. Lgl3SA expression inhibited invasion *in vitro* through decreased motility. In an orthotopic xenograft mouse model using primary glioblastoma cells, Lgl3SA expression promoted differentiation and decreased invasion. Therefore, *PTEN* loss, acting via PKCι and Lgl1, has a key role in maintaining glioblastoma in an undifferentiated, highly invasive state similar to what is observed following *Lgl* loss in *Drosophila*.

PREX1 was investigated as a potential link between *PTEN* loss and activation of PKCι. PREX1, a Rac activator, is synergistically activated by the PI3-kinase product PIP3 and G protein-coupled receptor (GPCR) βγ subunits. PREX1 expression was detected in primary glioblastoma cell cultures as well as the majority of patient tumour samples. Both PI3-kinase and GPCR βγ subunit activity is required for PREX1 to promote invasion in glioblastoma. In primary

glioblastoma cells, Rac1 preferentially associated with Par6a leading to activation of PKCι. Knockdown of PREX1 decreased activation of PKCι. Thus, PREX1 stimulates PKCι activity in glioblastoma likely by modulating the Rac1/Par6a/PKCι complex. The PI3-kinase pathway is activated by mutation in most glioblastomas and these results show this requires a context of GPCR signalling to promote invasion.

Acknowledgements

I would first like to express my gratitude to Dr. Ian Lorimer for his mentorship over the course of our many years together. Ian welcomed me into his lab as a fourth year honours student and introduced me to the world of scientific research. His enthusiasm for science sparks a genuine excitement from our whole team and his meticulous approach to problem solving has given me a solid foundation to conduct research. Ian, I am thankful for everything you have taught me and every time you have challenged me to improve. I know that your guidance will continue to support me in all aspects of my future career.

I would also like to thank my labmates, past and present. My research has greatly benefited from the way we discuss our results, help each other with experiments and solve problems as a team. From you I have learned that a chat and a good cup of coffee always helps when experiments fail and cells just don't grow.

Finally, I would like to thank my family for their love and support. I will forever appreciate your enthusiasm for my work even when sometimes it sounds like I'm speaking a different language. Megan, you have listened to all of my seminars many times over and helped edit just about every piece of work I turned in. Thank you for this and for always being there for me.

Table of contents

List of abbreviations

AGC	A, G, and C (PKA, PKG, PKC) family	nmMII	Non-muscle myosin II
Akt	Protein Kinase B	p53	Transformation-related protein 53
aPKC	Atypical protein kinase C	Par3	Partitioning defective mutant 3
BMP4	Bone morphogenetic protein 4	Par6	Partitioning defective mutant 6
CDC42	Cell division control protein 42	PDGF	Platelet-derived growth factor
DH	Diffuse B cell lymphoma (Dbl) homology	PDK1	3'-phosphoinositide-dependent kinase-1
Dlg	Discs large	PI3-kinase	Phosphoinositide 3-kinase
DRD2	Dopamine receptor D2	PIP2	Phosphatidylinositol 4,5-bisphosphate
ECM	Extracellular matrix	PIP3	Phosphatidylinositol (3,4,5)-trisphosphate
EGF	Epidermal growth factor	PREX	PtdIns(3,4,5)P3-dependent Rac exchanger
EGFR	Epidermal growth factor receptor	PriGO	Primary glioblastoma
FGF2	Basic fibroblast growth factor	PTEN	Phosphatase and Tensin homolog deleted on chromosome ten
GAP	GTPase activating protein	Rac	Ras-related C3 botulinum toxin substrate
G-CIMP	Glioma-CpG island methylator phenotype	Ras	Transforming oncogene found in rat sarcoma
GEF	Guanine nucleotide exchange factors	Rb	Retinoblastoma protein
GFAP	Cell division control protein 42	Rho	Ras homologous
GPCR	G-protein coupled receptor	Scrib	Scribble
GSCs	Glioma stem cells	SNAP	Soluble N-ethylmaleimide-sensitive factor attachment protein
GTICs	Glioblastoma tumor-initiating-cells	SNARE	Soluble N-ethylmaleimide-sensitive factor attachment protein receptor
HDAC	Histone deacetylase	SOX2	SRY (sex determining region Y)-box 2
Lgl	Lethal giant larvae	TCGA	The Cancer Genome Atlas
MDCK	Madin-Darby Canine Kidney	TUJ1	βIII-tubulin
MRI	Magnetic resonance imaging	VEGF	Vascular endothelial growth factor
mTOR	Mammalian target of rapamycin	Wnt	Wingless-related integration site

List of Figures

2. PTEN loss represses glioblastoma tumor initiating cell differentiation via inactivation of Lgl1

3. Inhibition of glioblastoma malignancy by Lgl1

4. PREX1 integrates G Protein-Coupled Receptor and Phosphoinositide 3-kinase signaling to promote glioblastoma invasion

5. Discussion

1. Introduction

1.1. Glioblastoma

1.1.1. Glioblastoma classification, prognosis and treatment

Astrocytomas are the most common brain tumour accounting for approximately 70% of malignant brain tumours (1). Astrocytomas are categorized in a four-grade scale established by the World Health Organization based on their morphological and pathological features (2, 3). Grade IV astrocytoma, also known as glioblastoma, is the most aggressive subtype and is distinguished by four histopathological criteria: 1) atypical cellular and nuclear morphology, 2) high cellularity and mitotic figures, 3) pseudopalisading necrosis, and 4) extensive neovascularization (4).

Multiple cells-of-origin have been speculated for glioblastoma. The subventricular zone and the subgranular zone of the hippocampus are the sites of adult neurogenesis in the brain and have been shown to be a site of origin for glioblastomas in genetic mouse models (5-8). Recent data also demonstrates that platelet-derived growth factor (PDGF) subunit-B induced gliomas can be established from committed glial progenitor cells (Oligodendrocyte progenitor cells) (9). Finally, with specific mutations, astrocytes and neurons can dedifferentiate to form gliomas in mice (10, 11). Thus, nearly all cells of neural origin have the potential to be the cell of origin for glioblastoma.

Glioblastoma is detected by neuroimaging mainly using magnetic resonance imaging (MRI) and confirmed by histopathological analysis (4, 12). The standard of care for glioblastoma is surgery combined with radiotherapy. Combining radiotherapy with the DNA alkylating temozolomide has been one of the more effective advances in treatment leading to prolonged survival, albeit, by months (13, 14). Bevacizumab, an inhibiting antibody to vascular

endothelial growth factor (VEGF), has demonstrated success in promoting progression-free survival measured by radiological imaging but failed to promote overall survival (15). Recently, Optune, a medical device that utilizes electromagnetic stimulation to inhibit tumour cell division has completed clinical trials in glioblastoma showing a small increase in overall survival (16). The mechanisms of action of this device are not well understood. However, none of these newer treatments are curative and there is a clear need for new therapeutic approaches to glioblastoma.

1.1.2. Glioblastoma invasion

A hallmark of glioblastoma is its high invasive potential. Early radical neurosurgery procedures involving removal of the entire hemisphere afflicted with glioblastoma resulted in eventual relapses in the contralateral hemisphere suggesting that cancer cells had already invaded into the opposite hemisphere (17). Even with modern neurosurgery, the diffuse borders of glioblastoma and high grade astrocytoma prevent complete resection. Recurrence mainly occurs in the 1-2cm area around the initial resection site (18). The ability to effectively excise brain cancers is a major prognostic factor; poorly invasive brain cancers including pilocytic astrocytomas, subependymal giant cell astrocytomas, gangliogliomas and pleomorphic xanthoastrocytomas can be readily excised which corresponds to increased survival with complete remission in many patients (19, 20).

Within the brain, glioblastoma demonstrates specific patterns of invasion that are distinct from systemic tumours that have metastasized to the brain. Glioblastoma cells have the potential to invade throughout the brain as single cells preferentially traveling along anatomically defined brain regions known as Scherer's secondary structures: white matter tracts, blood vessels and subpial glial space (21, 22). Glioblastoma tumours rarely metastasize out of the central nervous

system (23). At the cellular level, three key processes enable invasion: 1) adhesion to the brain parenchyma, 2) cellular motility via actin/myosin contractile motions, and 3) degradation of extracellular matrix components (24).

Interestingly, migration along white matter tracts and blood vessels is evident in adult neural precursor cells suggesting shared mechanisms for intracranial migration. During adult rodent neurogenesis, and to some extent in primates, precursor cells migrate along the rostral migratory stream to the olfactory bulb (22, 25). Bundles of vessels serve as apparent scaffolds for migration (22, 26). Glial progenitor cells can also migrate along white matter tracts across the midline of the brain (27). Finally, intracranial transplant experiments demonstrate that human embryonic stem cell derived neural precursor cells both recapitulate rostral migratory stream migration patterns and have the capacity to travel large distances along white matter tracts (28).

The structure of the brain presents two distinct compositions of extracellular spaces that glioblastoma cells navigate and invade through. The brain parenchyma is mainly composed of hyaluronan, proteoglycans, tenascin-C and thrombospondin. This is similar to the composition of cartilage, rather than the "classical" extracellular matrix (ECM) which is made up of protein such as laminin, collagen Type IV, fibronectin, and vitronectin. This "classical" ECM is found lining blood vessel walls and in the subpial space in the brain (22, 24).

1.1.3 Primary glioblastoma cultures

This study makes use of glioblastoma cell cultures isolated from patient samples and grown in serum-free neural stem cell culture media supplemented with growth factors (EGF and FGF2) as monolayers on laminin coated cell culture vessels at 5% O_2. Given that they are acquired directly from patient tumour samples they are referred to as primary glioblastoma cells

or PriGO cells in this study. Cells isolated and maintained under similar conditions have also been referred to as glioblastoma tumor-initiating-cells (GTICs) and glioma stem cells (GSCs). The conditions used preserve both the genetic profile in culture and invasive phenotype of the original tumour as intracranial xenografts in immunocompromised mice (29-32). Another characteristic of this population of cells is their differentiation potential which influences the heterogeneity of glioblastoma. Primary glioblastoma cell cultures express markers of neural stem cells including nestin, SOX2 and vimentin and have the capacity to differentiate along multiple lineages (29-31). While stem cell marker prominin-1/CD133 had initially been thought of as the essential marker of GSCs, subsequent studies have disputed this claim demonstrating that $CD133^-$ cells have tumour-forming capacity as well as the capability to form $CD133^+$ daughter cells (33). Serum-induced differentiation is non-specific leading to expression of multiple-lineage markers with aberrant co-expression of distinct lineage markers (29). Very few studies have identified specific lineage-promoting signalling pathways. Treatment with BMP4 demonstrates $GFAP^+$ astrocytic-lineage differentiation and treatment with Wnt3a, a notch inhibiting ligand, induces βIII-tubulin$^+$ neuronal-lineage differentiation (34, 35). Culture of primary glioblastoma cells in the presence of serum also results in an eventual loss of invasive potential both *in vitro* and *in vivo* with cells forming well circumscribed tumours (29, 36). Additionally, *in vivo*, nestin$^+$/$GFAP^-$ cells were observed to be enriched in the invasive periphery of the tumour mass while the $GFAP^+$ cells contribute more to the tumour mass (31). These findings suggest that the differentiation status of glioblastoma may correlate to its invasive potential.

1.1.4. Genetics of glioblastoma

The genetics of glioblastoma have been studied intensively. Traditionally, glioblastoma has been subdivided into two categories based on clinical behaviour: 1) primary (*de novo*) glioblastoma tumours without any previous history of lower grade astrocytoma that have frequent EGFR amplification, INK4A loss and PTEN loss, and 2) secondary glioblastoma which arises from initial lower grade astrocytoma. These have frequent PDGF/ FGF amplification, p53 mutation, Rb loss, and PTEN loss (1, 4, 8, 37). Based on RNA expression analysis of glioblastoma clinical samples led by The Cancer Genome Atlas (TCGA), glioblastoma has been reclassified by molecular subtype (38, 39). Initially, four subtypes were identified: classical, mesenchymal, neural and proneural (38). Further analysis revealed a fifth subtype, glioma-CpG island methylator phenotype (G-CIMP), which initially grouped with the proneural subtype (40). Clinical relevance of the subtypes has been suggested with the classical and mesenchymal subtypes benefitting more from intensive/ high cycle chemotherapy (38). In addition, patients with G-CIMP tumours experience significantly higher survival times (40). There is also substantial heterogeneity of gene expression within patient tumours. Single cell analysis revealed that within an individual tumour varying proportions of multiple molecular subtypes can be detected (41).

The homo or hemizygous loss of tumour suppressor *PTEN* in the 10q23 chromosome region occurs at a very high frequency across all subtypes (100% in classical, 87% in mesenchymal, 96% in neural and, 69% in proneural) (38). A recent bioinformatics study proposing that loss of *PTEN* via genomic loss in the 10q23 locus is an originating mutation across all molecular subtypes of glioblastoma (42). To a lesser extent, PTEN function is also affected by: 1) mutations, which are present in approximately 23% of TCGA samples analysed

(38), 2) transcriptional regulation by miR-26 (43) and miR-21 (44), and 3) protein degradation following C-terminal tail phosphorylation (45). Taken together, the loss of PTEN appears to be an essential step in gliomagenesis.

1.2. PTEN

1.2.1. Genetic and molecular roles of PTEN

Phosphatase and Tensin homolog deleted on chromosome Ten (PTEN) gene (also known as MMAC1) was initially mapped to a region on 10q23 which commonly undergoes loss of heterozygosity in multiple human tumours, especially so in glioblastoma (46, 47). *PTEN* germline mutations are found in three human autosomal dominant disorders - Cowden disease, Lhermitte-Duclos disease, and Bannayan-Zonana syndrome. Patients with these disorders commonly have multiple benign tumours (hamartomas) and increased susceptibility to malignant cancers such as breast, thyroid, and endometrial carcinoma (48, 49). Study of *PTEN* deletion in mouse models established it as a tumour suppressor (48, 50). Complete loss of *PTEN* is embryonic lethal with $PTEN^{-/-}$ embryonic stem cells demonstrating significant defects in germ layer differentiation (48). Chimaeras from $PTEN^{+/-}$ embryonic stem cells and mice have the histopathological signs of Cowden disease and the related disorders. In addition, $PTEN^{+/-}$ mice develop gastrointestinal and prostate hyperplasia, and have a very high tendency to develop spontaneous malignant tumours in multiple tissues (48).

PTEN was initially described as either a protein or lipid phosphatase (51, 52). Subsequent studies reinforced its role predominantly as a lipid phosphatase converting phosphatidylinositol 3,4,5-trisphosphate (PIP3) to form phosphatidylinositol 4,5-bisphosphate (PIP2) (53, 54). The lipid phosphatase activity of PTEN opposes the action of phosphoinositide

3-kinase (PI3-kinase) which, through PIP3 accumulation, activates 3'-phosphoinositide-dependent kinase-1 (PDK1). PDK1 supports the activation of many members of the AGC subfamily kinases through phosphorylation in the T-loop motif (55, 56). PIP3 accumulation also results in activation of Ras-related C3 botulinum toxin substrate (Rac) and cell division control protein 42 (CDC42), which promotes cell migration (57, 58).

1.2.2. PTEN in brain development

To overcome the embryonic lethality of *PTEN* deletion and explore the function of PTEN loss in brain development a conditional knockout mouse was developed by flanking exon 5 in the *PTEN* gene with *loxp* sequences ($PTEN_{loxp}$) and crossing with cre-recombinase driven by the *nestin* promoter (59). Neural specific loss of PTEN resulted in macrocephaly marked by increased progenitor proliferation and decreased cell death without disturbing multi-lineage differentiation (59). Single allele loss of *PTEN* was sufficient to increase the migratory capacity of neural progenitor cells in addition to inhibiting apoptosis and modestly increasing their proliferation (60). Subsequent analysis revealed that *PTEN* deletion promotes neural stem cell self-renewal; maintaining long-term proliferation with multi-lineage potential and restricting G_0 cell cycle exit and quiescence (61). In the adult mouse *PTEN* deletion under the *GFAP* promoter leads to increased neurogenesis in the subependymal zone, increased migration via the rostral migratory stream and as a result an increase in the olfactory blub mass and function (62). In related studies, *PTEN* deletion under the *GFAP* promoter promotes brain hypertrophy by increased post-natal astrocytic proliferation demonstrating similar pathology to Lhermitte-Duclos disease (63, 64).

1.2.3. PTEN loss in cancers

Loss of *PTEN* is sufficient to induce many cancer types including prostate, breast, endometrial, colon, and leukemia (48, 65, 66). However, within the brain *PTEN* loss mainly results in hyperplasia (59, 62, 64). Combined genetic mouse models demonstrate that *PTEN* loss cooperates with *P53* loss, PDGF-A expression or mutant constitutively active EGFR expression to form high-grade glioblastoma tumours (42, 67, 68).

Re-expression of PTEN in glioblastoma cells to supra-physiological levels using retroviral vectors resulted in a significant decrease in cell growth by inducing cell cycle arrest *in vitr*o and in subcutaneous xenograft mouse experiments (69, 70). In addition, expression of PTEN decreased the *in vitro* invasiveness of glioblastoma cell lines through focal adhesion kinase dephosphorylation and decreased matrix-metalloproteinase -9 expression (71, 72). In a more recent study, the effect of PTEN expression in glioblastoma tumour initiating cells was investigated (73). Expression of PTEN in glioblastoma cultures grown under serum-free conditions decreased neurosphere forming capability, a putative marker of self-renewal capacity (73).

In cancer, the best described consequence of PTEN loss is through promoting the activity of the PI3-kinase pathway resulting in increased concentration of the secondary messenger PIP3 and PDK1 activation. PDK1 activates many members of the AGC subfamily kinases of which Akt has been the most studied (54, 55). Activation of Akt promotes tumour growth and survival by modulating a magnitude of signalling molecules that regulate protein translation, progression through cell cycle, and resistance to apoptosis (74-78). In glioblastoma, targeting Akt and/or its substrate mTOR by small molecule inhibitors prevented tumour progression and promoted cell death (79-82). PDK1 also interacts with atypical PKC isoforms by direct binding. This leads to

phosphorylation of a threonine residue in its activation loop, an essential step in activation (83, 84). Atypical PKCs belong to the serine/threonine protein kinase C family of the ACG group kinases (85). Unlike the conventional (PKCα, PKCβ and PKCγ) and novel (PKCδ, PKCε, PKCθ and PKCη) PKCs, atypical PKCs (PKCι (PKCλ in mice) and PKCζ) are activated through protein interaction and not diacylglycerol nor Ca^{2+} (85-88). Of the two atypical PKC isotypes, PKCι/λ is most ubiquitously expressed. In the developing brain, PKCι/λ is the sole isotype expressed in the neocortex and midbrain (89). PKCι is overexpressed in many cancers and considered an oncogene (90). In glioblastoma cell lines, PKCι promotes cell invasion, proliferation, resistance to senescence and resistance to chemotherapeutics (91-95).

1.3. Lgl1

1.3.1. Function of Lgl in neuroblasts and neural stem cells

Lethal giant larvae (Lgl) was first discovered through *Drosophila* mutagenesis studies in which deletion of *Lgl* led to neoplastic overgrowth of larval ectodermal structures - neuroblasts and imaginal discs – and larvae death in the third instar stage (96). The resulting neoplastic growths are highly invasive when transplanted into secondary hosts (97). In mammals there are two forms of Lgl (Lgl1 and Lgl2) that are highly conserved in structure, sharing 71% sequence similarity (98). Lgl1 and Lgl2 appear to have distinct tissue distribution in mice with Lgl1 predominantly expressed in the brain and testes and Lgl2 in the kidney, liver, stomach, skin, lung and intestine (98). *Lgl1* knockout in mice is not embryonic lethal, however pups die shortly after birth due to severe hydrocephalus. *Lgl1*$^{-/-}$ mice have massive overgrowths of brain tissue producing a domed head phenotype. Neuroblastic rosettes reminiscent of pediatric neuroectodermal tumours are present (98).

Lgl function has been studied in detail in *Drosophila*. In asymmetrically dividing neuroblasts Lgl localizes to the basal cortex of the cell and promotes proper localization of cell fate determinants Miranda and Numb as well as the symmetry of neuroblast divisions (99, 100). Increased Notch pathway signalling by depletion of its negative regulator Numb promotes *Drosophila* neuroepithelial cell expansion and inhibits differentiation (101). Cell fate determination following neuroblast divisions is largely governed by the symmetry of division as regulated by alterations in cell polarity. Asymmetric cell division results in one neuroblast daughter cell and one ganglion mother cell – an intermediate cell that eventually generates post-mitotic neurons (102). Loss of *Lgl* promotes symmetric self-renewing divisions rather than asymmetric differentiating divisions resulting in an increased number of proliferating neuroblasts (103). Similarly, in the *Lgl1* knockout mouse the cell overgrowths are less differentiated, express neural progenitor marker nestin rather than neuronal marker βIII-tubulin, and have mislocalization of Numb and Notch signalling pathway activation (98).

In both *Drosophila* and mammalian cell models, aPKC phosphorylates conserved serine residues in the middle hinge region of Lgl inducing a conformational change and intramolecular association resulting in an inactive form (104, 105). Mutagenesis of the conserved serine sites to alanine prevents Lgl inactivation (104). Similarly to inactivation of Lgl by genetic loss, expression of active (membrane associated) aPKC into neuroblasts promotes self-renewing symmetric cell divisions by inactivating Lgl and this phenotype can be rescued by expression of non-phosphorylatable Lgl (Lgl3SA) (103, 106). aPKC and Lgl function in the context of the Par6/aPKC/Par3 complex where association of Par6, aPKC and GTP-bound CDC42/Rac1 form a complex to activate aPKC and phosphorylate Lgl. Active protein complex formation eventually

results in Par3 (Baz/Bazooka in *Drosophila*) binding in place of Lgl and a change of aPKC substrate specificity to Numb. Numb is phosphorylated and inhibited as a result (107-109).

1.3.2 Function of Lgl in apical-basolateral epithelial cell polarity

A highly studied aspect of Lgl is its function within polarity complexes to regulate establishment and proper function of apical-basolateral polarity in epithelial cells. Madin-Darby Canine Kidney (MDCK) cells undergo cell polarization and epithelial layer establishment induced by calcium addition to the culture medium (105). In this model, interactions of Lgl with aPKC and Par6 regulate formation of cell-to-cell contacts and apical-basolateral domain establishment. Immediately after calcium addition, Par6 and Lgl co-localize at sites of cell-to-cell contacts with phosphorylation of Lgl increasing throughout the polarization process. After cells are fully polarized, however, Par6 co-localizes with aPKC at the apical cortex of the cell with Lgl at the basolateral cortex. Overexpression of Lgl disrupts junction formation and active aPKC expression results in diffuse Lgl localization throughout the cell, providing evidence of both reciprocal inhibition of aPKC and Lgl and a stoichiometric relationship of polarity components for proper epithelial polarization (105). A follow-up study confirms these findings by demonstrating that depletion of Lgl levels disrupts the orientation of polarization (110). *Drosophila* epithelial cell polarization following growth demonstrates a temporal relationship between Par6/aPKC and Lgl. During polarization Par6 is recruited to the apical cortex in association with active CDC42 at which point the association with aPKC and Lgl results in Lgl phosphorylation and exclusion to the basolateral cortex (111). In the mammary epithelium, depletion of Lgl1 or Lgl2 disrupts normal three-dimensional acinar architecture and promotes cellular overgrowths without distinctly oriented apical-basolateral polarity (112).

In polarized epithelial MDCK cells Lgl1 directly interacts with the basolateral membrane exocytic soluble N-ethylmaleimide-sensitive factor attachment protein receptor (SNARE) components syntaxin 4 and SNAP23 (113). Both syntaxin 4 and SNAP23 are found at the target membrane of GLUT4 vesicles poised for exocytosis in the insulin secretion pathway (114). A closely related SNARE protein, SNAP25, is expressed in neurons and is essential for exocytosis of neurotransmitters (115). Syntaxin 4 has been shown to regulate the transport of membrane-type 1 matrix metalloproteinase to the membrane of gastric epithelial cells and cancer cells (116, 117). This suggests a link between polarized exocytic protein complexes and the invasive potential of cells.

1.3.3 Function of Lgl in cell motility

Multiple studies demonstrate that Lgl interacts with non-muscle myosin II, an actin binding protein with contractile properties (104, 118-120). In migrating cells, Lgl localizes to the leading edge together with aPKC and Par6 establishing front-rear polarity (93, 121). Lgl binds to the region on non-muscle myosin IIa (nmMIIA) important for filament assembly and promotes the monomeric unassembled state thus reducing contractibility (120). Depletion of Lgl in fibroblasts results in higher turnover activity at the leading edge of cells, a more elongated migrating cell morphology, more single cell migration and an overall increase in migration velocity (120). aPKCζ competes with nmMIIA to bind Lgl1 at the same domain with Lgl1 inactivation by phosphorylation demonstrating a similar phenotype to Lgl1 knockdown in the context of motility (121). These interactions are important to establish a leading edge rich in actin polymerization and focal adhesion assembly with polymerized nmMIIA providing contractile forces (120, 121).

1.3.4 Function of Lgl, Scribble and Discs large in polarity

In addition to the direct interactions with polarity proteins aPKC and Par6, Lgl functions in a common genetic pathway with Scribble (Scrib) and Discs large (Dlg) necessary for maintenance of epithelial cell polarity (122). In *Drosophila*, all three members are mutually dependent for proper cellular localization and *Scrib* and *Dlg* deletions phenocopy the neoplastic overgrowths observed upon deletion of *Lgl* (122). Loss of Scrib expression disrupts the three-dimensional organization of mammary cells in culture by inhibiting the apoptosis required for lumen formation (123). Transplants of Scrib-depleted cells into mouse mammary glands demonstrates abnormal morphogenesis marked by multilayered growths rather than normal glandular structures and in cooperation with c-myc forms mammary tumours (123). Similarly, loss of Scrib disrupts proper organization of epithelial cysts in three-dimensional cultures and upon inhibition in mice causes atypical and unorganized lung development linked to disruption of proper tight junctions (124).

Studies investigating interactions between Lgl/Scrib/Dlg suggest that physical interactions between these pathway members are possible. Scrib and Dlg co-localize in *Drosophila* and mammalian cells and interact via an intermediate protein (122, 125, 126). Lgl and Scrib can be shown to interact by co-immunoprecipitation when overexpressed in MDCK cells with Lgl binding the leucine-rich-repeat domain of Scrib (127). Recently, Lgl2 has been shown to interact with Dlg following phosphorylation on its hinge region serine residues (aPKC phosphorylation sites) (128).

In *Drosophila*, Lgl, Scrib and Dlg are neoplastic tumour suppressors because their loss results in tissue overgrowth with features that are present in high grade human cancers such as loss of tissue architecture and invasion (129). In normal colon mucosa and polyps Scrib and Dlg

are predominantly basolaterally localized (130). The progression to low-grade adenocarcinoma is marked by mislocalization of Scrib and Dlg to the cytoplasm and in high-grade adenocarcinoma the expression of Scrib and Dlg is lost in most cases (130). Similar patterns have been shown for Dlg in cervical cancer (131).

1.3.4. Dysregulation of Lgl in cancer

Compared to normal tissue, Lgl1 mRNA expression is lost or reduced in breast, prostate, ovarian and lung cancers as well as melanoma (132). Lgl2 is either lost or mislocalized in colon adenomas and adenocarcinomas by immunohistological analysis (133). Changes to Lgl expression have been linked to blood cancer malignancy and progression (134, 135). In an *Lgl* conditional knockout mouse model driven by a hematopoietic lineage promoter, loss of *Lgl1* increases the proliferation of hematopoietic stem cells and their competitive advantage in transplant studies (134). Both Lgl1 and Lgl2 have been implicated in acute myeloid leukemia malignancy: *Lgl1* loss correlates with a poor clinical prognosis and *Lgl2* is a key gene lost in the progression to leukemia (134, 135). Lgl1 expression is lost in melanoma cell lines and primary tumours and re-expression of Lgl1 decreases invasiveness *in vitro* (136). The mechanism for loss of Lgl expression is not fully understood. In breast cancer cell lines *Lgl2* expression is transcriptionally repressed by transcription factors such as Snail, which binds to E-box clusters in the core promoter region of *Lgl*, during epithelial-to-mesenchymal transition. This mechanism of transcriptional repression does not affect *Lgl1* (137).

1.4. PREX

1.4.1 Rac function

The Rho GTPases are members of the Ras superfamily of proteins acting as molecular switches controlling cellular signal transduction. GTPases cycle between GTP-bound active forms to GDP-bound inactive forms after hydrolysis. This binary switch is regulated by interacting proteins: GTPase activating proteins (GAPs) accelerate the rate of hydrolysis and limit the duration of activity, while guanine nucleotide exchange factors (GEFs) facilitate the exchange of GDP to GTP thereby promoting the activity of GTPases (138). Rac, Rho and CDC42 comprise the Rho GTPase family based on structural and functional similarity (138). Rho GTPases are best known for their function in potentiating different aspects actin cytoskeleton control: CDC42 promotes filopodia (finger-like extensions for sensing the extracellular enviroment) formation, Rac promotes lamellipodia (fan-like protrusions for cellular motility) formation, and Rho promotes stress fiber (actin bundles linked to cellular focal adhesions) formation (139). The Rac subgroup contains three isoforms: Rac1 which is ubiquitously expressed, Rac2 which is mainly expressed in the hematopoietic lineage, and Rac3 which is mainly expressed in the neural lineage (140, 141). Expression of activated forms of Rac1 and CDC42 that contain mutations disabling intrinsic hydrolysis of GTP, increase the motility of epithelial cells (58, 142). Increased Rac expression and activation has been observed in multiple forms of cancers (143). Rac proteins, particularly Rac1, promote an invasive phenotype in glioblastoma cell lines (144, 145) and in primary glioblastoma cell cultures (146).

In glioblastoma cell lines, Rac is stimulated by exogenous growth factor addition as well as PI3-kinase expression and PTEN deletion to promote migration (57, 58, 147). Rac activating GEFs such as Trio, Ect2, Vav3 and Dock180 have been described in glioblastoma cell lines but

few have been associated with PI3-kinase pathway activation (148, 149). Vav2, a Rac specific GEF has been shown to be activated in response to EGF stimulation by EGFR-mediated phosphorylation (150). Another commonly studied Rac GEF, Tiam, is activated through PI3-kinase stimulated tyrosine kinase Lck (151). These examples of activation by PI3-kinase pathway activity are either small in magnitude or through indirect mechanisms.

1.4.2 PREX function in cells

PtdIns(3,4,5)P3-dependent Rac exchanger 1 (PREX1) was first discovered in a study aiming to uncover a Rac1 activating guanine nucleotide exchange factor responsive to PIP3 (152). Subsequently PREX1 was found to be activated by both PIP3 and G-protein coupled receptor (GPCR) βγ subunit *in vitro* and in cells in a highly synergistic manner, such that activation by either component alone increases activity less than one-fold, whereas activation by both constituents increases activity nearly ten-fold (152). Analysis of PREX1 expression in human tissues revealed that it is largely expressed in the brain and blood leukocytes (152). The function of PREX1 was further investigated in mouse models. *PREX1* knockout mice are healthy and fertile with a mild elevation of peripheral blood leukocytes presenting as neutrophilia (153). When stimulated, *PREX1*$^{-/-}$ neutrophils demonstrate deficiency in NADPH-mediated reactive oxygen species (ROS) production and chemotaxis and when *PREX1*$^{-/-}$ mice are challenged in an infection-like inflammatory model, neutrophil recruitment to sites of inflammation is impaired (153, 154).

In mouse brain, PREX1 expression peaks in the late embryonic stages and remains constant into adulthood (155). Throughout development, PREX1 expression is detected in the hippocampal formation, olfactory bulbs, rostral migratory stream and cerebellum. Additionally,

PREX1 is expressed throughout the maturation of the cerebral cortex (155). Full-length PREX1 expression in cells promotes nerve growth factor (NGF) stimulated membrane ruffling and chemotaxis while a mutant without the DH domain functions as dominant negative and inhibits these functions (155). The PREX1 mutant lacking the Dbl-homology domain involved with GPCR βγ subunit binding (ΔDH-PREX1) acts as a dominant negative. Expression of ΔDH-PREX1 the developing mouse brain results in stalled neuron migration without affecting differentiation (155).

PREX2a and truncated splice variant PREX2b were later discovered by sequence similarity to PREX1. They are responsive to PI3-kinase stimulation resulting in Rac activation (156)(152). In mice, PREX2a is mainly expressed in the skeletal muscle, small intestine, and placenta while PREX2b is expressed in the heart (156). PREX2 has a similar distribution in humans, although expression in the brain has also been reported (157). Interestingly, the main phenotype of *PREX2* knockout mice is a mild loss of coordination due to improper development of Purkinje neurons in the cerebellum, which is worsened by double knockout of *PREX1* and *PREX2* (158).

1.4.3 PREX in cancer

Both PREX1 and PREX2 have been studied in the context of cancer and demonstrate distinct roles. PREX1 has been mainly studied in melanoma, prostate and breast cancers. In prostate cancer, PREX1 expression is elevated in human prostate cancer cell lines and metastatic clinical samples (159). PREX1 functions through Rac to promote the *in vitro* motility of prostate cancer cells and expression of GEF-dead dominant negative PREX1 decreases *in vitro* invasion in addition to lowering the incidence of lymph node metastasis in a prostate cancer xenograft

mouse model (159). Similarly, knockout of *PREX1* inhibits tumour invasion *in vivo* by restricting the incidence of metastasis in a genetic mouse model of melanoma (160). Finally, in breast cancer, PREX1 is overexpressed in cancer cell lines and tumours, with some specificity to the luminal subtype, and high expression of PREX1 correlates with decreased survival in breast cancer patients (161, 162). PREX1 promotes breast cancer *in vitro* migration via Rac and *in vivo* metastases and tumour growth in mouse models (161). Study of PREX1 in breast and prostate cancers also uncovered that *PREX1* expression is epigenetically modified by promoter methylation and histone acetylation. Treatment of prostate cancer cells with histone deacetylase inhibitor trichostatin A and treatment of breast cancer cells with a combination of trichostatin A and methyltransferase inhibitor 5'-aza-2'-deoxycytidine increased PREX1 levels (163, 164). Despite its apparent role in brain development, PREX1 has not been investigated in the context of brain malignancies.

PREX2 was linked to brain cancer in a study demonstrating that PREX2a binds the C-terminal of PTEN in a glioblastoma cell line (165). PREX2a inhibited the lipid phosphatase enzymatic activity of PTEN and co-expression of PTEN and PREX2a nullified the ability of PTEN to inhibit phosphorylation of Akt in glioblastoma and breast cancer cell lines (165). In breast cancer, PREX2a expression correlates with activating mutations of PI3-kinase (*PIK3CA* gene) (165). Follow-up study of these interactions suggests that PTEN has reciprocal inhibitory function on PREX2a activation of Rac1 (166). PREX2a is frequently mutated in cancers, particularly in those with high PTEN expression, where these mutations prevent binding and inhibition by PTEN (166). Thus, PREX2a appears to be relevant in cancers that do not experience PI3-kinase pathway activation by PTEN loss but rather through activating mutations on the PI-3kinase subunits.

1.5 Study rationale

The loss of Lgl in *Drosophila* leads to invasive neoplastic overgrowths within the larval brain tissue reminiscent of human brain tumours/ glioblastoma. Lgl loss in *Drosophila* neural stem cells (neuroblasts) promotes symmetric cell divisions leading to increased self-renewal/proliferation without differentiation. For this study we isolated glioblastoma cells from patient tumours (primary glioblastoma cell cultures). Primary glioblastoma cell cultures are the most clinically relevant model of glioblastoma as they recapitulate the genetic and the histopathological characteristics of the original patient's tumour. Additionally, primary glioblastoma cells exist in relatively undifferentiated state and have the potential for multi-lineage differentiation thereby linking their characteristics to the phenotype of *Drosophila* brain neoplasms formed by loss of Lgl1.

In glioblastoma, the loss of PTEN aberrantly activates the PI3-kinase pathway leading to activation of multiple downstream kinases including atypical protein kinase Cs. In *Drosophila* Lgl is phosphorylated and inactivated by aPKC thus demonstrating a potential link between PTEN loss and Lgl inactivation in glioblastoma. The mechanisms of aPKC activation via protein-protein interactions have been studied in the context of epithelial cell polarity where active Rac1 and CDC42 promote the formation of the Par6/aPKC/Par3 complex. PREX1 was discovered as a Rac1 guanine nucleotide exchange factor specifically activated by PIP3 binding and thus may link PI3-kinase pathway activation to aPKC activation in glioblastoma.

1.6 Hypothesis

In glioblastoma Lgl1 is inactivated through phosphorylation by PKCι as a consequence of PTEN loss. Inactivation of Lgl1 promotes glioblastoma malignancy through increased invasiveness and decreased differentiation recapitulating the characteristics of *Drosophila* brain tumour models. PREX1 links PTEN loss to activation of PKCι in glioblastoma.

1.7 Objectives

1. Investigate the link between PTEN loss and Lgl1
2. Investigate the role of Lgl1 in glioblastoma differentiation and invasive behavior
3. Investigate the role of PREX1 in promoting glioblastoma invasiveness
4. Investigate the link between PREX1 and PKCι activity via Rac1 facilitated interactions with Par6

2. PTEN loss represses glioblastoma tumor initiating cell differentiation via inactivation of Lgl1

Alexander Gont[1,2], Jennifer E L Hanson[1], Sylvie J Lavictoire[1], Doris A E Parolin[1], Manijeh Daneshmand[1,4], Ian J Restall[1,2], Mathieu Soucie[1,3], Garth Nicholas[1,5], John Woulfe[1,2,4], Amin Kassam[5], Vasco F Da Silva[5] and Ian AJ Lorimer[1,2,6]

[1]Centre for Cancer Therapeutics, Ottawa Hospital Research Institute, 501 Smyth Road, Ottawa, K1H 8L6, Canada
[2]Department of Biochemistry, Microbiology and Immunology, University of Ottawa, Ottawa, Ontario, Canada
[3]Faculty of Science, University of Ottawa, Ottawa, Ontario, Canada
[4]Department of Pathology and Laboratory Medicine, University of Ottawa, Ottawa, Ontario, Canada
[5]Department of Surgery, University of Ottawa, Ottawa, Ontario, Canada
[6]Department of Medicine, University of Ottawa, Ottawa, Ontario, Canada

Address correspondence to: Ian A. J. Lorimer, Ottawa Hospital Regional Cancer Centre, Centre for Cancer Therapeutics, 3rd floor, 501 Smyth Road, Ottawa, Ontario, Canada K1H 8L6. Phone (613) 737-7700 ext. 70332; Fax (613) 247-3524; E-mail ilorimer@ohri.ca

Keywords: glioblastoma, glioma, PTEN, PKCι, Lgl, tumor initiating cell

Contribution of authors: The content of this manuscript was written by A. Gont with the help of Dr. I.A.J. Lorimer. All of the experiments presented in this manuscript are the work of A. Gont except those specifically stated. Figure 2A was produced by M. Soucie. D.A.E. Parolin and J.E.L. Hanson performed CISH in Figures 4B, and 10A. J.E.L. Hanson provided the phase contrast images for Figures 4C, 9A and 10A. I. J. Restall quantified the membrane localization data in Figures 2C and 3B. PriGO cells cultures were established by J. E. L. Hanson with samples provided by Drs. A. Kassam and V. F. Da Silva. Drs. A. Kassam, V. F. Da Silva, G. Nicholas, and J. Woulfe provided consultation for the PriGO cell project. Drs. M. Daneshmand and J. Woulfe provided consultation for immunohistological and pathological experiments. S. J. Lavictoire provided consultation for plasmid construct development and lentiviral transductions.

Published: Oncotarget. 2013 Aug;4(8):1266-79.

Abstract

Glioblastoma multiforme is an aggressive and incurable type of brain tumor. A subset of undifferentiated glioblastoma cells, known as glioblastoma tumor initiating cells (GTICs), has an essential role in the malignancy of this disease and also appears to mediate resistance to radiation therapy and chemotherapy. GTICs retain the ability to differentiate into cells with reduced malignant potential, but the signaling pathways controlling differentiation are not fully understood at this time. *PTEN* loss is very common in glioblastoma multiforme and leads to aberrant activation of the phosphoinositide 3-kinase pathway. Increased signalling through this pathway leads to activation of multiple protein kinases, including atypical protein kinase C. In *Drosophila*, active atypical protein kinase C has been shown to promote the self-renewal of neuroblasts, inhibiting their differentiation along a neuronal lineage. This effect is mediated by atypical protein kinase c-mediated phosphorylation and inactivation of Lgl, a protein that was first characterized as a tumour suppressor in *Drosophila*. The effects of the atypical protein kinase C/Lgl pathway on the differentiation status of GTICs, and its potential link to *PTEN* loss, have not been assessed previously. Here we show that PTEN loss leads to the phosphorylation and inactivation of Lgl by atypical protein kinase C in glioblastoma cells. Re-expression of PTEN in GTICs promoted their differentiation along a neuronal lineage. This effect was also seen when atypical protein kinase C was knocked down using RNA interference, and when a non-phosphorylatable, constitutively active form of Lgl was expressed in GTICs. Thus *PTEN* loss, acting via atypical protein kinase C activation and Lgl inactivation, helps to maintain GTICs in an undifferentiated state.

Introduction

Glioblastoma multiforme is an aggressive type of adult brain tumor. Surgery is not curative, as this disease invariably exhibits extensive intracerebral dissemination at the time of diagnosis. Patients are also commonly treated with radiation and the alkylating agent temozolomide; this prolongs survival but is also not curative (167). A characteristic histological feature of glioblastoma is that glioblastoma cells show considerable phenotypic heterogeneity. One factor contributing to this heterogeneity is that glioblastoma cells exist in different differentiation states (168). A subset of glioblastoma cells are relatively undifferentiated; these are variously referred to as glioblastoma stem cells, glioblastoma stem-like cells or glioblastoma tumor-initiating cells (169, 170). The latter term is based on one of their defining properties, which is the ability to regenerate a tumor resembling the patient's original tumor when implanted in the brain of an immunocompromised mouse (169). These cells share some properties with normal adult neural stem cells, including the expression of stem cell-associated genes and the ability to differentiate along multiple lineages (31). Current data suggests that these undifferentiated cells are resistant to radiation therapy and temozolomide and therefore play a key role in glioblastoma recurrence (171, 172).

The genetics of glioblastoma are now understood in some detail. Loss of *PTEN* is a very frequent event in glioblastoma, with hemizygous or homozygous deletions occurring in over 90% of primary glioblastomas (38). PTEN catalyzes the inactivation of the second messenger phosphatidylinositol 3,4,5 trisphosphate. This second messenger is produced by the enzyme phosphoinositide 3' kinase (PI 3-kinase) after activation by tyrosine kinase receptors. Loss of PTEN therefore results in increased signaling through the PI 3-kinase pathway. Other glioblastoma mutations, including mutations in the *EGFR*, *PIK3CA* and *PIK3R1* genes, also

activate this pathway (38, 173). While much attention has focused on the role of Akt/PKB as a downstream mediator in the PI 3-kinase pathway, PI 3-kinase signaling results in the activation of multiple other downstream kinases (56). This includes atypical protein kinase C (PKC) family members (83). There are two atypical PKCs in humans, aPKCζ and aPKCι. Of these, PKCι is the most ubiquitously expressed in tissues and overexpressed PKCι has been shown to have the properties of an oncogene in several different tumor types (174). In studies using human glioblastoma cell lines, PKCι has been shown to have a role in both proliferation and invasion (92, 93, 175). Relatively little is known about the kinase substrates that mediate these effects. One of the more well-characterized substrates of the atypical PKCs is a protein known as Lgl.

Lethal Giant larvae (Lgl) was first identified as a gene in *Drosophila* that, when mutated, gave rise to a neoplastic phenotype characterized by overgrowth of imaginal epithelia and brain tissue (129). In *Drosophila* brain tissue, this overgrowth is the result of neuroblasts preferentially undergoing self-renewal rather than differentiating into neurons (103). Mammals have two genes with homology to *Drosophila* Lgl: *LGL1*, which in mice is broadly expressed with the highest expression in brain; and *LGL2*, which shows a more restricted expression pattern (98). Knockout of Lgl1 in mice causes a brain dysplasia phenotype (98). At the cellular level, Lgl proteins have multiple functions related to cell polarity, including asymmetric cell division (176). Additional cell polarity functions include the maintenance of apical/basolateral cell polarity (in epithelial tissue); polarized exocytosis; and cell motility (120, 177). Lgl proteins bind non-muscle myosin II and associate with the inner leaflet of the plasma membrane. They also bind the scaffolding protein Par6. Atypical PKCs also bind to Par6 and in this complex they are able to phosphorylate and inactivate Lgl. Inactivated Lgl no longer associates with the plasma membrane or with non-muscle myosin II (104).

Given its original characterization as a tumor suppressor in *Drosophila*, a possible role for Lgl as a tumor suppressor in human cancers has also been investigated. Human Lgl1 can rescue *Drosophila* Lgl mutants, showing conservation of function (132). Human Lgl1 mRNA and protein are reduced in multiple cancer types including colorectal cancer and melanoma (132, 136, 178). This reduced expression is not due to either Lgl1 gene mutations or promoter methylation, but instead is due to transcriptional repression (137). Although Lgl1 shows strong expression in brain and is known to control brain development in both *Drosophila* and mammals, there has been no detailed investigation of the role of Lgl1 in glioblastoma to date. Here we show that in glioblastoma, *PTEN* loss results in the inactivation of Lgl1 by phosphorylation. This inactivation of Lgl1 has a key function in the maintenance of undifferentiated glioblastoma tumor-initiating cell populations.

Results

Constitutive phosphorylation of Lgl1 in glioblastoma cells: A lentiviral vector for constitutive expression of Lgl1 was constructed and used to express Lgl1 in U87MG human glioblastoma cells. In addition a second lentiviral vector was made to express a non-phosphorylatable, constitutively active Lgl1 (designated Lgl3SA), in which the three major Lgl1 phosphorylation sites identified by Yamanaka *et al*. were mutated to alanine (105). Transduced Lgl1 and Lgl3SA were expressed at similar levels in U87MG glioblastoma cells (Figure 1A). U87MG cells express low levels of endogenous Lgl1, visible as a faint band in Figure 1A in the blot probed with Lgl1 antibody. To detect phosphorylated transduced Lgl1, a phospho-(Ser) PKC substrate antibody was used; in total cell extracts this labeled a prominent band of the expected size in cells transduced with Lgl1, but not in cells transduced with Lgl3SA (Figure 1B). Knockdown of Lgl1 with two different Lgl1 RNA duplexes also decreased the intensity of the band detected with the phospho-(Ser) PKC substrate antibody, confirming its identity (Figure 1C). Knockdown of PKCι (the sole atypical PKC isoform expressed in U87MG cells (93)) also reduced the intensity of this band, confirming that PKCι is responsible for Lgl1 phosphorylation in these cells (Figure 1D).

Effects of PTEN on Lgl1 activation: To assess the effects of PTEN on Lgl1 phosphorylation, a doxycycline-inducible expression system for PTEN was generated in U87MG cells, which do not express PTEN due to a mutation (179). This gave rapid, inducible expression of PTEN that was active, as assessed by its ability to decrease phosphorylation of Akt and PKCι (Figure 2A). These cells were transduced with Lgl1 cDNA and Lgl1 phosphorylation was assessed with phospho-(Ser) PKC substrate antibody as above. Induction of PTEN decreased levels of phosphorylated Lgl1 without significantly affecting the total levels of Lgl1 protein (Figure 2B).

Figure 1. Lgl1 is constitutively phosphorylated by PKCι in PTEN-null U87MG cells. (A) U87MG cells were transduced with lentiviral vectors expressing GFP (as a control), wild-type Lgl1, or a mutant non-phosphorylatable Lgl (Lgl3SA). Expression of Lgl was assessed by Western blotting of total cell lysates using antibodies to Flag epitope, Lgl1 and GAPDH (as a loading control); (B) U87MG cells were transduced with lentiviral vectors expressing either wild-type Lgl1 or Lgl3SA. Total cell lysates were analyzed by Western blotting using antibodies to phospho-PKC substrate, Lgl1 and GAPDH; (C) U87MG cell transduced with lentiviral vector expressing wild-type Lgl were mock transfected, transfected with control RNA duplex, or transfected with two different RNA duplexes targeting Lgl (LglA and LglB). 48 h after transfection, total cell lysates were collected and analyzed on separate Western blots with antibodies to Lgl and phospho-PKC substrate (GAPDH loading controls are shown for each blot). (D) U87MG cell transduced with lentiviral vector expressing wild-type Lgl were mock transfected, transfected with control RNA duplex, or transfected with two different RNA duplexes targeting PKCι (iotaA and iotaE). 48 h after transfection, total cell lysates were collected and analyzed by Western blotting for phospho-PKC substrate, PKCι and Lgl.

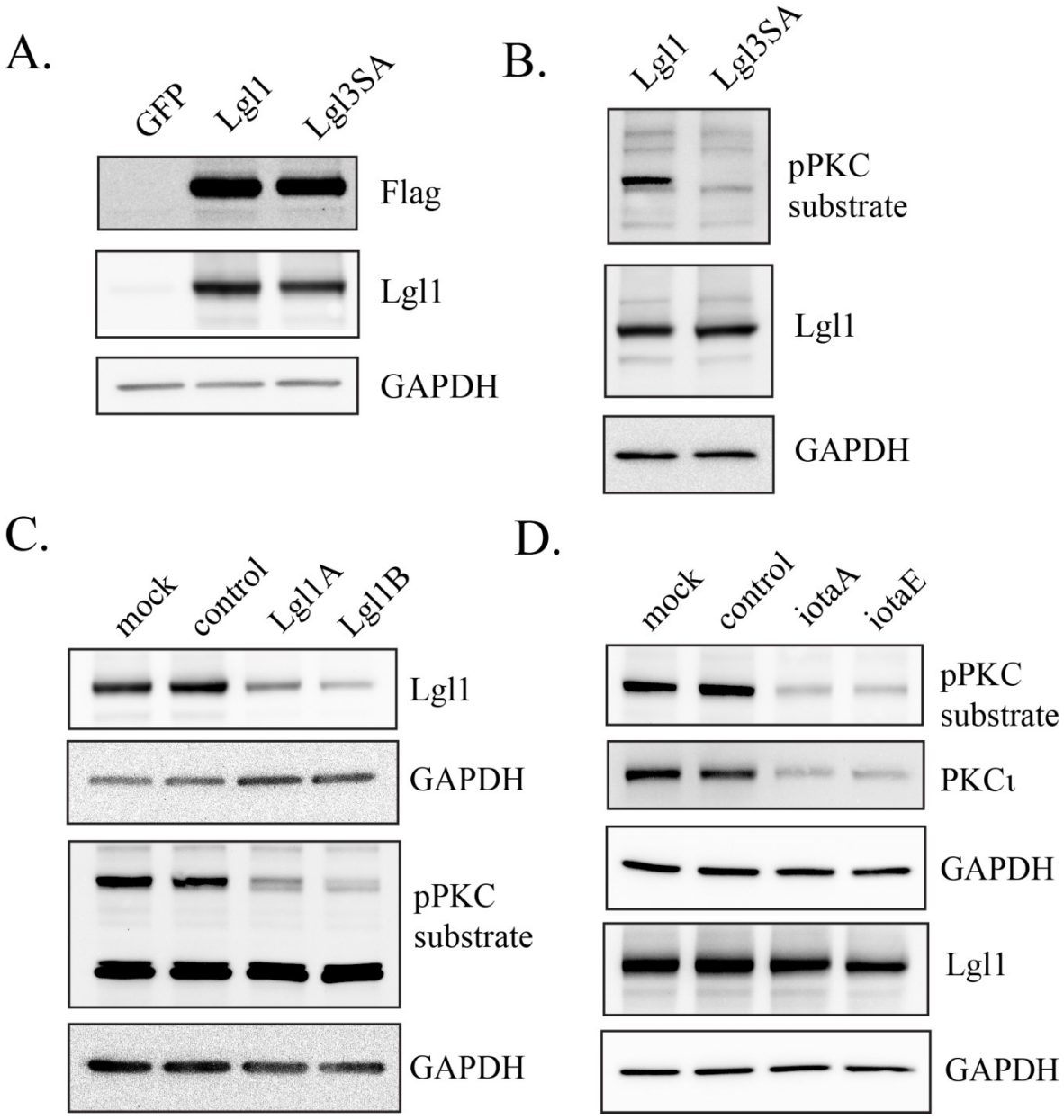
A.
GFP
Lgl1
Lgl3SA
Flag
Lgl1
GAPDH
B.
Lgl1
Lgl3SA
pPKC substrate
Lgl1
GAPDH
C.
mock
control
Lgl1A
Lgl1B
Lgl1
GAPDH
pPKC substrate
GAPDH
D.
mock
control
iotaA
iotaE
pPKC substrate
PKCι
GAPDH
Lgl1
GAPDH

Figure 2. Restoration of PTEN expression reduces Lgl phosphorylation and promotes its membrane association. (A) U87MG cells were transduced with lentiviral vectors expressing Tet activator and Tet-inducible PTEN. Cells were treated with or without 100 ng/ml doxycycline for the indicated period of time. Total cell lysates were then analyzed by Western blotting for PTEN expression (left panels). Total cell lysates from cell treated for 48 h with 100 ng/ml doxycycline were also analyzed by Western blotting for total and phosphorylated Akt and PKCι (right panels). (B) U87MG cells with doxycycline-inducible PTEN were treated for two days with doxycycline and then either mock-transduced or transduced with lentiviral vector constitutively expressing wild-type Lgl. Total cell lysates were collected two days after transduction and analyzed by Western blotting with phospho-PKC substrate antibody (shown), Lgl antibody and GAPDH antibody (not shown). Data from three independent experiments were analyzed for levels of total and phosphorylated Lgl (bar graphs at left). Data were first normalized to GAPDH levels and are shown normalized to the no doxycycline condition in the bar graphs. Data are shown as the mean ± SD. * indicates a p value less than 0.05. (C) U87MG cells with doxycycline-inducible PTEN were treated for two days with doxycycline and then transduced with lentiviral vector expressing wild-type Lgl. Two days after transduction, cells were fixed and analyzed by immunofluorescence with anti-Flag antibody. Examples of immunofluorescence staining are shown in the left two panels. The right panel shows the analysis for membrane localization from 15 randomly selected images per experiment assessed by an observer (IR) blinded to the treatment conditions. Data are the mean ± SD from three separate experiments. * indicates a p value less than 0.05.

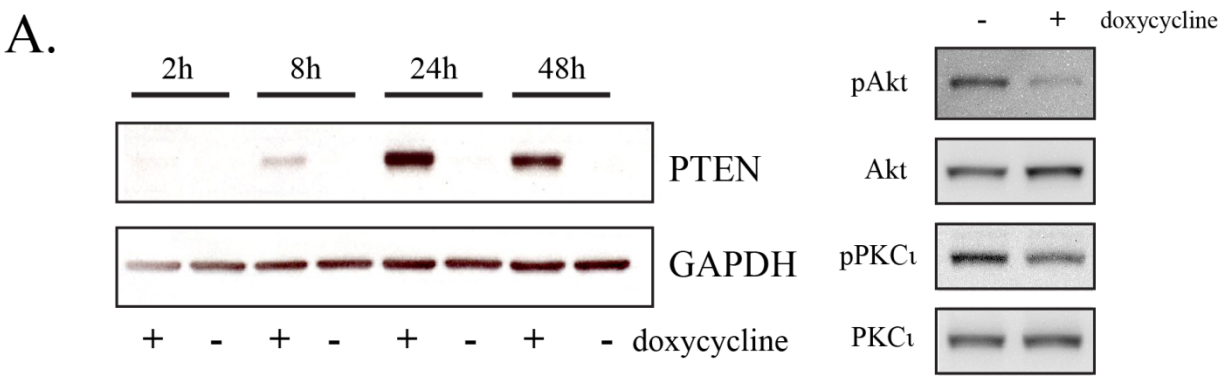
A.
2h
8h
24h
48h
PTEN
GAPDH
+ - + - + - + - doxycycline
- + doxycycline
pAkt
Akt
pPKCι
PKCι

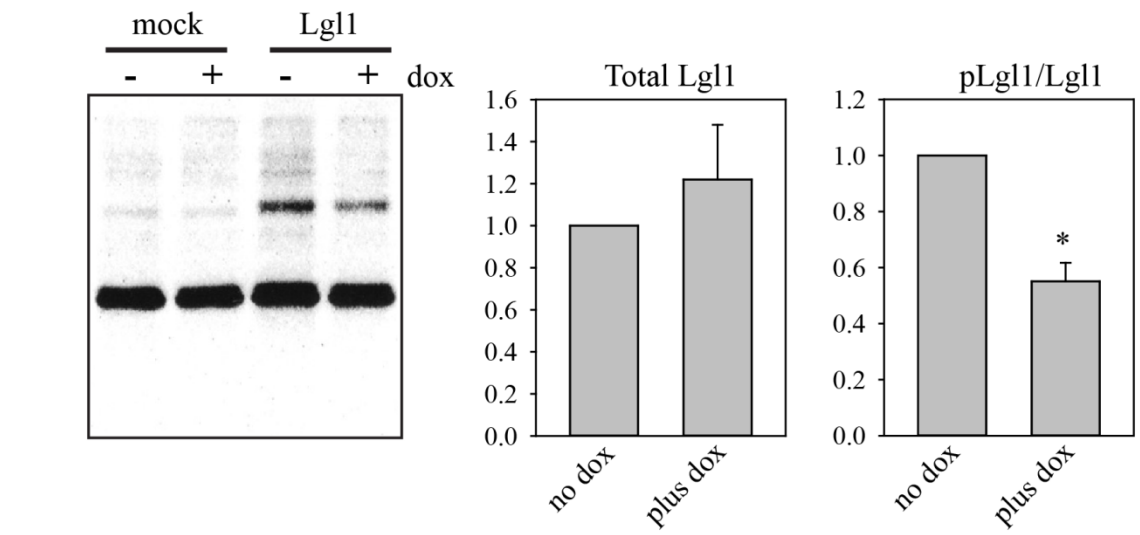
B.
mock
Lgl1
- + - + dox
Total Lgl1
1.6
1.4
1.2
1.0
0.8
0.6
0.4
0.2
0.0
no dox
plus dox
pLgl1/Lgl1
1.2
1.0
0.8
0.6
0.4
0.2
0.0
*
no dox
plus dox

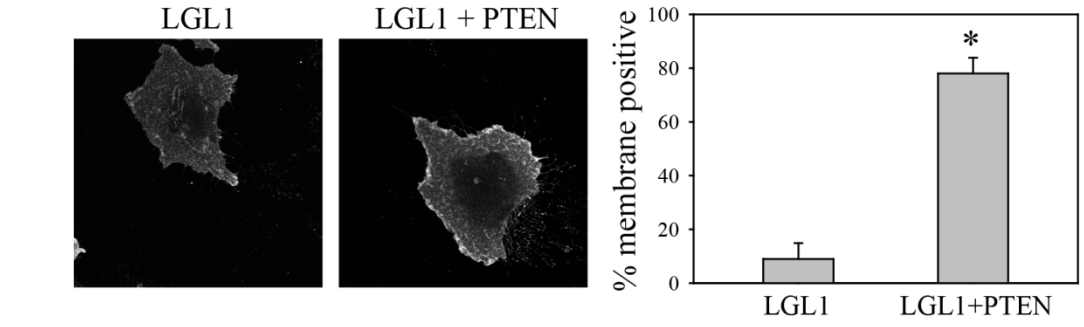
C.
LGL1
LGL1 + PTEN
% membrane positive
100
80
60
40
20
0
*
LGL1
LGL1+PTEN

Lgl1 in its active form is membrane-localized and inactivation by phosphorylation causes its translocation to the cytosol. In U87MG cells, transduced wild-type Lgl1 was localized in the cytoplasm. Induction of PTEN altered the subcellular localization of wild-type Lgl1, such that it was predominantly membrane-associated, consistent with its restoration to an active form (Figure 2C).

Membrane association of a non-phosphorylatable Lgl1 mutant in glioblastoma cells: A doxycycline-inducible expression system to express either wild-type Lgl or Lgl3SA was also made in U87MG cells. As with the constitutive expression system, both proteins were expressed at similar levels and were detectable within 6 h after induction of expression with doxycycline (Figure 3A). Induced Lgl and Lgl3SA showed different subcellular localizations in glioblastoma cells, with Lgl being predominantly cytoplasmic and Lgl3SA showing significant membrane association (Figure 3B). This membrane localization was particularly pronounced in mitotic cells; double staining for both Lgl and non-muscle myosin II (a known Lgl binding partner) in mitotic cells showed that Lgl3SA, but not Lgl, colocalized with non-muscle myosin II.

Characterization of glioblastoma tumor initiating cells (GTICs): GTICs were isolated from patients undergoing surgery for glioblastoma at The Ottawa Hospital. Cells were isolated following the procedure described by Pollard *et al*., in which GTICs are plated directly onto laminin-coated plates (31). Cells were cultured in 5% O_2, which significantly enhanced their growth rate compared to growth in atmospheric oxygen levels (20%). Enhanced growth in 5% O_2 has been observed previously for neural stem cells (180) and may be due in part to reduced

Figure 3. Non-phosphorylatable Lgl1 constitutively associates with the cell membrane in U87MG cells. (A) U87MG cells were transduced with lentiviral vectors expressing tet activator and tet-inducible Lgl or Lgl3SA. Cells were treated with 100 ng/ml doxycycline for the indicated periods of time and then analyzed by Western blotting with anti-Flag antibody. (B) U87MG cells with inducible Lgl or Lgl3SA expression were treated with 100 ng/ml doxycycline for 4 days and then analyzed by immunofluorescence microscopy using anti-Flag antibody. Membrane localization was quantitated as describe in Figure 2C. (C) U87MG cells with inducible Lgl or Lgl3SA expression were treated with 100 ng/ml doxycycline for 4 days and then analyzed by confocal immunofluorescence microscopy with antibodies to Flag epitope (red) and non-muscle myosin IIa (green). Cells were counterstained with DAPI. Examples of confocal images of mitotic cells expressing Lgl and Lgl3SA are shown.

A.

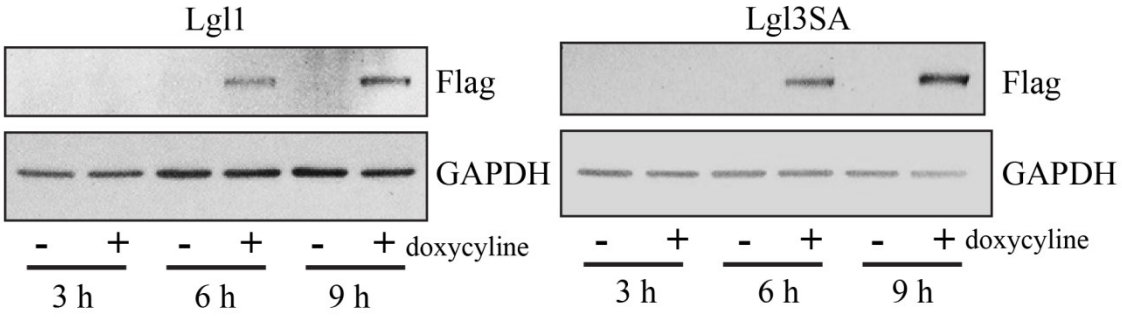
Lgl1
Lgl3SA
Flag
Flag
GAPDH
GAPDH
- + - + - + doxycyline
- + - + - + doxycyline
3 h
6 h
9 h
3 h
6 h
9 h

B.

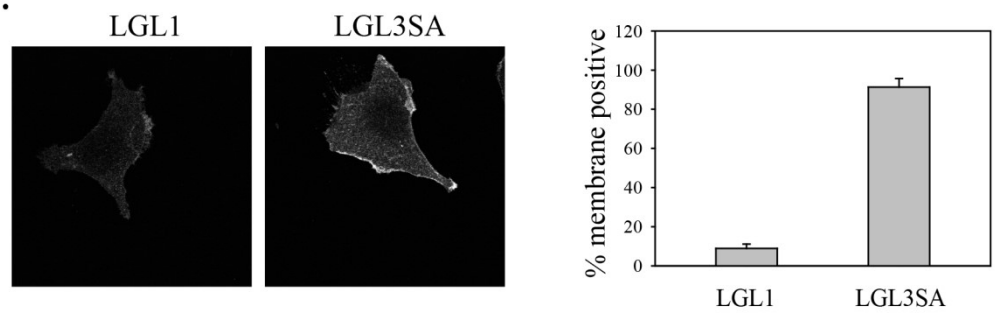
LGL1
LGL3SA
% membrane positive
120
100
80
60
40
20
0
LGL1
LGL3SA

C.

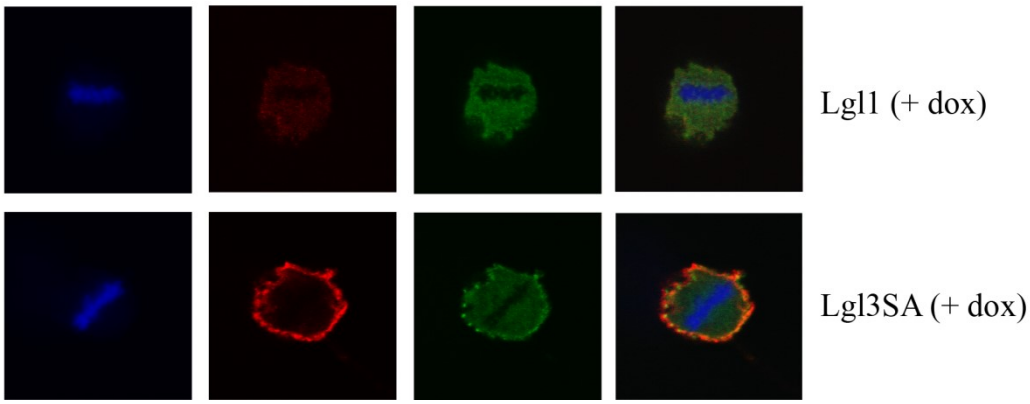
DAPI
Lgl1
NMMII
merged
Lgl1 (+ dox)
Lgl3SA (+ dox)

senescence (181). This level is also more physiologically appropriate than atmospheric oxygen levels (20%), as it is similar to oxygen levels in the adult brain (29). GTICs were used at low passage numbers (less than 20 passages), as this has been shown to be important for maintaining multipotency (182). Analysis of GTIC cultures from three different patients showed that they all expressed Lgl1 and PKCι, with expression of Lgl1 being considerably higher than in U87MG cells (Figure 4A). Cells from two patients showed detectable expression of PTEN, while cells from one patient (PriGO8A cells) showed a complete absence of PTEN expression, as in U87MG cells (Figure 4A). The latter were chosen for further detailed analysis. Chromogenic in situ hybridization showed that PriGO8A cells had three copies of the *EGFR* gene, likely reflecting a gain of chromosome 7, a characteristic genetic feature of glioblastoma (Figure 4B). When grown in the absence of laminin, the cells readily formed neurospheres resembling those seen in neural stem cell culture (Figure 4C). The cells also uniformly stained positive for nestin, a standard marker of neural stem cells (Figure 4D). When injected intracerebrally into immunocompromised mice, these cells formed a diffuse glioblastoma that was highly invasive (Figure 5A). The pattern of invasion was typical of glioblastoma, with extensive movement of cells into the uninjected hemisphere occurring along the corpus callosum. Thus these cells have the characteristic features of GTICs described in previous publications (30, 31).

The ability of PriGO8A cells to differentiate in response to standard differentiation induction methods (serum addition, with or without growth factor withdrawal) was assessed (Figure 5B and C). To assess neuronal differentiation, neuron-specific class III β-tubulin (TUJ1) antibody was used; differentiation along the astrocytic lineage was assessed using antibody to glial fibrillary acidic protein (GFAP). These markers have been used extensively to assess differentiation along neuronal and astrocytic lineages in both GTICs and normal adult neural

Figure 4. Characterization of PriGO8A cells. (A) Western blot analysis of PTEN, Lgl1 and PKCι expression in GTIC cultures from three patients. Total cell extracts from U87MG cells with doxycycline-inducible PTEN were also run for comparison. (B) Chromogenic in situ hybridization was performed on PriGO8A cells using an EGFR probe. Examples of two nuclei are shown. The three dark spots in the nuclei indicate a gain for this region of chromosome 7. (C) Left panel, phase contrast microscopy of PriGO8A cells grown in the presence of laminin; right panel, phase contrast microscopy of PriGO8A cells grown in the absence of laminin, showing neurosphere formation. (D) Immunofluorescence microscopy for nestin in PriGO8A cells growing on laminin. Cells were counterstained with DAPI. A control in which the primary antibody was omitted during staining is also shown.

A.

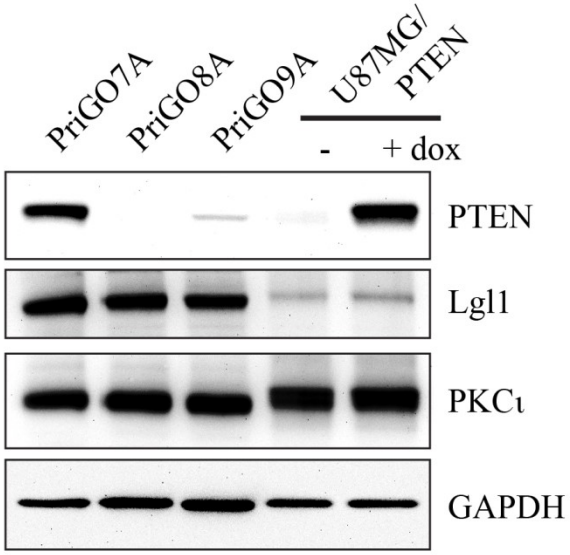

B.

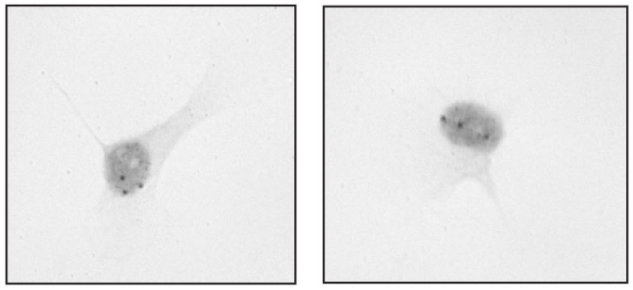

C.

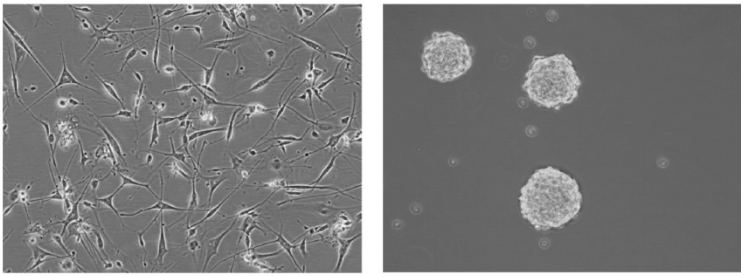

laminin

no laminin

D.

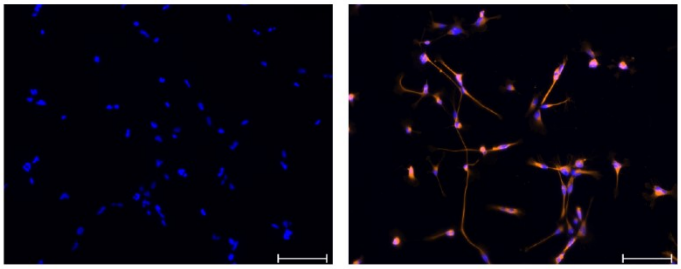

DAPI
no primary

DAPI
nestin

Figure 5. In vivo growth of PriGO8A cells and differentiation of PriGO8A cells in response to serum and/or growth factor withdrawal. (A) Growth of PriGO8A cells three months after intrastriatal injection in the right hemisphere. Hematoxylin and eosin stained whole brain sections (left panel) show extensive growth and invasion into the left hemisphere across the corpus callosum. The close-up (right panel) shows a border area between cancer cells and normal brain. (B) PriGO8A cells were grown in: regular media; media supplemented with 10% fetal calf serum; media supplemented with 10% fetal calf serum without EGF and FGF growth factors. Seven days later cells were fixed and immunofluorescence microscopy was performed for either TUJ1 or GFAP. (C) Quantitation of the results in B. Data are shown as the mean ±SE.

A.

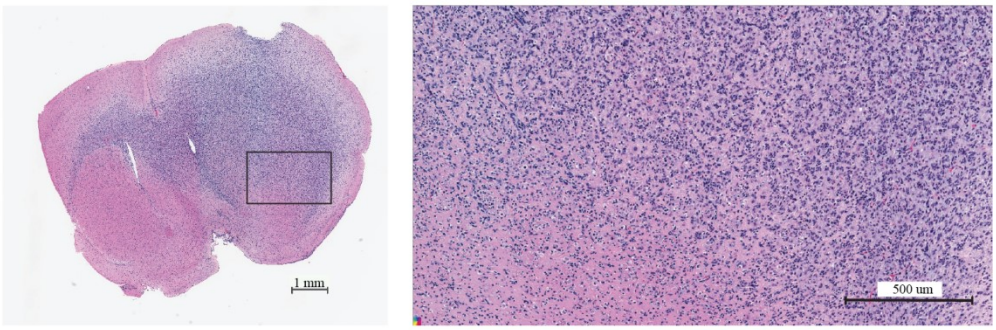
1 mm
500 um

B.

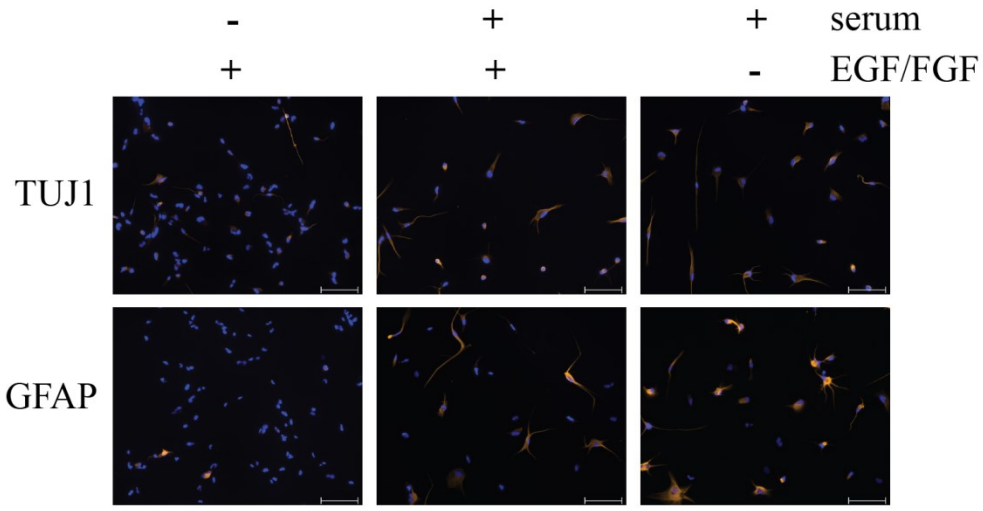
-
+
+
serum
+
+
-
EGF/FGF
TUJ1
GFAP

C.

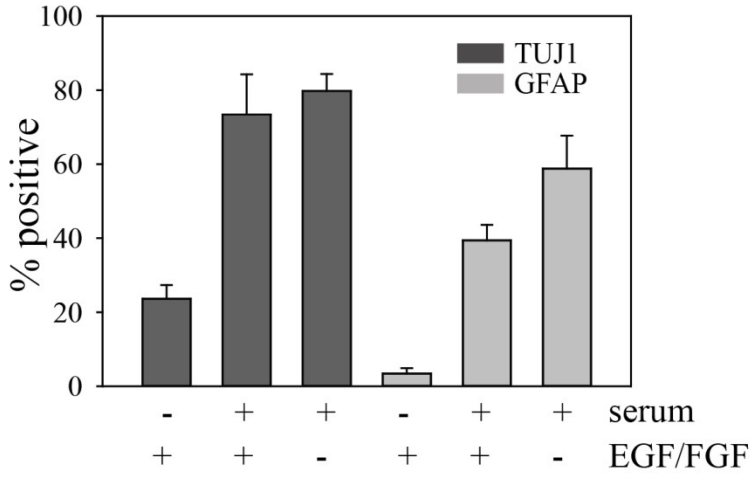
100
80
60
40
20
0
% positive
TUJ1
GFAP
- + + - + + serum
+ + - + + - EGF/FGF

stem cells (169).The addition of serum, either in the presence or absence of growth factors, increased the percentage of cells expressing TUJ1 and the percentage of cells expressing GFAP, indicating that PriGO8A cells differentiate along both neuronal and astrocytic lineages in the presence of serum. Although double labeling experiments were not performed here, the percentages of positive cells suggest that some of the differentiation observed is aberrant, giving rise to TUJ1/GFAP double positive cells, as observed previously (29, 30).

Effects of PTEN, PKCι and Lgl1 on GTIC differentiation: To assess the effects of PTEN on differentiation, PriGO8A cells were engineered for inducible expression of PTEN as described above for U87MG cells. Treatment with doxycycline induced PTEN expression in a dose-dependent fashion (Figure 6A). As in U87MG cells, PTEN induction reduced the phosphorylation of transduced Lgl1 (Figure 6B). PTEN-induction in PriGO8A cells significantly increased the relative proportion of cells that were TUJ1 positive (Figure 6C and D). This was not seen in unmodified PriGO8A cells treated with doxycycline, showing that the effect is dependent on PTEN induction (Figure 6D). PTEN induction had no effect on differentiation along the astrocytic lineage (Figure 6D).

To assess the role of PKCι in PriGO8A differentiation, transient knockdown of PKCι was performed using two different RNA duplexes at a 10 nM concentration (Figure 7A). Knockdown with both duplexes, but not with a control duplex used at the same concentration, resulted in increased differentiation along the neuronal lineage without any effects on astrocytic differentiation (Figure 7B and C).

To assess the role of Lgl1 phosphorylation, PriGO8A cells were transduced with lentiviral vector expressing Lgl3SA. As with U87MG cells, Lgl3SA, but not Lgl1, showed

Figure 6. Effects of PTEN on PriGO8A differentiation. (A) PriGO8A cells were transduced with Tet activator lentivirus and selected with G418 for four days. Selected cells were then transduced with inducible PTEN lentivirus and selected with puromycin for four days. Selected cells were treated with the indicated concentrations of doxycycline for 48 h. Total cell lysates were then analyzed by Western blotting for expression of PTEN. (B) PriGO8A cells with inducible PTEN were treated with 500 ng/ml doxycycline for two days and then either mock transduced or transduced with lentivirus constitutively expressing wild-type Lgl1. One day later cells were switched to media without EGF. Total cell extracts were collected one day later and analyzed by Western blotting with antibodies to phospho-PKC substrate and Flag epitope. (C) PriGO8A cells with inducible PTEN were untreated or treated with 500 ng/ml doxycycline for 7 days. Cells were then fixed and immunocytochemistry for TUJ1 and GFAP expression was performed. (D) Quantitation of data from C. The left graph shows doxycycline treatment of PriGO8A cells with inducible PTEN. The right graph shows doxycycline treatment of parental PriGO8A cells (as a control for effects of doxycycline alone). Quantitation was performed as described in Material and Methods. Data are shown as the mean ± SE. * indicates a p value less than 0.05.

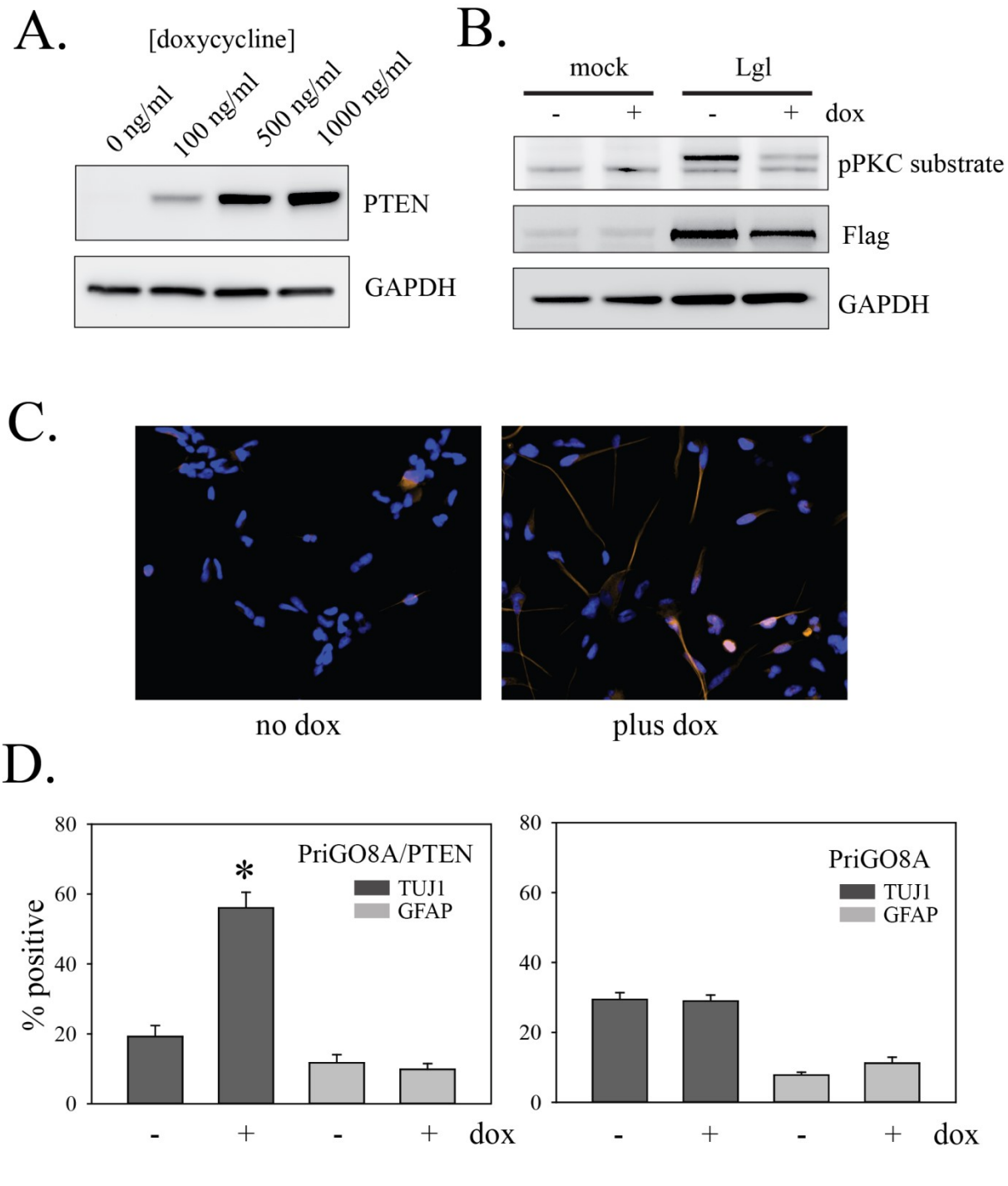
A.
[doxycycline]
0 ng/ml
100 ng/ml
500 ng/ml
1000 ng/ml
PTEN
GAPDH
B.
mock
Lgl
- + - + dox
pPKC substrate
Flag
GAPDH
C.
no dox
plus dox
D.
PriGO8A/PTEN
TUJ1
GFAP
% positive
80
60
40
20
0
*
- + - + dox
PriGO8A
TUJ1
GFAP
80
60
40
20
0
- + - + dox

Figure 7. Effects of PKCι on PriGO8A differentiation. (A)PriGO8A cells were transfected with control RNA duplex or two different RNA duplexes targeting PKCι. Three days later, total cell lysates were collected and analyzed for PKCι expression by Western blotting. (B) Cells were transfected as in A. Seven days later cells were fixed and immunofluorescence with antibodies to TUJ1 and GFAP was performed. Representative images of TUJ1 immunofluorescence are shown. (C) Quantitation of TUJ1 and GFAP immunofluorescence seven days after PKCι knockdown. Quantitation was performed as described in Material and Methods. Data are shown as the mean ± SE. * indicates a p value less than 0.05.

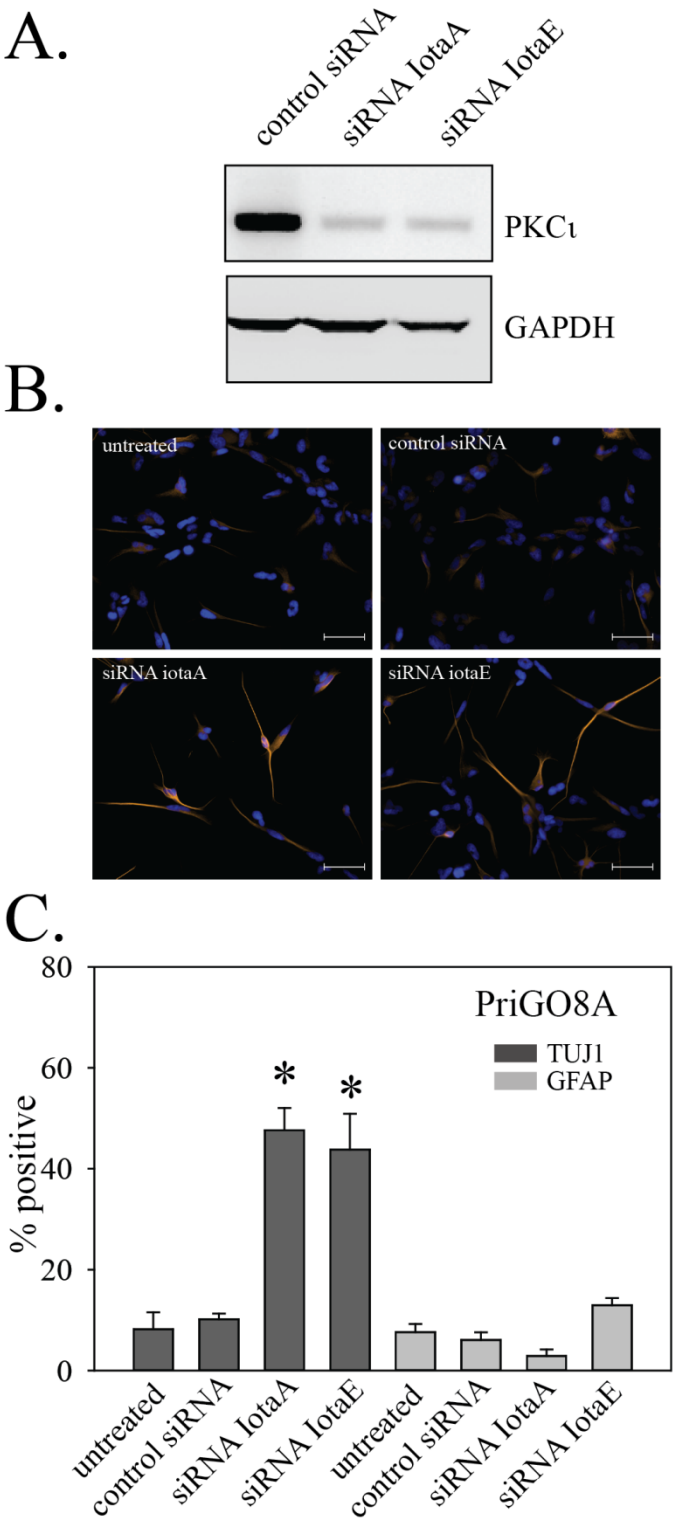
A.
control siRNA
siRNA IotaA
siRNA IotaE
PKCι
GAPDH
B.
untreated
control siRNA
siRNA iotaA
siRNA iotaE
C.
PriGO8A
TUJ1
GFAP
% positive
80
60
40
20
0
*
*
untreated
control siRNA
siRNA IotaA
siRNA IotaE
untreated
control siRNA
siRNA IotaA
siRNA IotaE

marked membrane localization in mitotic cells (Figure 8A). As with PTEN transduction and PKCι knockdown, transduction of Lgl3SA also induced PriGO8A cell differentiation along the neuronal lineage, but not the astrocytic lineage (Figure 8B and 8C).

GTICs from different patients have been reported to show variability in their differentiation behavior (31). To determine the generalizability of the above findings, the effects of PKCι knockdown and Lgl3SA expression on GTIC differentiation were also assessed in cell populations isolated from two other patients, designated PriGO9A and PriGO7A. As with PriGO8A cells, PriGO9A and PriGO7A cells were able to form neurospheres when grown in the absence of laminin, were uniformly nestin positive and were able to undergo differentiation along neuronal and astrocytic lineages when exposed to serum (Figure 9A-B and 10A-B). Western blot analysis of PriGO9A and PriGO7A cells for expression of PTEN, Lgl1 and PKCι was shown in Figure 4A. Both show similar levels of PKCι and Lgl1 to those seen in PriGO8A cells. PriGO9A cells showed very low but detectable levels of PTEN, while PriGO7A cells show higher levels. PriGO7A cells were also examined by chromogenic in situ hybridization for EGFR copy number, which showed amplification in this region (Figure 10A). Both knockdown of PKCι and Lgl3SA transduction induced differentiation along the neuronal lineage in PriGO9A and PriGO7A cells without affecting astrocytic differentiation, similar to what was observed in PriGO8A cells (Figures 9C and 10C).

Figure 8. Effects of Lgl3SA on PriGO8A differentiation. (A) PriGO8A cells were transduced with either Lgl (left) or Lgl3SA (right). Four days later cells were fixed and immunofluorescence with anti-Flag antibody was performed. Representative examples of mitotic cells are shown. (B) PriGO8A cells were transduced with either empty vector control (pLVX) or vector expressing Lgl3SA. Seven days later cells were fixed and immunofluorescence for TUJ1 and GFAP was performed. Representative images for TUJ1 staining are shown. (C) Quantitation of TUJ1 and GFAP immunofluorescence seven days after transduction with Lgl3SA. Data are shown as the mean ± SE. * indicates a p value less than 0.05.

A.

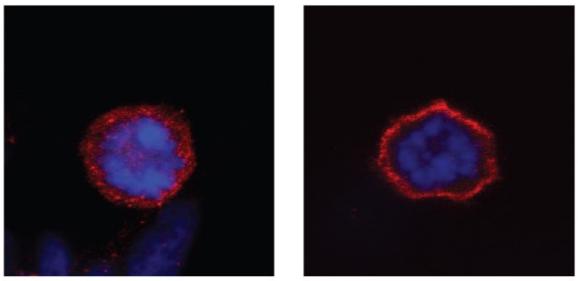

Lgl1 Lgl3SA

B.

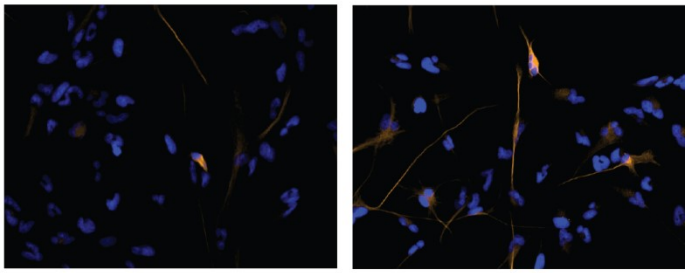

pLVX Lgl3SA

C.

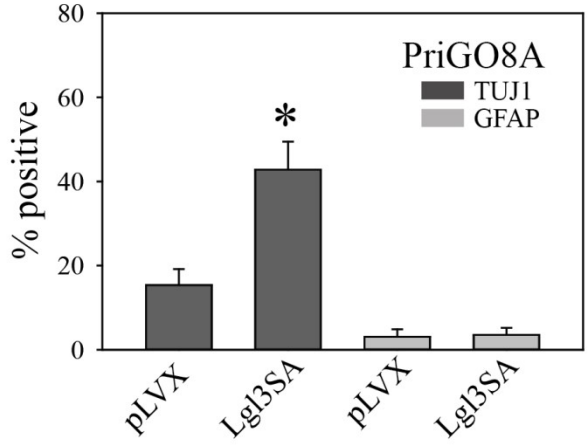

Figure 9. Effects of PKCι and Lgl3SA on PriGO9A cell differentiation. (A) Morphology under phase contrast microscopy (top left panel), neurosphere formation (top middle panel) and nestin immunofluorescence (top right panel) for PriGO9A cell cultures. (B) Differentiation of PriGO9A cells after exposure to serum with or without growth factor withdrawal, determined as described in Figure 5. (C) Bar graphs show the effects of PKCι knockdown (left panel) and Lgl3SA transduction (right panel) on PriGO9A differentiation, determined as described in Figure 7.

A.

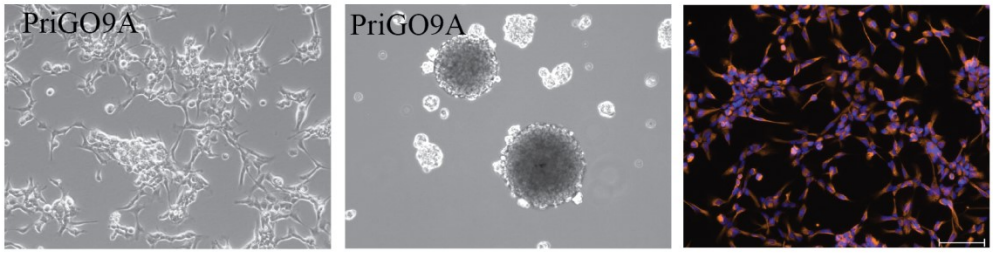
PriGO9A
PriGO9A

B.

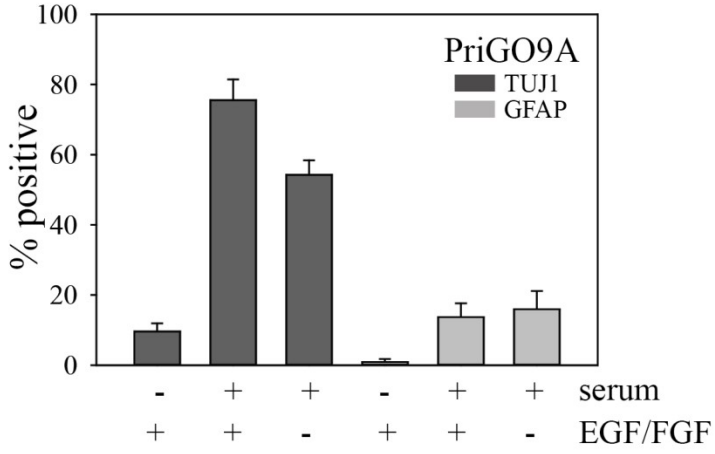
PriGO9A
TUJ1
GFAP
% positive
100
80
60
40
20
0
- + + - + + serum
+ + - + + - EGF/FGF

C.

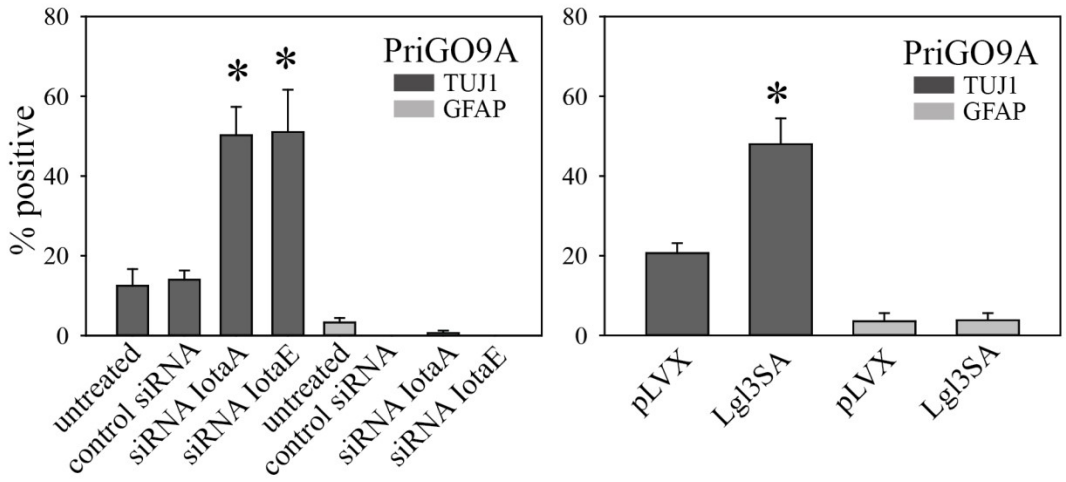
PriGO9A
TUJ1
GFAP
% positive
80
60
40
20
0
*
*
*
untreated
control siRNA
siRNA IotaA
siRNA IotaE
untreated
control siRNA
siRNA IotaA
siRNA IotaE
pLVX
Lgl3SA
pLVX
Lgl3SA

Figure 10. Effects of PKCι and Lgl1 on PriGO7A differentiation. (A) Morphology under phase contrast microscopy (top left panel), neurosphere formation (top right panel), nestin immunofluorescence (lower left panel) and EGFR chromogenic in situ hybridization for PriGO7A cells (lower right panel). (B) Differentiation of PriGO7A cells after exposure to serum or growth factor withdrawal. (C) Bar graphs show the effects of PKCι knockdown (left panel) and Lgl3SA transduction (right panel) on PriGO7A differentiation.

A.

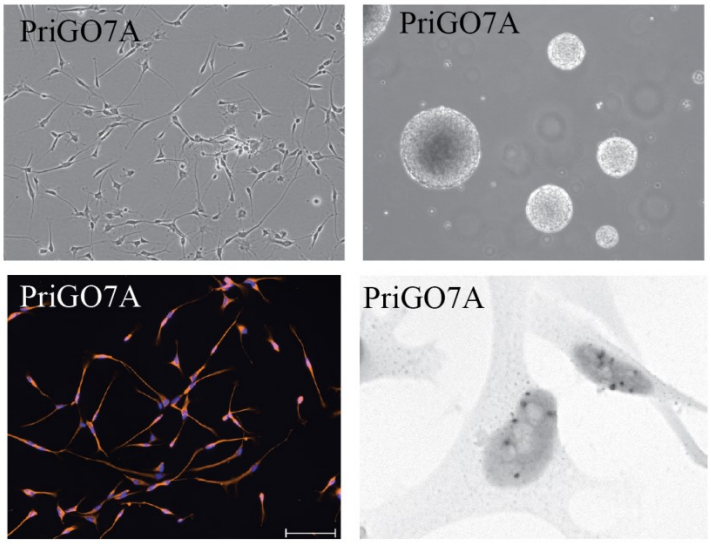
PriGO7A
PriGO7A
PriGO7A
PriGO7A

B.

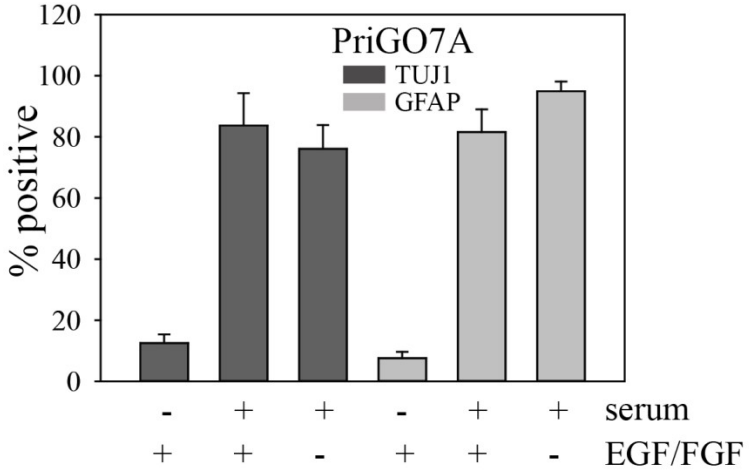
PriGO7A
TUJ1
GFAP
% positive
120
100
80
60
40
20
0
- + + - + + serum
+ + - + + - EGF/FGF

C.

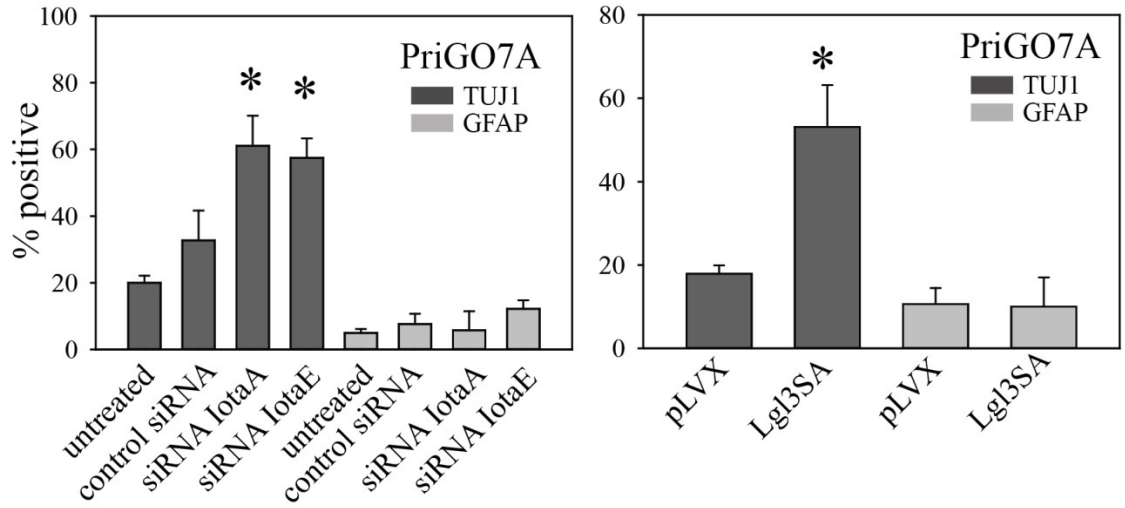
PriGO7A
TUJ1
GFAP
% positive
100
80
60
40
20
0
*
*
untreated
control siRNA
siRNA IotaA
siRNA IotaE
untreated
control siRNA
siRNA IotaA
siRNA IotaE
PriGO7A
TUJ1
GFAP
80
60
40
20
0
*
pLVX
Lgl3SA
pLVX
Lgl3SA

Discussion

Partial or complete loss of the tumor suppressor *PTEN*, by either hemizygous deletion, homozygous deletion or mutation, is a frequent event in glioblastoma. In this study, we demonstrate that loss of this tumor suppressor leads to the inactivation of a second protein with tumor suppressor-like functions, Lgl1. Previous work has shown both that Lgl is inactivated by phosphorylation and that the atypical PKCs are responsible for this (104, 120, 177). The key finding here is the link between this and the loss of *PTEN*: we show that restoration of PTEN results in a decrease in Lgl1 phosphorylation as well as an increase in its membrane association, which is a marker of functional Lgl1. The effects of PTEN on Lgl1 phosphorylation were seen both in U87MG cells and in GTICs. This finding represents a second mechanism by which Lgl1 can be inactivated in cancer cells, as previous studies have shown that Lgl1 is downregulated at both the mRNA and protein levels in several cancer types, including colorectal cancer and melanoma, compared to normal tissue (136, 178). Lgl1 inactivation therefore appears to be a very frequent event in human cancers.

The effects of the PTEN/aPKC/Lgl1 pathway on the differentiation state of glioblastoma tumor initiating cells (GTICs) were assessed. GTICs were isolated from multiple patients using previously described culture techniques that preserve their ability to generate tumors in mice that mimic the pathology of human glioblastoma (30, 31). Cultures were screened for PTEN expression levels. GTICs from one patient (PriGO8A cells) were chosen for detailed study, as these showed complete loss of PTEN expression, in common with U87MG cells. PriGO8A cells showed the common features of GTICs that have been described previously in the literature (29, 31), including nestin expression, the ability to form neurospheres, the ability to differentiate

along both neuronal and astrocytic lineages in response to serum exposure, and the ability to form invasive tumors in immunocompromised mice.

PriGO8A cells were engineered for inducible expression of PTEN. As in U87MG cells, induction of PTEN in PriGO8A cells reduced the phosphorylation of Lgl1. Induction of PTEN also resulted in differentiation. This finding is similar to previous findings in adult neural stem cells and other non-cancer stem cell types, where loss of PTEN represses differentiation (183). Although serum exposure resulted in differentiation of these cells along both neuronal and astrocytic lineages, with PTEN induction differentiation was exclusively along the neuronal lineage. This contrasts with the previously reported effects of BMP-4 on GTIC differentiation, where differentiation occurred primarily along the astrocytic lineage (34). In most human glioblastoma tumors, the bulk of the cells are GFAP-positive, indicating that differentiation occurs primarily along the astrocytic lineage. Results here suggest the possibility that this is a consequence of strong repression of neuronal differentiation by *PTEN* loss and subsequent PI 3-kinase pathway activation.

As with PTEN induction, knockdown of PKCι also reduced the phosphorylation of Lgl1. In addition, knockdown of PKCι in PriGO8A cells resulted in differentiation along the neuronal lineage, phenocopying what was seen with PTEN induction. This indicates that PKCι is the key mediator of PI 3-kinase pathway effects on GTIC differentiation.

A non-phosphorylatable constitutively-active mutant of Lgl1 (designated Lgl3SA) was also expressed in PriGO8A cells. This was able to associate with the cell membrane; importantly this indicates that the human homologs of the *Drosophila* tumor suppressors Scribble and Discs large are functional in these cells, as these proteins are known to be required for Lgl membrane association (129). As with PTEN induction and PKCι knockdown, expression of Lgl3SA

induced differentiation exclusively along the neuronal lineage, indicating that Lgl is a key substrate mediating the effects of PKCι on GTIC differentiation.

The effects of Lgl3SA were also assessed in GTIC cells from two additional patients. PriGO9A cells, which showed low but detectable levels of PTEN, also underwent differentiation along a neuronal lineage when transduced with Lgl3SA. This effect was also seen in PriGO7A cells. These cells express high levels of PTEN, but show evidence of amplification of EGFR. Thus the role for Lgl1 does not appear to be restricted to GTICs in which PTEN expression is completely lost, but is also functional in GTICs where the PI 3-kinase pathway is hyperactivated by other mechanisms such as EGFR amplification.

The above findings for PKCι and Lgl1 are consistent with previous studies in *Drosophila* showing that atypical PKC and Lgl mediate the decision between neuroblast self-renewal and differentiation (103). The data here show that this pathway is conserved in human GTICs and, critically, is linked to PTEN and PI 3-kinase signaling pathway status. The fact that partial or complete loss of PTEN expression is very common suggests that it is an early event in gliomagenesis. Thus inactivation of Lgl1 may also be an early event in gliomagenesis, leading to the expansion of a population of undifferentiated tumor initiating cells, the cell population that is the key driver for glioblastoma malignancy (168).

Materials and methods

Antibodies and chemicals: Anti-Flag M2 mouse monoclonal antibody, non-muscle myosin II rabbit polyclonal antibody and GFAP mouse monoclonal were from Sigma-Aldrich (Oakville, ON, Canada). PKCι mouse monoclonal and phospho-threonine 555 PKCι rabbit polyclonal antibodies were from BD Transduction Laboratories (Mississauga, ON, Canada) and Invitrogen (Carlsbad, CA, USA) respectively. The Akt goat polyclonal was from Santa Cruz Biotechnology (Santa Cruz, CA, USA). Phospho-AKT (Ser473) rabbit polyclonal, phospho-(Ser) PKC Substrate (P-S3-101) antibody (a mix of three rabbit monoclonal antibodies), and PTEN rabbit monoclonal antibody were from Cell Signaling Technology (Danvers, MA, USA). Lgl1 rabbit polyclonal antibody and GAPDH mouse monoclonal (6C5) antibody were from Abcam (Cambridge, MA, USA). TUJ1 rabbit monoclonal antibody was from Covance (Princeton, NJ, USA). Nestin mouse monoclonal antibody was from R&D Systems (Minneapolis, MN, USA).

Cell Culture: U87MG cells were grown in Dulbecco's Modified Eagle medium supplemented with 100 units/ml penicillin, 100 μg/ml streptomycin and 10% fetal bovine serum at 37°C and 5% CO_2. Cells were used at low passage number and were routinely checked and shown to be free of mycoplasma. GTIC cultures were isolated following a protocol approved by the Ottawa Hospital Research Ethics Board. Surgical samples were harvested from consented patients undergoing surgery for suspected glioblastoma (and without a history of previous lower grade brain tumor) using a Nico Myriad surgical device (NICO Corporation, Indianapolis, IN, USA). Cultures were digested with Accutase, filtered through 100 μM and 40 μM nylon mesh filters, and plated on laminin-coated plates as described by Pollard *et al*. (31). Accutase and laminin were from Sigma-Aldrich, Oakville, ON, Canada. Cultures were grown in Neurobasal A medium

supplemented with B27, N2 (all from Life Technologies, Burlington, ON, Canada), EGF and FGF (Peprotech, Rocky Hill, NJ, USA) at 37°C in 5% O_2/CO_2 .

Plasmid constructs: Full-length cDNA encoding Lgl1 mRNA was produced as described previously (14). Site-directed mutagenesis was used to add an amino terminal Flag tag using the QuikChange XL Site-Directed Mutagenesis kit (Stratagene, La Jolla, CA, USA). Site-directed mutagenesis was also used to change the codons for serine 656, 660 and 664 to alanine to generate Flag-tagged Lgl3SA cDNA. For constitutive lentiviral vector production, Flag-tagged wild-type Lgl or Lgl3SA were PCR amplified to add Xba1 and Sal1 5' and 3' restriction sites and subcloned into pLenti-CMV GFP Puro (Addgene Plasmid 17448) which had been digested with the same restriction enzymes to remove the GFP cDNA. For inducible expression, PTEN cDNA, Flag-tagged Lgl cDNA and Flag-tagged Lgl3SA cDNA were subcloned into the Tet-inducible lentiviral vector pLVX-Tight-Puro (Clontech, Mountain View, CA, USA).

Transduction with lentiviral vectors: Replication-incompetent lentiviral particles were made by the four-plasmid transfection method described by Wiederschain *et al*. (184). U87MG were transduced by incubation for 24 h with lentivirus-containing supernatant added to regular media supplemented with 10 μg/ml polybrene (for U87MG transductions; polybrene was omitted for tumor initiating cell transductions). For inducible expression, cells were first transduced with lentivirus made with Tet-activator plasmid (Clontech, Mountain View, CA, USA) and selected with G418 (500μg/ml); these cells were then transduced again with lentivirus made with the inducible cDNA vectors described above and selected with puromycin (1μg/ml for U87MG and 0.5μg/ml for PriGO cells).

Western blotting: Western blotting was done as described previously (175). Chemiluminescence from HRP conjugated secondary antibodies was detected with the Alpha Innotech Fluorchem system (Santa Clara, CA, USA) and quantitated using Alphaview software.

Immunofluorescence microscopy: Immunofluorescence microscopy was done as described previously (93). For differentiation experiments using TUJ1 and GFAP antibodies, images were taken of five random fields of view (chosen under DAPI filter) per condition per experiment. Analysis was carried out in ImageJ software (National Institutes of Health, Bethesda, Maryland, USA). The proportion of positive cells to total nuclei was assessed per condition +/- SE for each experiment.

Chromogenic in situ hybridization: Chromogenic *in situ* hybridization was used to detect EGFR gene copy number changes in PRIGO cells. ZytoDot SPEC EGFR Probe (Cat. ZTV-C-3007-400) and ZytoDot CISH Implementation Kit were from Cedarlane (Burlington, ON, Canada) and were used according to the manufacturer's recommendations.

Intracerebral xenografts: Experiments were carried out in accordance with the recommendations of the Animal Care Committee at the University of Ottawa.

5 X 10^5 PriGO cells in 10μL sterile PBS were injected intrastriatal (right side of the skull approximately 0.5mm above the coronal suture and 2mm from the sagittal suture) into 4-6 week old SCID/beige mice (Charles River Laboratories, Wilmington. MA). Endpoint was reached after approximately three months when mice became symptomatic. Whole brains were harvested, formalin fixed and paraffin embedded. Sections were cut, stained with hematoxylin and eosin, and reviewed by a neuropathologist (JW).

Statistics: SigmaPlot12 software was used for statistical analyses. Comparisons between two groups were performed using two-tailed t-tests with a p value <0.05 considered significant.

Acknowledgments

We thank Julie Wells and Sharon Kelly at the Ottawa Hospital Regional Cancer Centre for their invaluable help in obtaining patient consent for isolation of GTICs. This work was supported by a grant from the Canadian Institutes of Health Research (to IAJL). AG is supported by a Queen Elizabeth II Graduate Scholarship in Science and Technology.

3. Inhibition of glioblastoma malignancy by Lgl1

Alexander Gont[1,2], Jennifer E L Hanson[1], Sylvie J Lavictoire[1], Manijeh Daneshmand[1,3], Garth Nicholas[1,5], John Woulfe[1,2,3], Amin Kassam[4*], Vasco F Da Silva[4] and Ian AJ Lorimer[1,2,5]

[1]Centre for Cancer Therapeutics, Ottawa Hospital Research Institute, 501 Smyth Road, Ottawa, K1H 8L6, Canada
[2]Department of Biochemistry, Microbiology and Immunology, University of Ottawa, Ottawa, Ontario, Canada
[3]Department of Pathology and Laboratory Medicine, University of Ottawa, Ottawa, Ontario, Canada
[4]Department of Surgery, University of Ottawa, Ottawa, Ontario, Canada
[5]Department of Medicine, University of Ottawa, Ottawa, Ontario, Canada

Address correspondence to: Ian A. J. Lorimer, Ottawa Hospital Regional Cancer Centre, Centre for Cancer Therapeutics, 3rd floor, 501 Smyth Road, Ottawa, Ontario, Canada K1H 8L6. Phone (613) 737-7700 ext. 70332; Fax (613) 247-3524; E-mail ilorimer@ohri.ca

Keywords: Glioblastoma, glioma, Lgl, Lgl1, PTEN, invasion

**current address*: Aurora St. Luke's Medical Center, Aurora Health Care, Milwaukee, WI 53215, USA

Contribution of authors: The content of this manuscript was written by A. Gont with the help of Dr. I.A.J. Lorimer. All of the experiments presented in this manuscript are the work of A. Gont. PriGO cells cultures were established by J. E. L. Hanson with samples provided by Drs. A. Kassam and V. F. Da Silva. Drs. A. Kassam, V. F. Da Silva, G. Nicholas, and J. Woulfe provided consultation for the PriGO cell project. Drs. M. Daneshmand and J. Woulfe provided consultation for immunohistological experiments. S. J. Lavictoire provided consultation for plasmid construct development and lentiviral transductions.

Published: Oncotarget. 2014 Nov 30;5(22):11541-51.

Abstract

lethal giant larvae (*lgl*) was first identified as a tumor suppressor in *Drosophila*, where its loss repressed the differentiation and promoted the invasion of neuroblasts, the *Drosophila* equivalent of the neural stem cell. Recently we have shown that a human homolog of Lgl, Lgl1 (LLGL1), is constitutively phosphorylated and inactivated in glioblastoma cells; this occurs as a downstream consequence of *PTEN* loss, one of the most frequent genetic events in glioblastoma. Here we have investigated the consequences of this loss of functional Lgl1 in glioblastoma *in vivo*. We used a doxycycline-inducible system to express a non-phosphorylatable, constitutively active version of Lgl1 (Lgl3SA) in either a glioblastoma cell line or primary glioblastoma cells isolated under neural stem cell culture conditions from patients. In both types of cells, expression of Lgl3SA, but not wild type Lgl1, inhibited cell motility *in vitro*. Induction of Lgl3SA in intracerebral xenografts markedly reduced the *in vivo* invasion of primary glioblastoma cells. Lgl3SA expression also induced the differentiation of glioblastoma cells *in vitro* and *in vivo* along the neuronal lineage. Thus the central features of Lgl function as a tumor suppressor in *Drosophila* are conserved in human glioblastoma.

Introduction

In *Drosophila*, loss of the *lgl* gene results in overgrowth of both brain and imaginal disc tissue, resulting in death at the late larval stage (132) . Brain overgrowth was shown to be due to overproliferation of neuroblasts, the *Drosophila* equivalent of the neural stem cell. Normal neuroblasts undergo repeated rounds of asymmetric cell divisions to generate a new neuroblast and a daughter cell with limited proliferative capacity that goes on to form the mature cell types (neurons and glia) of the adult fruit fly brain. In *lgl* mutants, instead of these asymmetric divisions, neuroblasts undergo repeated rounds of symmetric cell divisions to generate two neuroblasts (103). This results in expansion, rather than maintenance, of the neuroblast population, explaining the apparent increase in proliferation described early on for *lgl* mutants. Along with increased proliferation, neuroblasts in *lgl* mutant *Drosophila* spread throughout the larval brain causing abnormalities in brain structure. Transplantation studies showed that brain tissue from *lgl* mutant *Drosophila* was invasive when transplanted into wild type hosts; this invasion was mainly restricted to within the larval brain, with metastases outside the brain being relatively infrequent (97).

Here we are addressing the extent to which the behavior of *Drosophila lgl* mutants is recapitulated in the human adult brain tumor known as glioblastoma. Humans contain two genes with homology to *Drosophila* Lgl; we have focused on Lgl1 (encoded by the *LLGL1* gene) as it is the only homolog that is expressed in mammalian brain tissue (98). In both *Drosophila* and mammals, Lgl activity is controlled by atypical PKC, which phosphorylates Lgl at its hinge region leading to its inactivation (104, 177). We have shown previously that Lgl1 is constitutively phosphorylated and inactivated in glioblastoma cells (185). This inactivation is a downstream consequence of *PTEN* loss, one of the most frequent genetic events in glioblastoma

(38, 186). Currently glioblastoma is an incurable disease with a median survival time of about one year after diagnosis (167). A key aspect of its malignancy is its highly invasive nature. This invasiveness gives glioblastoma primary tumors their characteristic diffuse borders, and can result in the spread of glioblastoma cells throughout the central nervous system, with frequent involvement of both hemispheres. The pattern of glioblastoma invasion is distinctive, with single cancer cells preferentially traveling along white matter tracts and the outside walls of blood vessels (23). Another well known aspect of glioblastoma is its phenotypic heterogeneity. Some of this heterogeneity appears to be due to the fact that glioblastoma cells can exist in a range of differentiation states. A subset of cells exists in an undifferentiated neural stem cell-like state; glioblastoma cells in this undifferentiated state are thought to be the key drivers of glioblastoma malignancy (169). We have previously shown that expression of a non-phosphorylatable, constitutively active version of Lgl1 induces the differentiation of glioblastoma cells from multiple patients along the neuronal lineage in cell culture, a finding that is consistent with the behavior of Lgl in *Drosophila* (185). Here we have investigated the *in vivo* effects of Lgl1 on glioblastoma malignancy, using a xenograft model that closely mimics the invasive behavior of this disease that is seen in patients.

Results

Inhibition of glioblastoma cell motility in cell culture: We first tested the effects of Lgl1 on the invasive properties of the human glioblastoma cell line U87MG. For these experiments, a constitutively active version of Lgl1 was used in which the three hinge region phosphorylation sites were mutated to alanine (105). This was expressed using a doxycycline-inducible system as described previously (185). Invasion was evaluated in Transwell membranes coated with Matrigel. As shown in Figure 1A, expression of Lgl3SA caused a 58% reduction in U87MG cell invasion. This effect was not seen in U87MG cells transduced with control vector and treated with doxycycline. Lgl3SA had no effect on total cell numbers under the conditions used here (Figure 1B). To determine if this was an effect of Lgl3SA on the ability of cells to degrade Matrigel, or an effect on motility, we repeated this assay using Transwell membranes without Matrigel. As shown in Figure 1C, Lgl3SA reduced U87MG motility to a similar extent to that seen in the presence of Matrigel, indicating that Lgl3SA is primarily affecting motility. No effect on motility was seen when wild type Lgl was tested for effects on motility, consistent with our previous finding that Lgl is largely inactivated by phosphorylation downstream of *PTEN* loss in these cells (Figure 1D).

Although U87MG cells are motile and invasive in cell culture, they are not invasive *in vivo*. We therefore assayed the effects of Lgl3SA on the motility of primary glioblastoma cells isolated from patients under conditions that preserve their invasive properties and that enrich for glioblastoma cells with neural stem cell-like features (185). We have described the properties of these cells (designated PriGO8A cells) previously (185); their neural stem cell like characteristics include expression of the neural stem cell markers nestin and sox2, the ability to

Figure 1. Inhibition of U87MG cell invasion and motility by Lgl3SA. (A) Invasion of U87MG cells was assessed using Transwell chambers coated with Matrigel. U87MG cells were transduced with Tet activator and either empty vector (pLVX) or vector expressing Lgl3SA (pLVX-Lgl3SA). Cells were then treated with or without doxycycline for three days. Equal numbers of cells were then plated in Transwell plates and 24 h later the number of cells that had crossed the membrane was determined. Data are shown normalized to the untreated doxycycline controls and are the mean of three independent experiments each performed in triplicate. (B) Total viable cell counts for U87MG cells with inducible Lgl3SA, with and without treatment with doxycycline for three days. (C) To assess motility, U87MG cells transduced with Tet activator and vector expressing Lgl3SA were assayed as in A, except that Transwell membranes without Matrigel were used. Data are shown normalized to the untreated doxycycline controls and are the mean of three independent experiments each performed in triplicate. (D) U87MG cells were transduced with Tet activator and vector expressing wild type Lgl1 and assayed as in C. Data shown are from one independent experiment performed in triplicate, normalized to the mean value for untreated cells. Error bars show the mean ± standard deviation. * indicates a p value < 0.05.

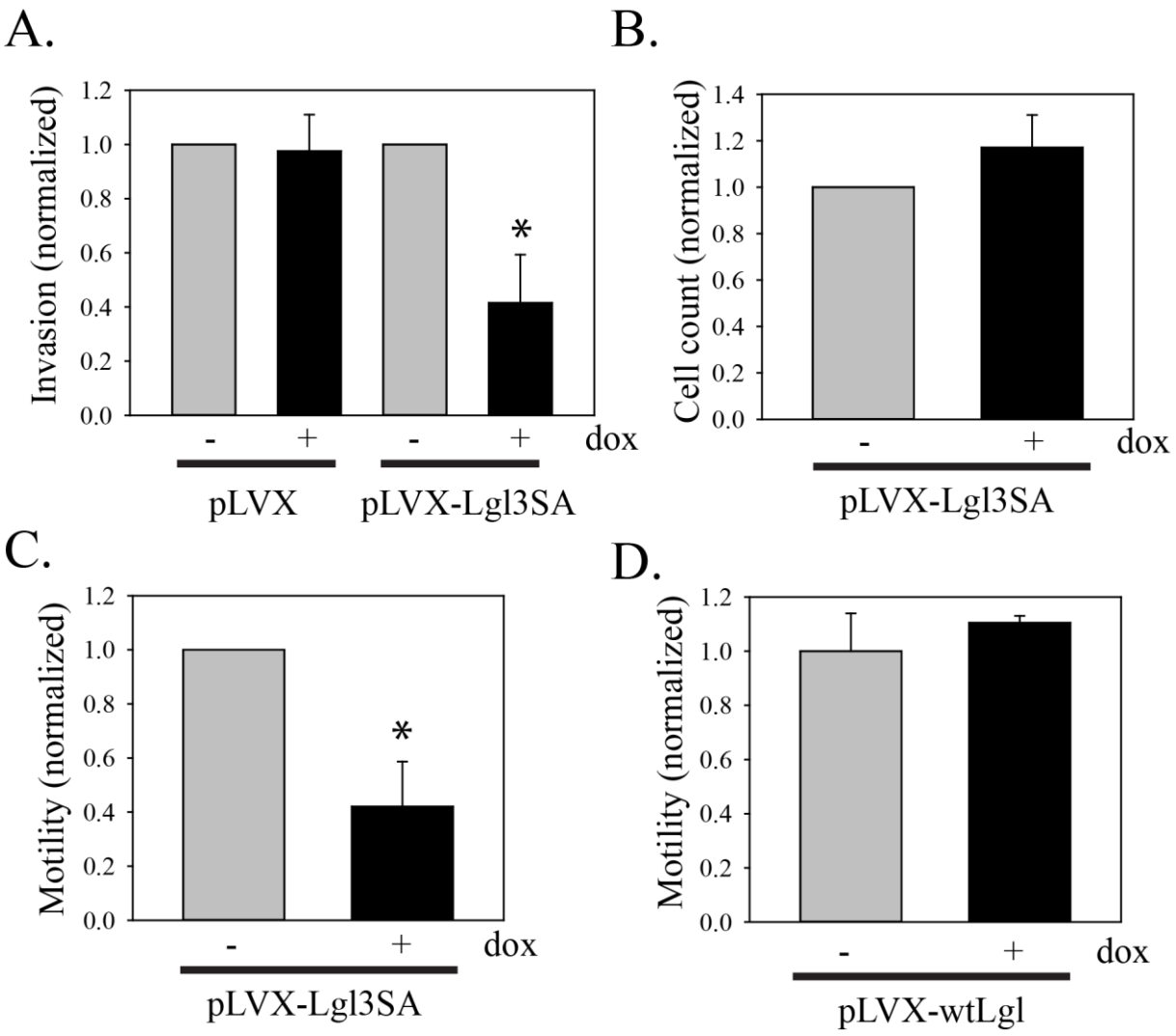
A.
Invasion (normalized)
1.2
1.0
0.8
0.6
0.4
0.2
0.0
*
- + - +
dox
pLVX
pLVX-Lgl3SA
B.
Cell count (normalized)
1.4
1.2
1.0
0.8
0.6
0.4
0.2
0.0
- +
dox
pLVX-Lgl3SA
C.
Motility (normalized)
1.2
1.0
0.8
0.6
0.4
0.2
0.0
*
- +
dox
pLVX-Lgl3SA
D.
Motility (normalized)
1.2
1.0
0.8
0.6
0.4
0.2
0.0
- +
dox
pLVX-wtLgl

undergo differentiation along multiple lineages, and the ability to form neurospheres when plated on plastic. In addition these cells form invasive disease in immunocompromised mice; this invasion closely resembles that seen in patients, with single cells invading along white matter tracts including the *corpus callosum* and the external capsule (see Figure 3C). These cells were transduced with lentiviral vectors for doxycycline-inducible expression of Lgl3SA as for U87MG cells (Figure 2A). Testing of these cells for motility in Transwell assays showed that expression of Lgl3SA caused a 65% decrease in their motility (Figure 2A). As seen with U87MG cells, expression of wild type Lgl at similar or higher levels than Lgl3SA had no effect on motility of PriGO8A cells (Figure S1A and B). Similar effects of Lgl3SA on motility were seen in cells isolated from a second patient (Figure 2B). Lgl3SA did not reduce total cell numbers under the conditions used, showing that this effect is not an artifact of effects on proliferation (data not shown). Neither wild type Lgl nor Lgl3SA affected the phosphorylation state of PKCι on Thr555, indicating that they were not suppressing global activation of PKCι (Figure S1C).

As a second method to assess motility that is independent of proliferation, we used time lapse videomicroscopy to monitor motility. PriGO8A cells are highly motile under the culture conditions used (Figure 2C; see also supplementary movies S1 and S2). Tracking of single cells using this method showed that expression of Lgl3SA reduced overall motility to a similar extent to that seen using the Transwell assay technique.

To assess effects of Lgl3SA on glioblastoma invasion *in vivo*, we made use of the doxycycline inducible system to turn on Lgl3SA expression after injection of cells into the cerebrum of immunocompromised mice (Figure 3A). The use of an inducible system avoids potential artifacts due to differences in the ability of genetically modified cells to survive the

Figure 2. Inhibition of PriGO cell motility by Lgl3SA. (A) PriGO8A cells were transduced with Tet activator and either empty vector (pLVX) or vector expressing Lgl3SA (pLVX-Lgl3SA). To confirm inducible expression, cells were treated with doxycycline for 24 h and then analyzed by Western blotting for expression of flag-tagged Lgl3SA and GAPDH as a loading control. The bar graph shows the results of motility assays. Cells were treated with or without 500 ng/ml doxycycline for three days. Equal numbers of cells were then plated in Transwell plates and 24 h later the number of cells that had crossed the membrane was determined. Data are shown normalized to the untreated doxycycline controls and are the mean of three independent experiments each performed in triplicate. (B) Cells from a second patient (PriGO9A) were transduced with tet activator plasmid and vector expressing Lgl3SA. Confirmation of inducible expression and effects on motility were determined as in A. (C) PriGO8A cells transduced with Tet activator and vector expressing Lgl3SA cells were plated in videomicroscopy dishes. After treatment with or without doxycycline for three days, cell movement was recorded by videomicroscopy for 20 h. Tracks of individual cells over 20 h are shown by the colored lines, with each cell assigned a different color. The bar graph shows the mean total distance traveled for ten randomly selected cells under each condition. For all bar graphs in this figure, error bars show the mean ± standard deviation. * indicates a p value < 0.05.

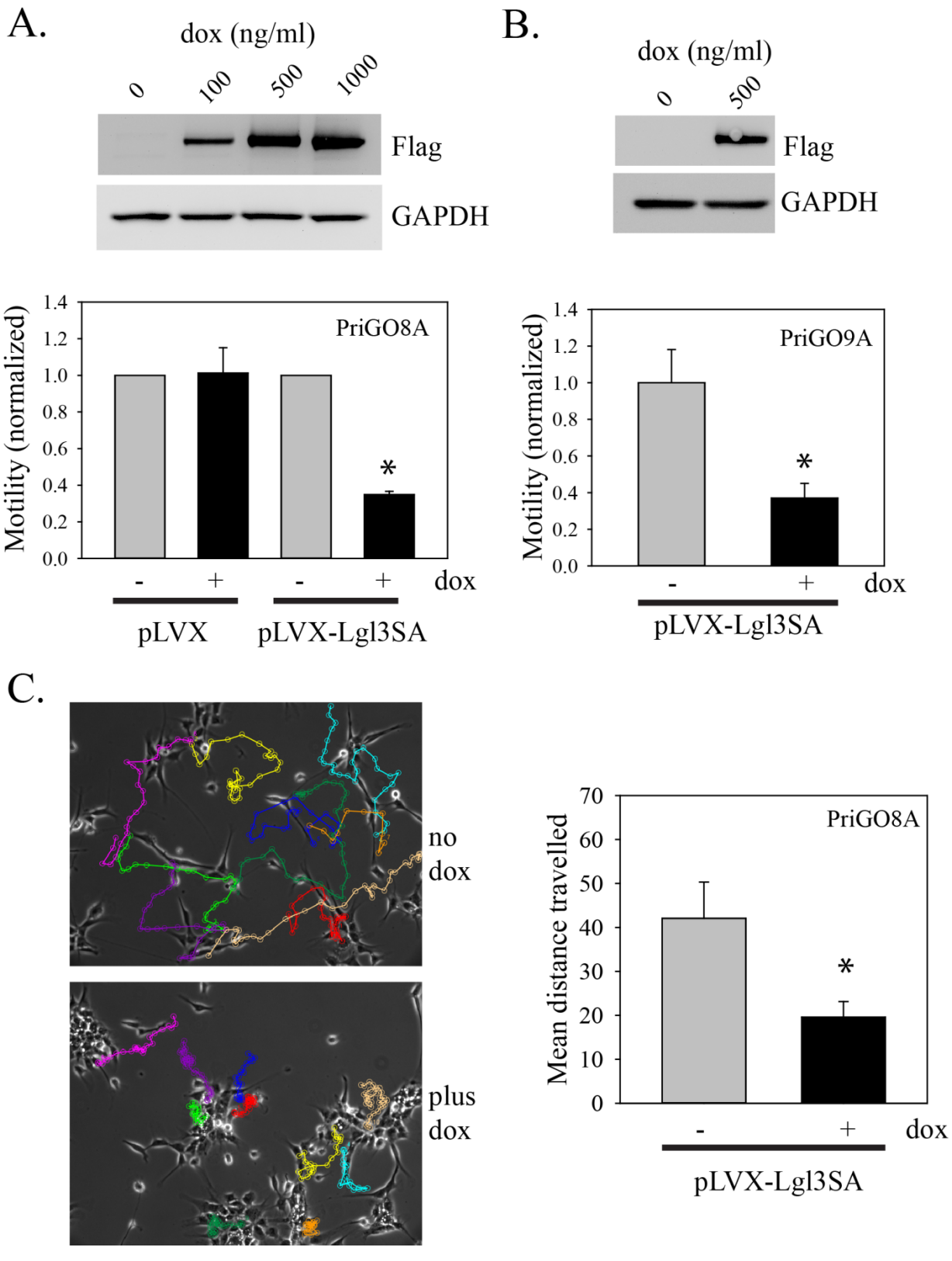
A.
dox (ng/ml)
0
100
500
1000
Flag
GAPDH
B.
dox (ng/ml)
0
500
Flag
GAPDH
Motility (normalized)
PriGO8A
PriGO9A
dox
pLVX
pLVX-Lgl3SA
C.
no dox
plus dox
Mean distance travelled
PriGO8A
pLVX-Lgl3SA

Figure 3. Induction of Lgl3SA in vivo. (A) Experimental design for *in vivo* invasion experiments. (B) PriGO8A cells were transduced with lentivirus expressing Tet activator and lentivirus expressing Flag-tagged Lgl3SA under control of the doxycycline-inducible P_{tight} promoter. Cells were then injected intracerebrally in SCID/beige mice. One month after injection of cells, mice were randomized to regular chow or chow with doxycycline. Mice were euthanized one month after randomization. Representative examples of STEM121 and Flag epitope immunohistochemistry performed on serial sections are shown for a mouse that was not treated with doxycycline (top panels) and one that was treated with doxycycline (bottom panels). (C) Brain section from a no doxycycline control mouse showing features of invasion in this model. NT, needle track; CC, *corpus callosum*; EC, external capsule.

A.

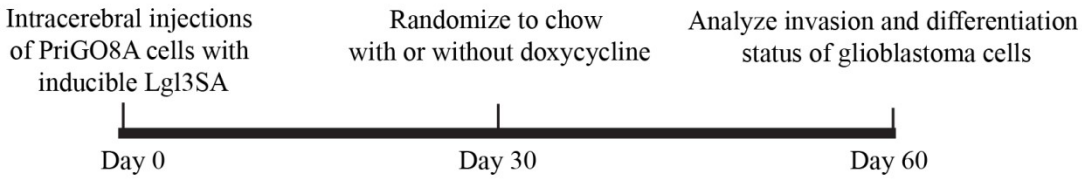
Intracerebral injections of PriGO8A cells with inducible Lgl3SA
Randomize to chow with or without doxycycline
Analyze invasion and differentiation status of glioblastoma cells
Day 0
Day 30
Day 60

B.

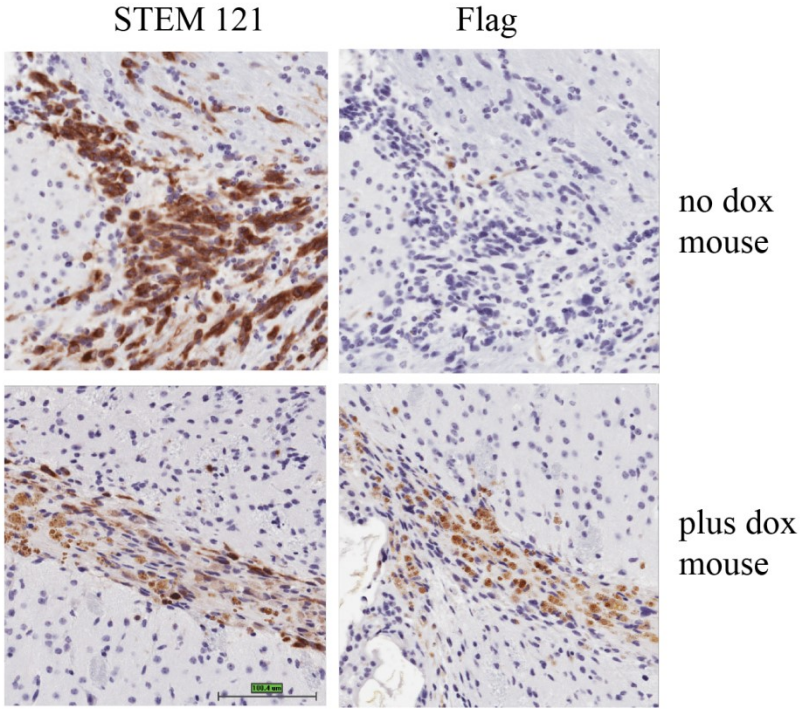
STEM 121
Flag
no dox mouse
plus dox mouse

C.

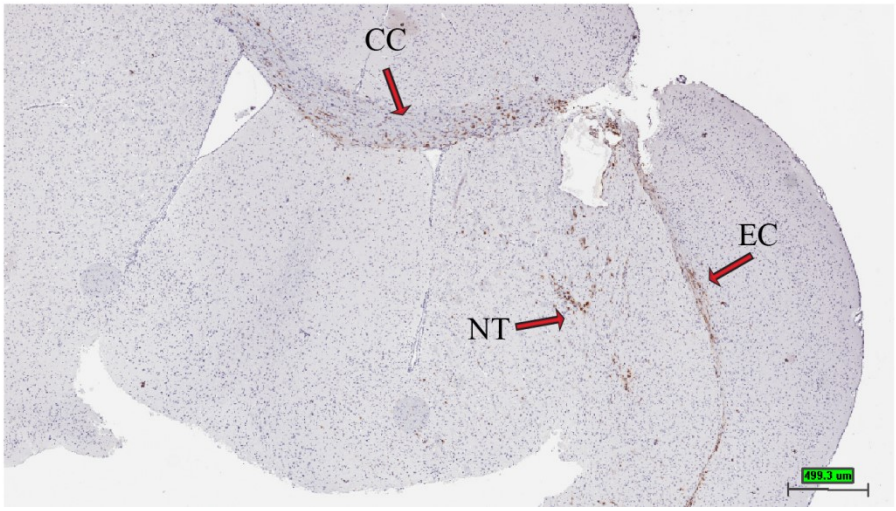
CC
EC
NT
499.3 um

transplant process into mice; in addition it gives an indication of the potential value of targeting this pathway in established disease. Cells were injected into mice and allowed to establish for a period of one month. Mice were then randomized to regular chow or chow containing doxycycline. One month later, mice brains were analyzed by immunohistochemistry. We first confirmed that Lgl3SA was being expressed in the mice fed chow with doxycycline. To detect injected cells, we used the antibody STEM121, which detects human cells regardless of their differentiation status (187). Expression of Lgl3SA was detected using antibody to its amino terminal Flag epitope. Figure 3B shows that effective induction of Lgl3SA expression was achieved in mice fed doxycycline chow. STEM121 staining of control mice also showed that cells had invaded extensively in the two month period of the experiment, with invasion along the corpus callosum into the uninjected hemisphere being evident (Figure 3C).

As an objective way to compare the extent of invasion in control and doxycycline-treated mice, total STEM121 positive pixel counts were recorded for the non-injected hemisphere. This was done for four sections from each mouse, taken approximately 20-40 μm apart. An example of this analysis is shown in Figure 4A. Results of the analyses of all the mice are shown in Figure 4B. In mice in which Lgl3SA was induced, there was an 89% reduction in the number of STEM121 positive pixels in the non-injected hemisphere of doxycycline-treated mice and this reduction was statistically significant (Figure 4B). As this could be an indirect effect of a reduction in overall cell numbers, we also recorded total numbers of positive pixels in both hemispheres; these were reduced by 44% (Figure 4C). This difference was not statistically significant and is too small to explain the difference in invasion observed. As a control, we performed a separate experiment using PriGO8A cells transduced with tet activator alone. Mice

Figure 4. Induction of Lgl3SA reduces invasion in vivo. (A) Representative images from mice on regular chow or doxycycline chow, showing invasion into the non-injected hemisphere, primarily along the *corpus callosum*. The area of analysis is the non-injected hemisphere. Within this area, human cells, identified by STEM121 antibody, are shown pseudocoloured red and negative pixels are pseudocoloured blue. (B) Bar graph showing the extent of invasion *(i.e.* positive staining for STEM121 in the uninjected hemisphere). Data are from three mice per group, with four sections analyzed per mouse. (C) Bar graph showing total numbers of STEM121 positive pixels in both hemispheres in mice from the regular and doxycycline chow mice. (D) As a control, mice were injected with PriGO8A cells transduced with Tet activator lentiviral vector only. One month later mice were randomized to chow with or without doxycycline. After one more month, mice were analyzed for invasion of PriGO8A cells into the non-injected hemisphere as above. Data are from five mice per group, with three sections analyzed per mouse. (E) Bar graph showing STEM121 positive pixels in both hemispheres in mice from the regular and doxycycline chow mice from the experiment in D. Error bars show the mean ± standard deviation. * indicates a p value < 0.05.

A.

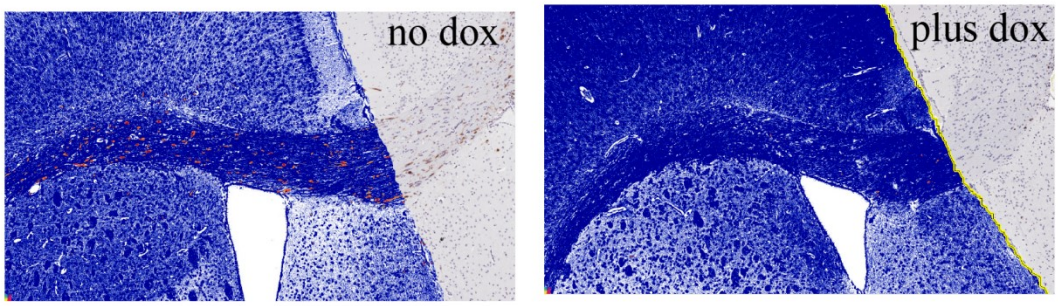
no dox
plus dox

B.

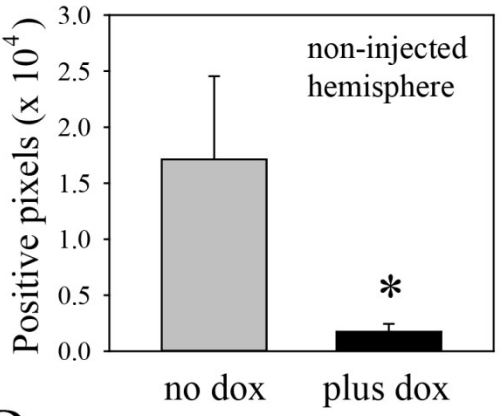
Positive pixels (x 10^4)
3.0
2.5
2.0
1.5
1.0
0.5
0.0
non-injected hemisphere
*
no dox
plus dox

C.

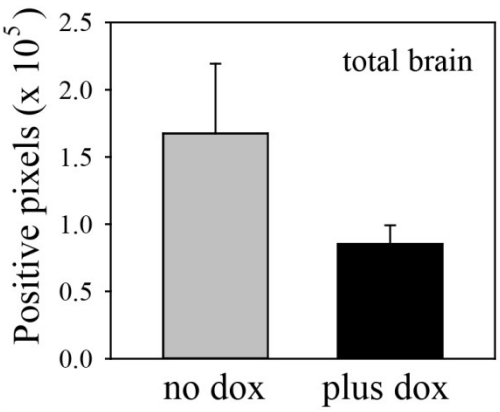
Positive pixels (x 10^5)
2.5
2.0
1.5
1.0
0.5
0.0
total brain
no dox
plus dox

D.

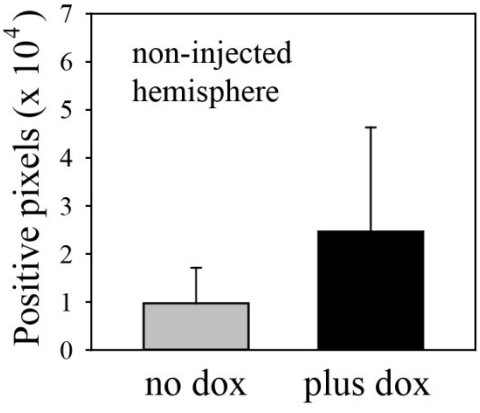
Positive pixels (x 10^4)
7
6
5
4
3
2
1
0
non-injected hemisphere
no dox
plus dox

E.

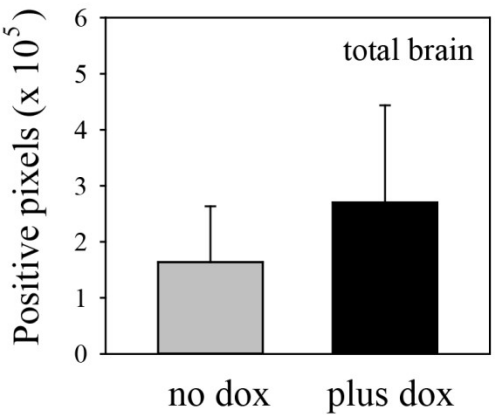
Positive pixels (x 10^5)
6
5
4
3
2
1
0
total brain
no dox
plus dox

were injected and randomized to chow with or without doxycycline as above. There was no decrease in invasion in the doxycycline treated animals in this model (Figure 4D and E).

As we had previously shown that expression of Lgl3SA induced differentiation of glioblastoma cells along the neuronal lineage in cell culture, we also used this experiment to determine if this phenomenon occurred *in vivo*. Our previous work made use of TUJ1 as an early marker of differentiation along the neuronal lineage. Analysis of an additional early neurogenesis marker, doublecortin (188), in cell culture supported this finding (Figure 5A and B). The rise in markers of neuronal differentiation was only seen in cells transduced with Lgl3SA, not wild type Lgl, again consistent with the idea that Lgl is inactivated by phosphorylation in these cells (Figure 5A and B). The increase in TUJ1 was seen after seven and fourteen days of Lgl3SA induction, but not after one day of induction (Figure S1D). To assess differentiation *in vivo*, sections from the mouse experiment were analyzed by double immunofluorescent immunohistochemistry for STEM121 and TUJ1. Examples of this are shown in Figure 5C and in Figure S2. Figure 5D shows the data for all mice, with three different sections analyzed per mouse. Induction of Lgl3SA resulted in a 4.5 fold increase in the numbers of pixels that were double positive for STEM121 and TUJ1, showing that induction of Lgl3SA promotes differentiation along the neuronal lineage *in vivo*.

Figure 5. Induction of Lgl3SA promotes differentiation in vivo. (A and B) Analysis of TUJ1 (A) and doublecortin (B) expression in PriGO8A cells transduced with control empty lentiviral vector (EV), or lentiviral vectors expressing wild-type Lgl or Lgl3SA. Immunofluorescence for TUJ1 and doublecortin was performed on the indicated number of days after transduction and the percent of positive cells was counted. Data are the mean ± standard error from five randomly selected fields per condition. (C) Immunohistochemistry for STEM121/TUJ1 double positive cells. Each section was stained with STEM121 antibody (green: identifies human cells) and TUJ1 (red: identifies cells differentiated along the neuronal lineage in both human and mouse tissue). White areas show cells that are both STEM121 and TUJ1 positive. Representative images from one untreated and one doxycycline-treated mouse are shown. Larger versions of these images, along with additional images, are shown in Figure S2. (D) Bar graph showing the percent of STEM121 positive pixels that are also TUJ1 positive in mice under the two conditions. Data are from three mice per group, with three sections analyzed per mouse. Error bars show the mean ± standard deviation. * indicates a p value < 0.05.

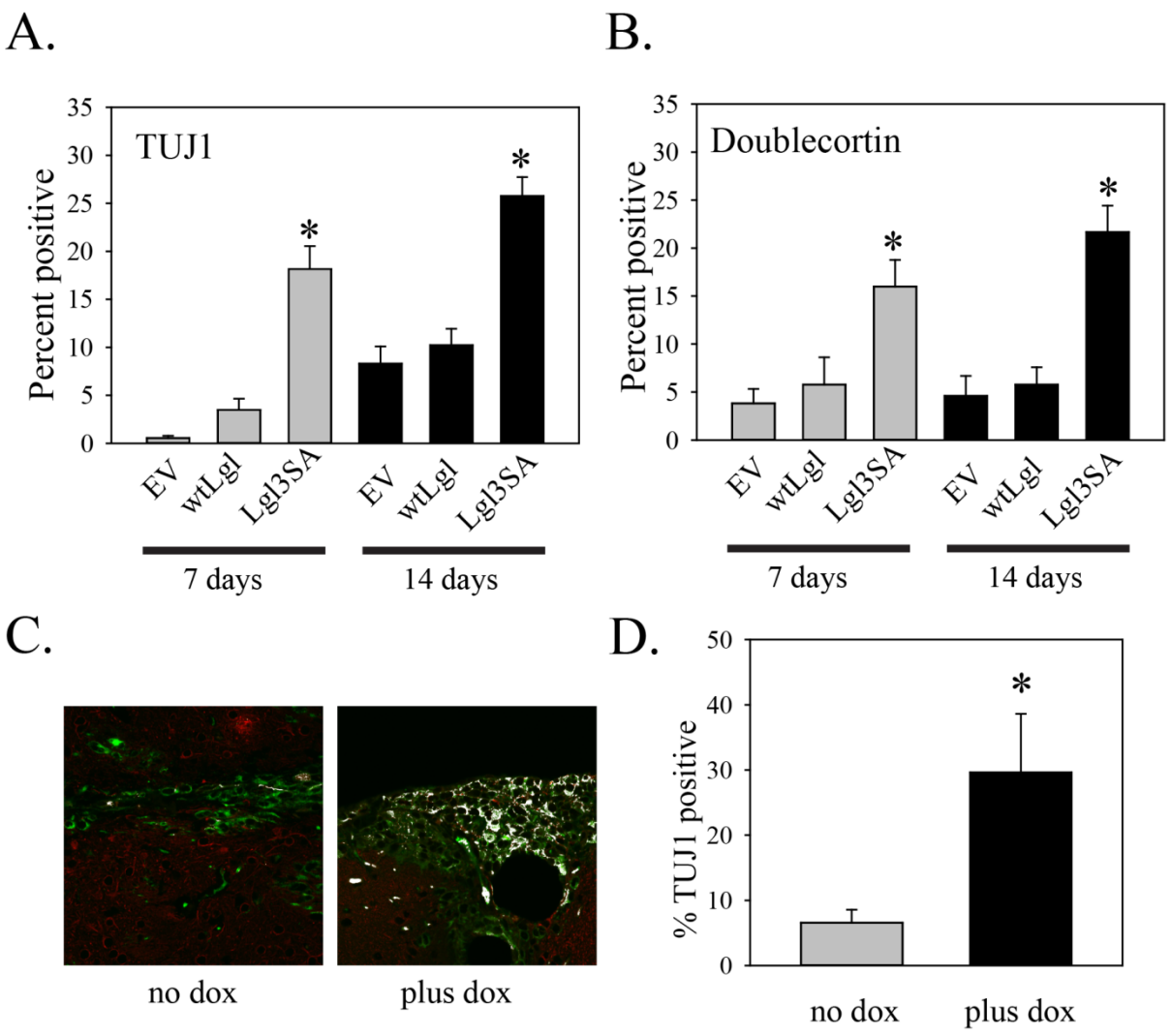
A.
TUJ1
Percent positive
35
30
25
20
15
10
5
0
*
*
EV
wtLgl
Lgl3SA
EV
wtLgl
Lgl3SA
7 days
14 days
B.
Doublecortin
Percent positive
35
30
25
20
15
10
5
0
*
*
EV
wtLgl
Lgl3SA
EV
wtLgl
Lgl3SA
7 days
14 days
C.
no dox
plus dox
D.
% TUJ1 positive
50
40
30
20
10
0
*
no dox
plus dox

Discussion

Drosophila lgl mutants showed two key changes with respect to neuroblast behavior: first, the neuroblast population expands as a consequence of its inability to differentiate; second the neuroblasts disseminate throughout the larval brain, while showing limited ability to metastasize to other sites. We show here that Lgl inactivation in human glioblastoma has similar consequences. A key difference between *Drosophila lgl* mutants and human glioblastoma is the mechanism of Lgl inactivation. In human glioblastoma, Lgl1 is not inactivated by mutation; instead it is inactivated by constitutive phosphorylation that is a consequence of *PTEN* loss. Consistent with this, we found that the effects of Lgl1 on both invasion and differentiation were only seen when a non-phosphorylatable, constitutively active version of Lgl1 was used. As partial or complete loss of *PTEN* occurs in 85% of glioblastomas, and *PTEN* loss is thought to be an early genetic event, this would appear to be a key pathway in gliomagenesis. The Strand laboratory has previously described a mechanism for Lgl inactivation in human cancer (primarily breast cancer) in which Lgl expression is repressed by the transcription factor Snail as an essential step in the epithelial to mesenchymal transition (189). This effect was restricted to Lgl2, with Snail having no effect on Lgl1 expression; as Lgl2 expression is absent in mammalian brain this pathway is unlikely to play a role in glioblastoma (98). In theory, the two pathways could act in concert in some cancer types to repress both Lgl1 and Lgl2 function.

As we see effects on both differentiation and invasion, one question is whether the effects on invasion are a consequence of differentiation. This interpretation is suggested by the well documented ability of neural stem cells to migrate through the brain in response to injury (190). In addition, it has been shown that glioblastoma cells treated with serum express differentiation markers and lose their invasive properties (29). However our data suggest that

Lgl1 primarily has a direct effect on glioblastoma cell motility that is independent of its effects on differentiation, because it is also seen in U87MG cells, which do not have the differentiation potential of the primary glioblastoma cells. This effect on motility may reflect a need to inactivate Lgl1 to allow the dynamic changes in the cell polarity required for coordinated cell movement (191). Biochemically, the repression of cell motility by Lgl1 may be mediated in part by its effects on cytoskeletal non-muscle myosin IIA (93, 120, 121). Although the effects of Lgl3SA appear to be primarily a direct consequence of the inhibition of motility, it is possible that differentiation contributes further to reduced invasion *in vivo*. This possibility is suggested by the fact that Lgl3SA effects on invasion *in vivo* (assessed after one month of Lgl3SA induction) are larger than those seen *in vitro*. We also see a trend towards a reduction in total cell numbers *in vivo*. As this is not seen in short term *in vitro* experiments, this may also be a long term consequence of differentiation, with a concomitant reduction in proliferative potential. A current model depicts cancer cells as stochastically transitioning between differentiation states to reach a phenotypic equilibrium (including transitions from non stem-like to stem-like) (192). In the context of this model, Lgl inactivation in glioblastoma would shift this equilibrium so that on average a greater number of cells occupy a less differentiated state. Further studies are required to determine whether this affects response to radiation and temozolomide therapy.

In summary, our data support a novel mechanism for gliomagenesis, in which loss of *PTEN* leads to inactivation of a second tumor suppressor, Lgl1, which in turn promotes invasion while repressing differentiation. Lgl1 inactivation is due to phosphorylation by PKCι, which is activated by *PTEN* loss. Our findings, along with recent data showing a lack of toxicity for neuron-specific PKCι knockouts in mice (193), support further study of PKCι as a therapeutic target for glioblastoma.

Methods

Antibodies: The following antibodies were used: FlagM2 mouse monoclonal (Sigma-Aldrich, Oakville, ON, Canada); Stem121 mouse monoclonal (Stemcells Inc., Newark, CA, USA); TUJ1 rabbit monoclonal antibody (Covance, Princeton, NJ, USA); doublecortin rabbit polyclonal antibody (Cell Signaling Technology, Danvers, MA, USA). PKCι mouse monoclonal antibody was from BD Transduction Laboratories (Mississauga, ON, Canada) and anti-Phospho (Thr555)-PKCι rabbit polyclonal antibody was from Invitrogen (Carlsbad, CA, USA).

Cell Culture: U87MG cells were grown in Dulbecco's Modified Eagle medium supplemented with 100 units/ml penicillin, 100 μg/ml streptomycin and 10% fetal bovine serum at 37°C and 5% CO_2. PriGO cells were described previously (185) and were grown on laminin-coated plates in Neurobasal A medium supplemented with B27, N2, EGF and FGF2 at 37°C in 5% O_2/CO_2. PriGO cells were used at passage < 20 to avoid potential loss of multipotency (194). Cells with inducible transgene expression were generated by transduction with lentiviral vector expressing Tet activator (Clontech, Mountain View, CA, USA) and selection in G418, followed by transduction with inducible lentiviral vectors made from pLVX-Tight-Puro (Clontech, Mountain View, CA, USA) and selection in puromycin, as described previously (185).

In vitro invasion and motility assays: U87MG or PriGO cells transduced with a doxycycline inducible empty vector, wildtype Lgl or LGL-3SA cDNA were incubated with or without doxycycline for three days (100ng/mL for U87MG and 500ng/mL for PriGO8A). Cells were then counted and re-plated in the top compartment of 8μm Transwell inserts with or without Matrigel (Corning BioCoat, Corning, NY, USA) and in parallel in a 24 well plate. For U87MG experiments 10% serum containing media was added to the bottom compartment. For PriGO cells laminin was added directly to the media in both the top and bottom compartments.

Doxycycline was added to both compartments at the corresponding doses. After 22-24 hour incubation, cells remaining in the top compartment were scraped off with a swab. Cells were fixed and stained using the Kwik Diff staining kit (ThermoElectron, Pittsburgh, PA, USA). Migrated cells were counted within 5 random fields at 40x magnification of 3 separate replicates and counts were normalized to the average cell count of each experimental condition from the parallel 24 well plate.

Videomicroscopy: PriGO8A cells transduced with doxycycline inducible Lgl3SA were plated on laminin coated Bioptechs delta-T dishes (Butler, PA, USA) in 1mL media. Cells were grown for three days at 37°C in 5% O_2/CO_2 in the presence or absence of 500ng/mL doxycycline in the media. Cells were maintained at 37°C in a sealed chamber for the duration of the image acquisition. Phase contrast images of the cells were taken at 5 min intervals for 17 h using the through 10x objective of the ZiessAxiovert 200 M microscope equipped with a AxioCamHRm CCD camera(Zeiss, Göttingen, Germany). Motility was quantified as the average distance per point every five frames of ten cells per condition using the MtrackJ plugin (195) in ImageJ software (National Institutes of Health, Bethesda, Maryland, USA).

Mouse model: Experiments were carried out in accordance with the recommendations of the Animal Care Committee at the University of Ottawa. PriGO8A cells were transduced with a doxycycline inducible lentiviral vector for Lgl3SA cDNA expression. 1 x 10^5 cells in 10µL sterile PBS were injected intrastriatally (right side of the skull approximately 0.5mm above the coronal suture and 2mm from the sagittal suture) into 4-6 week old Fox Chase SCID/beige mice (Charles River Laboratories, Wilmington. MA). Mice were kept under normal conditions for 4 weeks after which mice were randomized into two groups. One group was fed regular chow as

control and one group was fed nutrient matched doxycycline containing chow (Rodent Diet #2018 - 625 Doxycycline, Harlan, IN, USA).

Immunohistochemistry: Whole brains were harvested, and fixed in formalin for 48h. Brains were cut in the coronal plane at the site of injection and paraffin embedded. Antigen retrieval on 5µm sections was performed in citrate buffer (Vector, Burlingame, CA, USA) in a decloaking chamber (Biocare Medical, CA, USA). For colorimetric immunohistochemistry the DakoEnVision+ system HRP labeled polymer was used (Dako North America, Carpinteria, CA, USA) and sections were developed using DAB Peroxidase Substrate Kit (Vector, Burlingame, CA, USA) and counterstained with haematoxylin (Vector; Burlingame, CA, USA). For fluorescent immunohistochemistry double labeling experiments Alexa-flour conjugated secondary 488 and 555 antibodies were used (Life Technologies, Eugene, OR, USA). Colorimetric immunohistochemistry slides were scanned using the ScanScope CS2 (Aperio, CA, USA). Fluorescent immunohistochemistry images were acquired under 40x magnification using the Zeiss Observer Z1 microscope connected to a Zeiss LSM 510 Meta confocal unit (Zeiss, Göttingen, Germany). Positive pixel counts of immunohistochemistry slides were performed using Aperio ImageScope software (Version 11.2.0.780, Aperio, CA, USA). Fluorescent IHC double positive pixel counts of TUJ1:Stem121 were quantified using Zen 2008 software (Zeiss, Germany) Double positive pixels were highlighted and pseudocolored white using the "co-localization finder" plugin in ImageJ software (http:rsb.info.nih.gov/ij/plugins/colocalization-finder.html).

Statistical analyses: All statistical analyses were performed using SigmaPlot12 software. Comparisons between two groups were performed using two-tailed t-tests with a p value <0.05 considered significant.

Acknowledgements

This work was supported by a grant from the Canadian Institutes of Health Research (to IAJL) and funds from the Ottawa Regional Cancer Foundation and the Ottawa Hospital Foundation (to IAJL). IAJL is also supported by the J. Adrien and Eileen Leger Chair in Cancer Research at the Ottawa Hospital Research Institute.

Figure S1: (A) PriGO8A cells were transduced with Tet activator and vector expressing wild type Lgl (pLVX-wtLgl). Cells were treated with or without 500 ng/ml doxycycline for three days. Equal numbers of cells were then plated in Transwell plates and 24 h later the number of cells that had crossed the membrane was determined. Data are shown normalized to the untreated doxycycline controls and are the mean of three independent experiments each performed in triplicate. (B) Comparison of inducible expression of wild type Lgl and Lgl3SA in PriGO8A cells. PriGO8A cells were transduced with Tet activator and either vector expressing wild type Lgl (pLVX-wtLgl or vector expressing Lgl3SA (pLVX-Lgl3SA). To confirm inducible expression, cells were treated with doxycycline for 48 h and then analyzed by Western blotting for expression of flag-tagged Lgl and Lgl3SA. GAPDH was used as a loading control. (C) Effects of Lgl expression on PKCι activation. PriGO8A cells were transduced with lentiviral vectors expressing either wild type Lgl or Lgl3SA. 24 h later cells were analyzed for effects on PKCι activation, as assessed by Western blotting with antibody to PKCι phosphorylated on Thr555 as well as total PKCι levels. (D) Analysis of TUJ1 expression in PriGO8A cells transduced with Tet activator and vector expressing Lgl3SA after 24 hours of doxycyline treatment. Immunofluorescence for TUJ1 was performed and the percent of positive cells was determined. Data are the mean ± standard error from five randomly selected fields per condition.

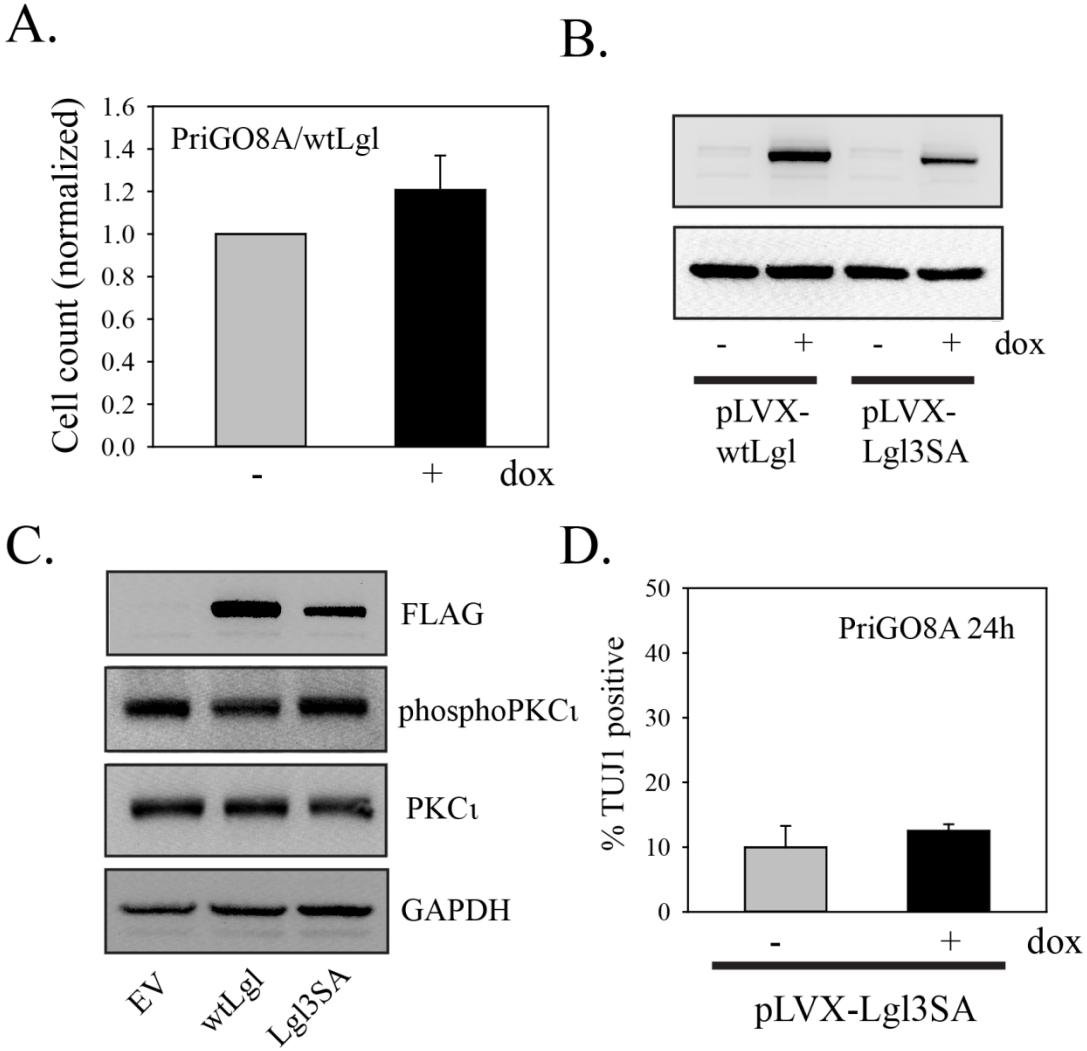
A.
B.
C.
D.
Cell count (normalized)
1.6
1.4
1.2
1.0
0.8
0.6
0.4
0.2
0.0
PriGO8A/wtLgl
-
+
dox
-
+
-
+
dox
pLVX-
wtLgl
pLVX-
Lgl3SA
FLAG
phosphoPKCι
PKCι
GAPDH
EV
wtLgl
Lgl3SA
% TUJ1 positive
50
40
30
20
10
0
PriGO8A 24h
-
+
dox
pLVX-Lgl3SA

Figure S2: The top two panels are enlarged versions of the images shown in Figure 5C. Four additional images, each from a different mouse (two on regular chow and two on doxycycline-containing chow), are also shown**.** Details of the analysis performed are described in Figure 5C.

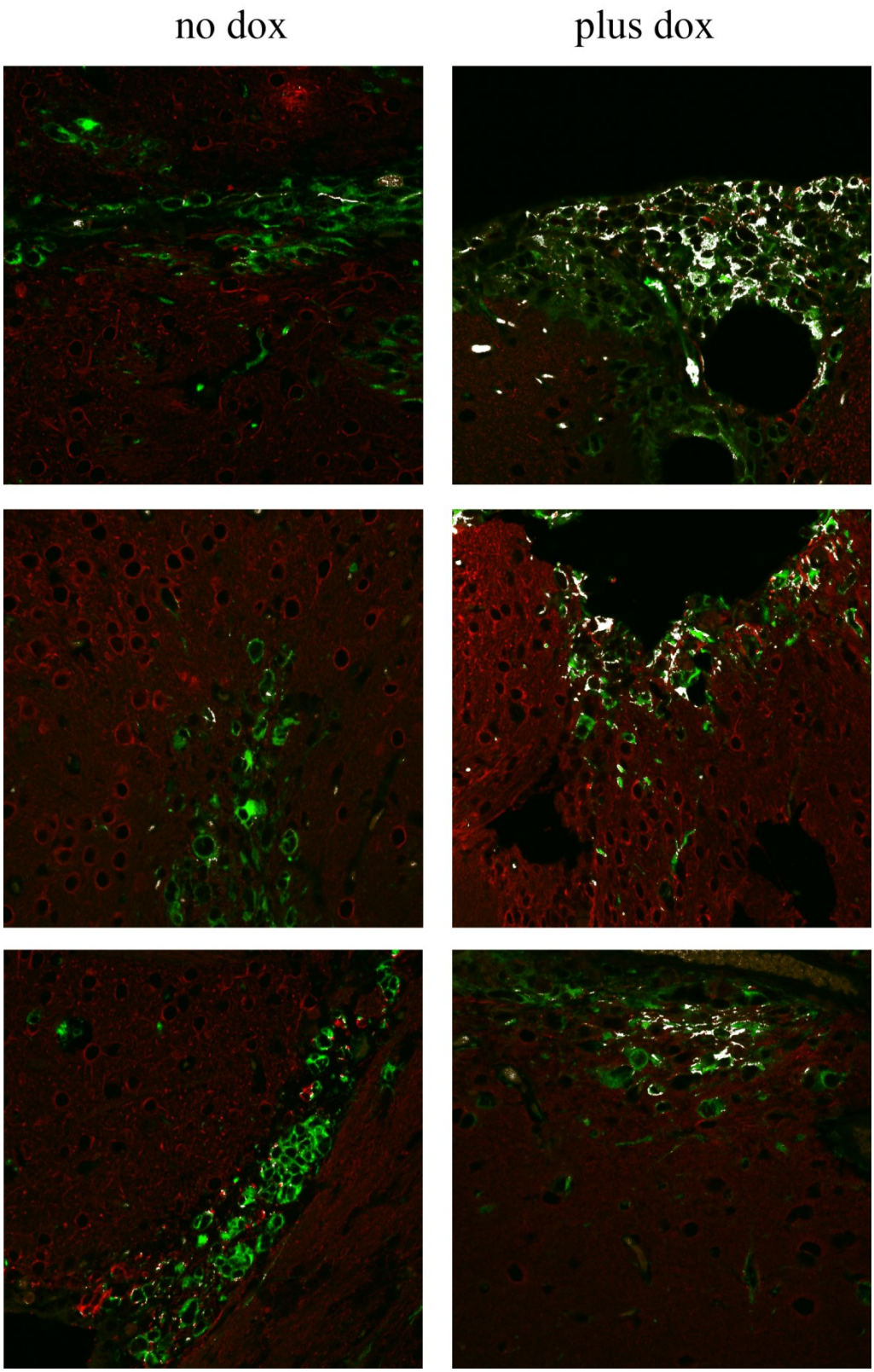
no dox
plus dox

4. PREX1 integrates G Protein-Coupled Receptor and Phosphoinositide 3-kinase signaling to promote glioblastoma invasion

Alexander Gont[1,2], Manijeh Daneshmand[1,3], John Woulfe[1,2,3], Sylvie J Lavictoire[1] and Ian A Lorimer[1,2,4].
[1]Centre for Cancer Therapeutics, Ottawa Hospital Research Institute, 501 Smyth Road, Ottawa, K1H 8L6, Canada
[2]Department of Biochemistry, Microbiology and Immunology, University of Ottawa, Ottawa, Ontario, Canada
[3]Department of Pathology and Laboratory Medicine, University of Ottawa, Ottawa, Ontario, Canada
[4] Department of Medicine, University of Ottawa, Ottawa, Ontario, Canada

Address correspondence to: Ian A. J. Lorimer, Ottawa Hospital Regional Cancer Centre, Centre for Cancer Therapeutics, 3rd floor, 501 Smyth Road, Ottawa, Ontario, Canada K1H 8L6. Phone (613) 737-7700 ext. 70332; Fax (613) 247-3524; E-mail ilorimer@ohri.ca
Keywords: Glioblastoma, glioma, PREX1, PI3-kinase, GPCR, invasion

Contribution of authors: The content of this manuscript was written by A. Gont with the help of Dr. I.A.J. Lorimer. All of the experiments presented in this manuscript are the work of A. Gont with the exception of Figure 3. Immunohistochemistry was performed by Dr. M. Daneshmand and quantification was performed by Drs. M. Daneshmand and J. Woulfe. Figure 3C was generated by Dr. I.A.J. Lorimer. Sylvie J Lavictoire constructed the Par6 expression vector used in Figure 7.

Manuscript prepared for submission

Abstract

A defining feature of the brain cancer glioblastoma is its highly invasive nature. The Rac subclass of Rho GTPases has been shown to promote invasive behaviour in glioblastoma. PREX1 was originally identified as a Rac activator PREX1 that is synergistically activated by binding the PI3-kinase product PIP3 and GPCR βγ subunits. This makes it of particular interest in glioblastoma as the PI3-kinase pathway is aberrantly activated by mutations in nearly all glioblastoma cases. PREX1 expression was detected in primary glioblastoma cells grown in cell culture and in orthotopic mouse xenografts. Analysis of a tissue microarray showed that PREX1 was expressed in most clinical cases of glioblastoma, whereas PREX1 expression was low or absent in normal brain tissue. PREX1 was studied in primary glioblastoma cells that recapitulate the molecular profile and invasive phenotype of the original clinical case. Knockdown of PREX1 with siRNA duplexes decreased cell invasion through coated transwell chambers and decreased motility in time-lapse videomicroscopy experiments, while exhibiting no effects on cell growth. To investigate the upstream activators of PREX1, gallein, a GPCR βγ subunit inhibitor, and BKM120, a type I PI3-kinase inhibitor were used. PREX1 required both PI3-kinase and GPCR βγ subunit activity for glioblastoma motility. Glioblastoma cell motility was also inhibited by haloperidol, suggesting that ligand-mediated GPCR activity may contribute to PREX1 function. In primary glioblastoma cells, Rac1 preferentially associated with Par6a leading to activation of PKCι and knockdown of PREX1 decreased activation of PKCι. Thus, PREX1 stimulates PKCι activity in glioblastoma likely by modulating the Rac1/Par6a/PKCι complex. In conclusion, our data demonstrates a novel context for *PTEN* loss and aberrant PI3-kinase signalling in glioblastoma whereby PREX1 integrates GPCR signalling via the βγ subunit and PI3-kinase pathway signalling to promote glioblastoma invasive behaviour.

Introduction:

Glioblastoma is a devastating brain tumour with a dismal prognosis. A defining feature of glioblastoma is its highly invasive nature within the brain. Glioblastoma cells efficiently migrate through the perivascular space and the brain parenchyma often following anatomical extracellular routes including along white matter tracts and blood vessels (22). Radical resections of the entire inflicted hemisphere in the early 1900s (17) were not curative and even sophisticated modern neurosurgery results in eventual recurrence centimeters from the resection site (18).

Multiple studies examining the invasive nature of glioblastoma have suggested an important role for the Rac subclass of Rho GTPases in glioblastoma cell lines (144, 145). These findings were consistent when studied in patient-derived primary glioblastoma cell lines (146). In its active form Rac is bound to GTP. The association with GTP is enhanced by the action of Rac-specific guanine-nucleotide exchange factors (GEFs). One such GEF, PREX1, is a 185 kDa protein that was originally identified as a Rac GEF specifically responsive to the phosphoinositide 3-kinase (PI3-kinase) pathway second messenger phosphatidylinositol 3,4,5 trisphosphate (PIP3) (152). This makes it of particular interest in glioblastoma, as the PI 3-kinase pathway is aberrantly activated in almost all glioblastomas through partial or complete loss of *PTEN*, amplification of growth factor receptors, or mutation of PI 3-kinase itself (39). Further research has shown that PREX1 is synergistically activated by PIP3 and G-protein coupled receptor $\beta\gamma$ subunits (152).

PREX1 is mainly expressed in mouse brain and neutrophils and has major physiological roles in promoting efficient neuroblast migration and proper neutrophil recruitment and function, where PREX1 is required for efficient stimulated migration and ROS production (153-155).

Given its clear role in promoting cell motility PREX1 has been studied in the context of multiple cancers. Overexpression of PREX1 has been linked to increased migration and metastases in melanoma, prostate and breast cancers. PREX1 is highly expressed in a large fraction of human breast cancer cell lines and tumours with some specificity to the luminal subtype. Additionally, high expression of PREX1 correlates with decreased survival in breast cancer patients (161, 162). PREX1 promotes breast cancer *in vitro* migration and *in vivo* metastases and tumour growth in a mouse model (161). In melanoma and prostate cancer PREX1 is similarly upregulated in metastatic tumours and functions to promote metastatic behaviour without affecting growth and survival suggesting some cell-type specific functions (159, 160). PREX1 has not been investigated in the context of brain cancer.

The goal of this study is to investigate the role of PREX1 in human glioblastoma. We show that PREX1 is overexpressed in many glioblastomas, and is enrichmed in the classical subtype. PREX1 is also expressed in glioblastoma cells isolated from patients, where it integrated signals from both PI3-kinase pathway and G protein-coupled receptors to drive invasion.

Results

PREX1 expression in primary glioblastoma cell cultures: PREX1 expression was examined by Western blotting in primary glioblastoma cultures. A single band of roughly 184,000 kDa was detected in each primary culture sample, similar to the reported 186,000 kDa for PREX1 isoform 1 (Figure 1A). Knockdown of PREX1 with two different PREX1-specific duplexes reduced the intensity of this band, indicating that the antibody was specific to PREX1 (Figure 1B). PREX1 expression varied across primary glioblastoma cell cultures from different patients, with the highest expression in PriGO7A cells and the lowest expression in PriGO17A cells (Figure 1A). Expression in primary glioblastoma cell cultures was considerably higher than in the U87MG human glioblastoma cell line, where a faint band was detected only with long exposures (Figure 1A). Levels of PREX1 have been reported to be regulated by promoter histone acetylation in prostate cancer (163) and by subtype-specific promoter methylation in breast cancer (164). To test whether such mechanisms could explain the relatively low expression of PREX1 in PriGO17A cells, these cells were treated with the histone deacetylase inhibitor Trichostatin A. This led to an increase in PREX1 levels in PriGO17A (Figure 1C), supporting a role for histone modifications in controlling PREX1 expression in glioblastoma.

To investigate the expression of PREX1 in primary glioblastoma cells within their physiological microenvironment, PriGO cells were grown as xenografts in SCID/Beige mice and analyzed for PREX1 expression by immunohistochemistry. The *in vivo* growth of PriGO8A cells has been described previously (196). They do not form a distinct tumor mass, but rather grow diffusely in the injected hemisphere with extensive invasion along white matter tracts into the uninjected hemisphere. PriGO9A cells showed a similar pattern of growth (Figure 2).

Figure 1: PREX1 expression in glioblastoma cells. (A) PREX1 expression in glioblastoma cell line U87MG and glioblastoma cells isolated from patients under serum-free conditions (PriGO 7A, 8A, 9A and 17A) was analyzed by Western blotting. GAPDH was used as a loading control. Tick marks annotations correspond to molecular weight markers (top down): 170, 130, 93, 70, 53, 41, 30 and 22kDa (B) PriGO8A cells were mock transfected or transfected with control siRNA duplex, or with two different siRNA duplexes targeting PREX1 (siPREX1a and siPREX1b). Two days after transfection cell lysates were collected and analyzed by Western blotting. (C) PriGO17A cells were treated with 100ng/mL histone deacetylase inhibitor Trichostatin A for 24 hours after which cell lysates were collected and analyzed by Western blotting.

A.

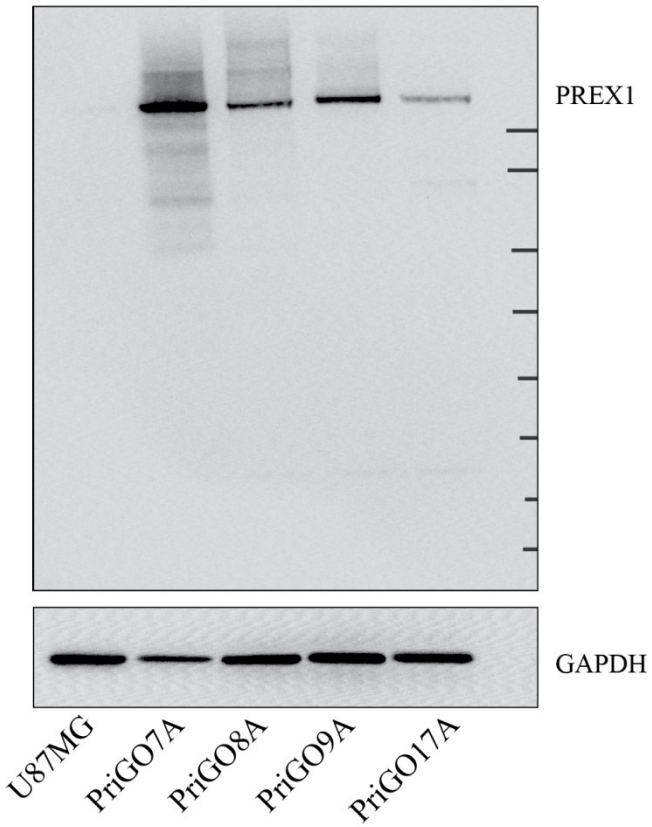
PREX1
GAPDH
U87MG
PriGO7A
PriGO8A
PriGO9A
PriGO17A

B.

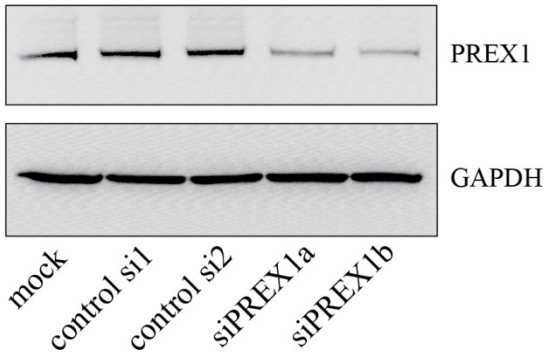
PREX1
GAPDH
mock
control si1
control si2
siPREX1a
siPREX1b

C.

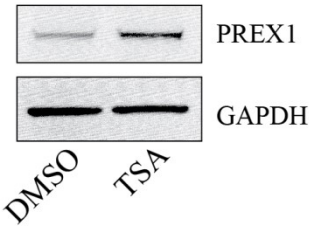
PREX1
GAPDH
DMSO
TSA

Figure 2: PREX1 expression in glioblastoma tumour xenografts. (A) PREX1 expression was assessed in PriGO8A tumour-bearing mice by immunohistochemistry. (B) PriGO9A cells were injected intracranial in SCID/beige mice and intracranial tumours were analysed for PREX1 expression by immunohistochemistry after 6 months of growth (right). SOX2 (left) marks cancer cells. (C) PriGO7A cells were injected intracranial in SCID/beige mice and intracranial tumours were analysed for PREX1 expression by immunohistochemistry after 6 months of growth. Stem121 was used to detect cancer cells. Cancer cell distribution and PREX1 expression is shown at the cortical subarachnoid space (bottom panels). Scale bars are 500µm and 200µm (panel A right image and panel C bottom images)

A.

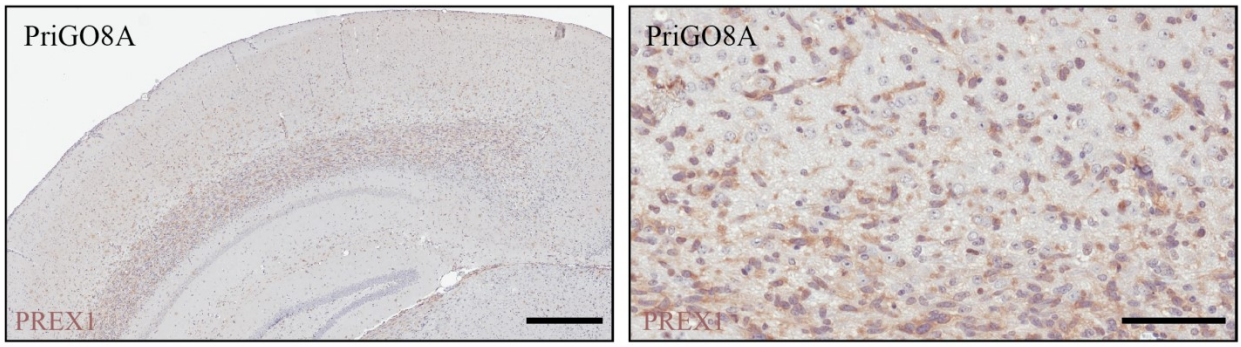
PriGO8A
PREX1
PriGO8A
PREX1

B.

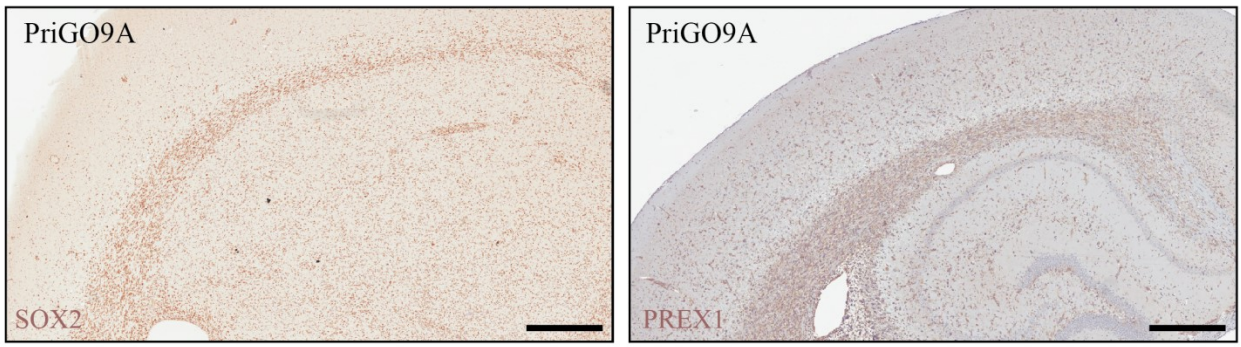
PriGO9A
SOX2
PriGO9A
PREX1

C.

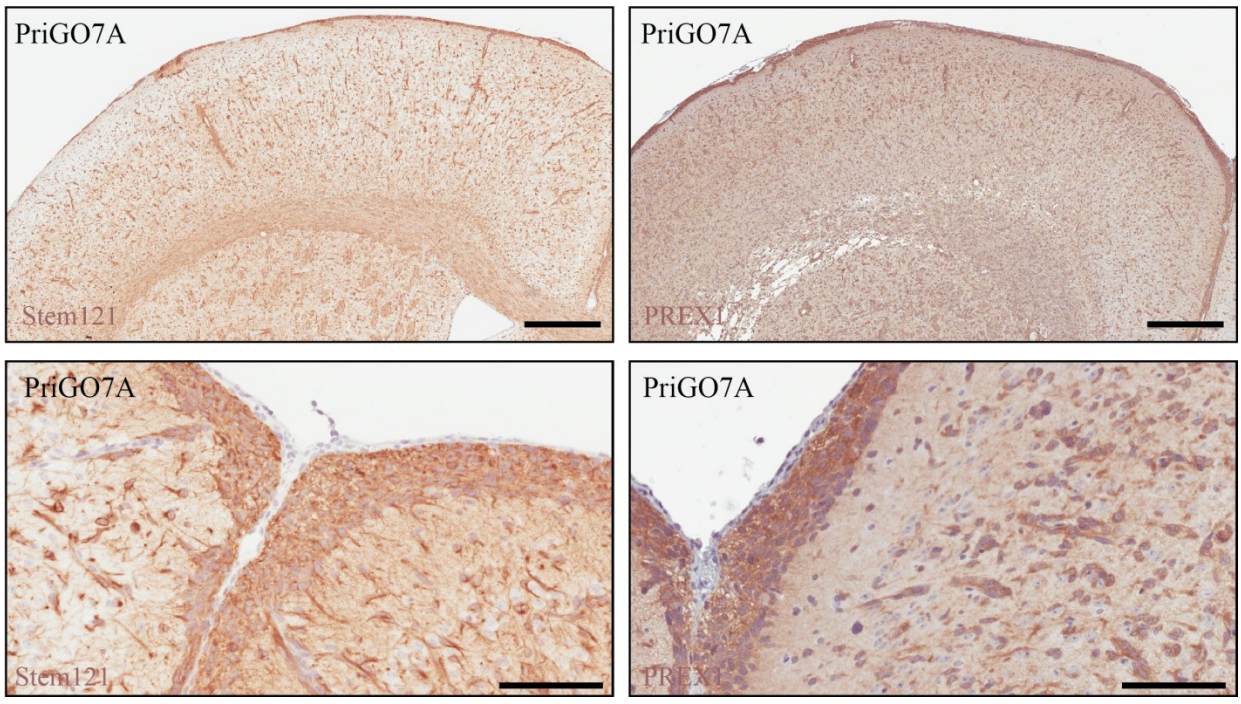
PriGO7A
Stem121
PriGO7A
PREX1
PriGO7A
Stem121
PriGO7A
PREX1

PriGO7A cells were also highly invasive, with a greater tendency to invade through the parenchyma and accumulate in the subpial space. Intracranial growths of primary glioblastoma cultures showed a uniform expression pattern of PREX1 with the intensity of signal proportional to the Western blot intensities across the PriGO7A, 8A and 9A cell cultures (Figure 2).

PREX1 expression in glioblastoma clinical samples: PREX1 protein expression and distribution within tumour tissue by was analysed by immunohistochemistry on a commercial tissue microarray of 35 individual cases (two cores per case) consisting of mostly high grade astrocytoma/glioblastoma and five cases of normal cerebral tissue (two cores per case). Each core was scored from 0 to 3 for both the overall intensity of the staining and the frequency of positive signal. Representative examples of staining are shown (Figure 3A). While in normal brain tissue PREX1 staining was absent or low, 91% of glioblastoma cases showed some level of PREX1 expression (Figure 3). As in the PriGO cells, expression intensity varied, with about one third of the cases showing high expression. Analysis of PREX1 mRNA levels in the TCGA database (38, 39) using cBioPortal (197) showed that PREX1 mRNA levels trended to be higher in the classical subtype (Figure 3). Consistent with this, PREX1 mRNA levels are also positively correlated with phosphoEGFR ($p=0.021$ and $p=0.022$ for Y1173 and Y1068 phosphorylation, respectively) and EGFR protein expression levels ($p=0.028$). This analysis also showed that PREX1 is almost never amplified or mutated in glioblastoma. The association of higher PREX1 levels in the classical subtype fits with the Western blot analysis shown in Figure 1A, as microarray expression analysis of PriGO7A, PriGO8A and PriGO9A cells showed that they are predominantly classical molecular subtype, while PriGO17A cells have more characteristics of the mesenchymal subtype (Kumar *et al*., *submitted for publication*).

Figure 3: PREX1 expression in glioblastoma clinical cases. (A) PREX1 was analysed by immunohistochemistry in a tissue microarray (USBioMax, GL805a) containing samples from thirty five glioblastoma patients, with two adjacent brain tissue cores and three normal brain tissue cores. Representative cores of normal brain tissue, low intensity staining, and high intensity staining are shown. (C) Intensity of staining (0 – negative, 1, 2 and 3) and frequency of positive staining (0 – no cancer cells positive, 1 – 0-33%, 2- 33-66% and 3 – 66%-100%) were scored independently by MD and JW with scoring discrepancies averaged. (B) PREX1 RNAseqV2 mRNA expression from the Cell 2013 TCGA dataset was analysed by cancer subtype using cBioPortal.

A.

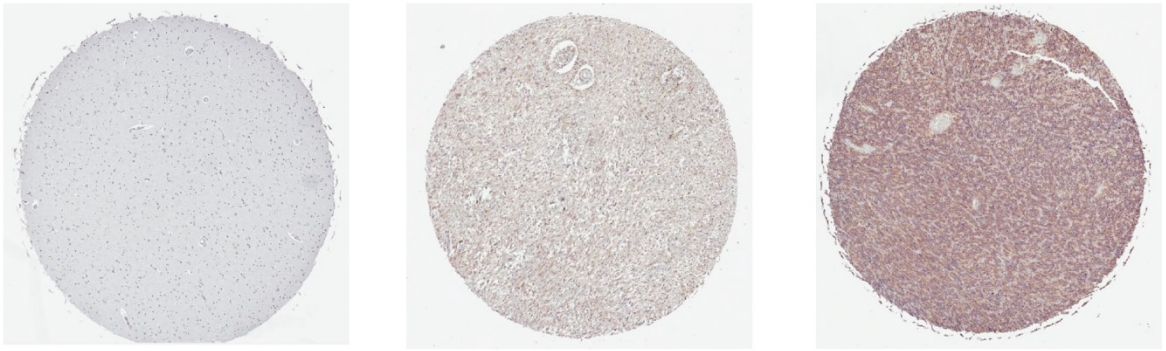
Normal brain
1 frequency, 1 intensity
3 frequency, 3 intensity

B.

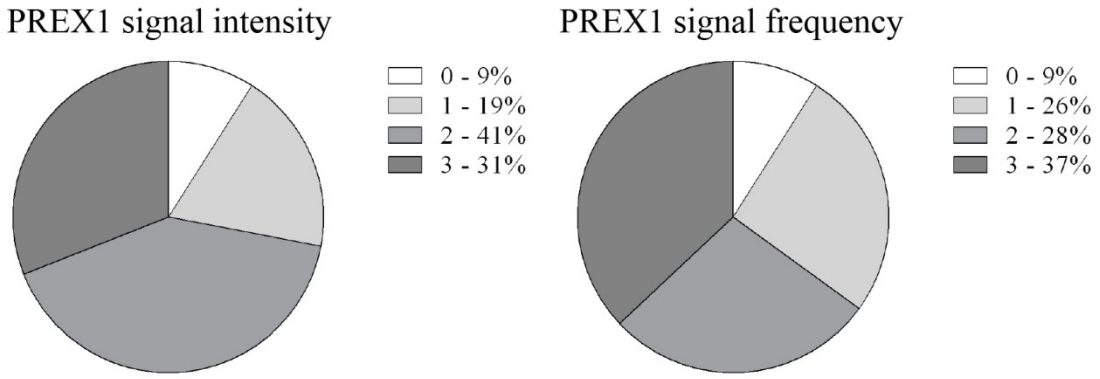
PREX1 signal intensity
0 - 9%
1 - 19%
2 - 41%
3 - 31%
PREX1 signal frequency
0 - 9%
1 - 26%
2 - 28%
3 - 37%

C.

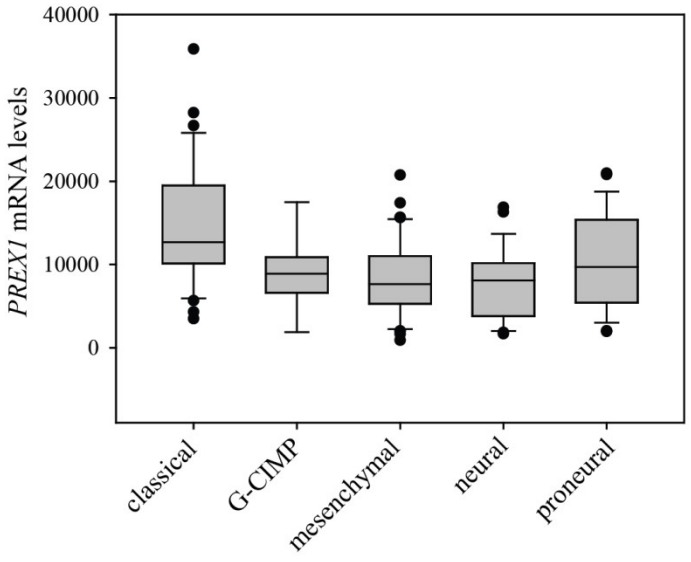
40000
30000
20000
10000
0
PREX1 mRNA levels
classical
G-CIMP
mesenchymal
neural
proneural

PREX1 in glioblastoma invasion and motility: In vitro invasion was assessed using Matrigel-coated Transwell chambers. PREX1 knockdown resulted in a significant reduction in the invasiveness of PriGO8A cells (Figure 4A). This was seen with two different RNA duplexes targeting PREX1 and knockdown of PREX1 did not significantly affect cell growth in PriGO8A cells over the time frame of the invasion assays (Figure 4B). A similar reduction in invasion was seen with knockdown of Rac1, indicating that PREX1 is the principal activator of Rac1 in these cells (Figure 4A). Loss of invasive behaviour can be a consequence of reduced ability to degrade cell matrix or a reduction in motility. Motility of PriGO8A cells was determined using time-lapse videomicroscopy and quantified as the average distance travelled by a cell per frame. Knockdown of PREX1 significantly reduced the motility of PriGO8A cells (Figure 4C). Similar to the results of the invasion assays, knockdown of Rac1 had a similar effect on motility as with knockdown of PREX1 (Figure 4C).

Upstream regulation of PREX1 activity in glioblastoma: G protein βγ subunits and PIP_3 binding synergistically activate PREX1 (153). To inhibit G protein βγ subunit binding and activation of PREX1, the compound gallein was used (198). Gallein binds purified Gβγ with a Kd of approximately 400 nM at a site that interferes with its interaction with downstream effectors (198). In addition, gallein has been shown to inhibit the Gβγ-dependent activation of Rac1 in neutrophils (198). Motility of PriGO8A cells was assessed by time-lapse videomicroscopy as in Figure 4. Gallein treatment resulted in a significant decrease in migration (Figure 5A). As one control for drug specificity, the same experiment was performed on U87MG cells that have very low, if any, PREX1 expression. Gallein did not significantly affect the motility of these cells (Figure 5B). BKM120, a pan-PI3K inhibitor (199), was used to inhibit PIP_3 levels.

Figure 4: PREX1 depletion inhibits glioblastoma invasion through decreased motility. (A) PREX1 levels were depleted in PriGO8A cells using siRNA as shown in figure 1B. *In vitro* invasion was assessed using Transwell chambers coated with Matrigel basement membrane matrix three days after siRNA-mediated knockdowns. Mock, siControl2, siControl3 and siPREX1a treatments were done in three independent replicates demonstrating consistent results. Shown are results from one experiment done in duplicate with extra siRNA treatment conditions. Mean +/- SEM; * $P<0.05$ (B) Three days after siRNA-mediated knockdowns live PriGO8A cell counts were quantified by trypan blue exclusion from three independent experiments. Mean +/- SD; * $P<0.05$. (C) Cell motility was assessed three days after siRNA-mediated knockdowns by time-lapse video microscopy. Cell movement per ten minute frame was quantified in ImageJ with the MTrackJ plug-in and displayed as the average of twenty cells per condition with each condition done in two to three independent experiments. * $P<0.05$.

A.

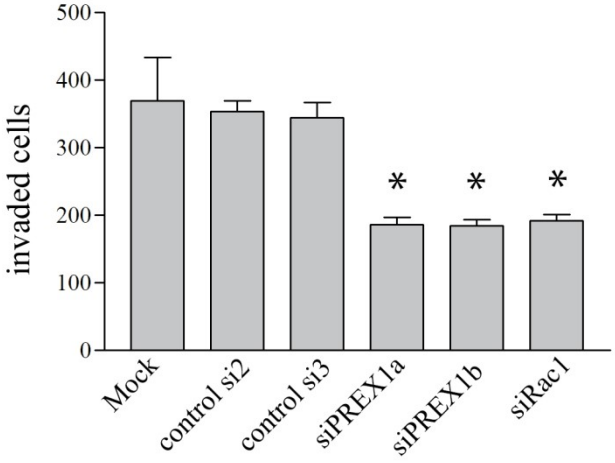
invaded cells
500
400
300
200
100
0
*
*
*
Mock
control si2
control si3
siPREX1a
siPREX1b
siRac1

B.

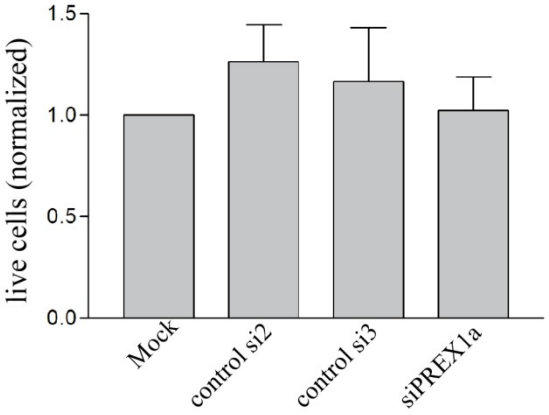
live cells (normalized)
1.5
1.0
0.5
0.0
Mock
control si2
control si3
siPREX1a

C.

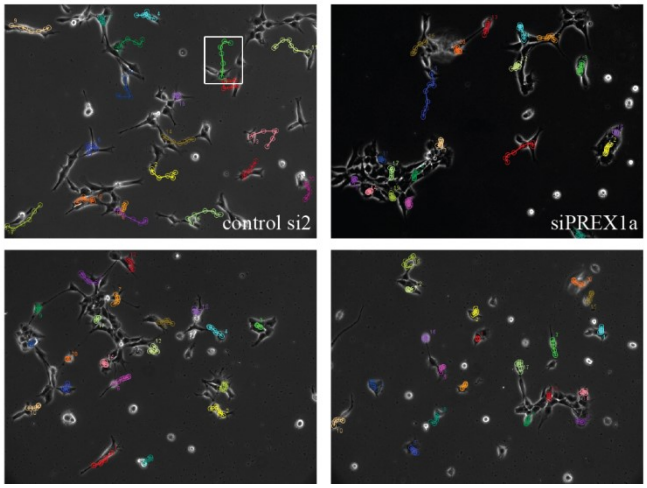
control si2
siPREX1a

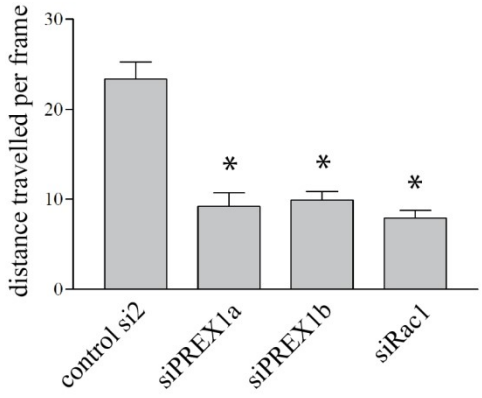
distance travelled per frame
30
20
10
0
*
*
*
control si2
siPREX1a
siPREX1b
siRac1

Figure 5: PI3-kinase and G-Protein coupled receptor inhibition decreases glioblastoma motility via Rac1. (A) PriGO8A cells were treated with 30μM gallein and/or 1μM BKM120 with DMSO used as solvent control. Cell motility was assessed 24 hours after treatment by time-lapse video microscopy as in figure 4. (B) U87MG cells were treated with 30μM gallein and 24h later cell motility was assessed by time-lapse video microscopy. (C) PriGO8A cells transduced with a PTEN cDNA doxycycline inducible lentiviral vector were treated with doxycycline at 1μg/mL for 24 hours in media containing $1/10^{th}$ of the EGF and FGF2 supplements. Cell motility was assessed by time-lapse video microscopy. Inducible expression of PTEN is shown in right panel by Western blot. (D) PriGO8A cells were treated with 10μM haloperidol and 24h later cell motility was assessed by time-lapse video microscopy. (E) PriGO8A cells were treated with a single dose of gallein, BKM120, haloperidol or DMSO at the concentrations used above. Relative cell amounts were assessed by crystal violet signal intensity (OD 570nm). Mean +/- SEM is shown; * $P<0.05$.

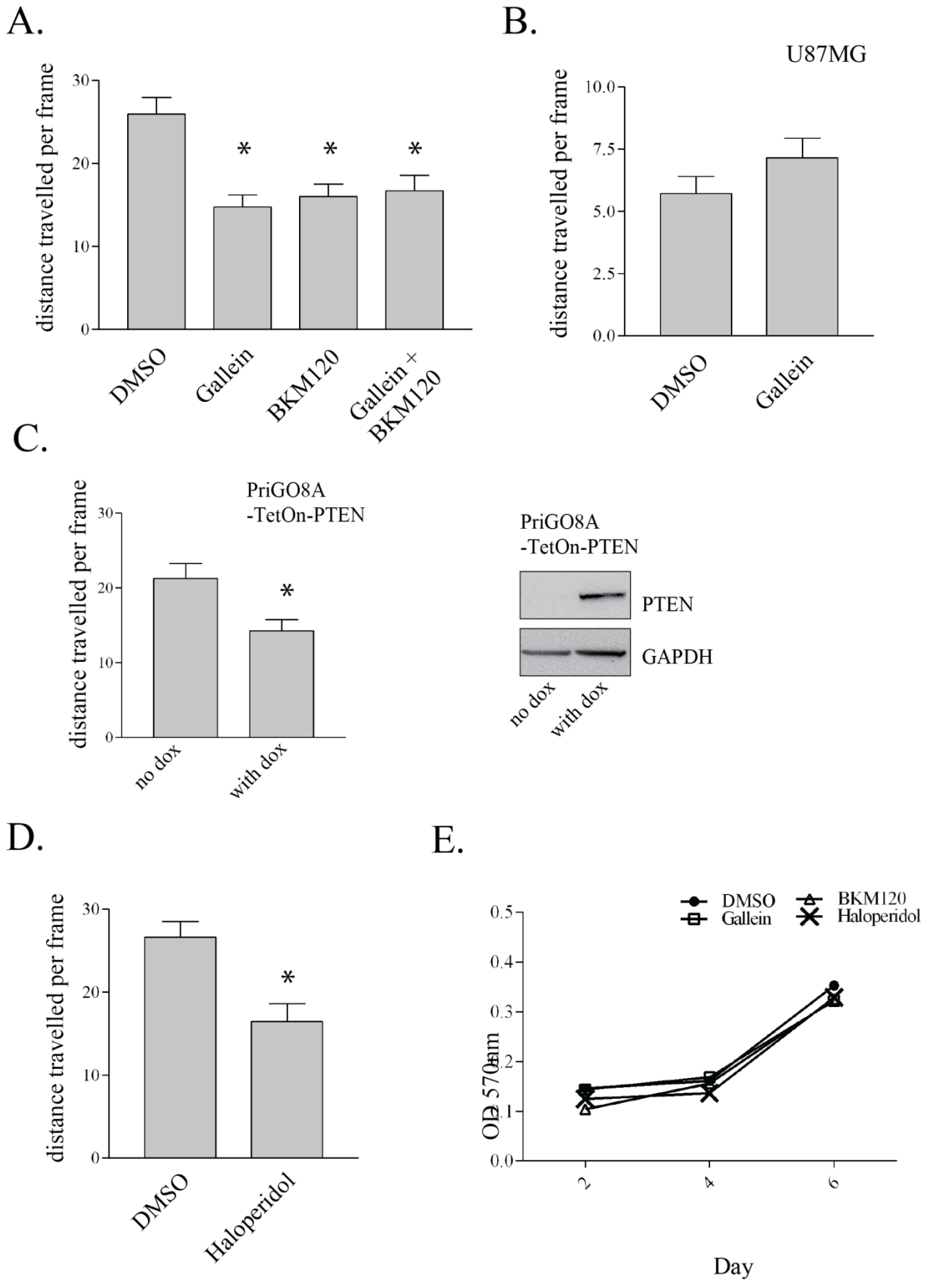
A.
distance travelled per frame
30
20
10
0
*
*
*
DMSO
Gallein
BKM120
Gallein + BKM120
B.
U87MG
distance travelled per frame
10.0
7.5
5.0
2.5
0.0
DMSO
Gallein
C.
PriGO8A
-TetOn-PTEN
distance travelled per frame
30
20
10
0
*
no dox
with dox
PriGO8A
-TetOn-PTEN
PTEN
GAPDH
no dox
with dox
D.
distance travelled per frame
30
20
10
0
*
DMSO
Haloperidol
E.
DMSO
Gallein
BKM120
Haloperidol
OD 570nm
0.5
0.4
0.3
0.2
0.1
0.0
2
4
6
Day

Treatment with BKM120 reduced cell motility to the same extent as gallein treatment (Figure 5A). A similar decrease in motility was observed when PIP_3 levels were repressed by expression of PTEN (Figure 5C). A combination of gallein and BKM120 also repressed motility, but this effect was not greater than the effect seen with either compound alone (Figure 5A). Gallein and BKM120 did not affect the growth of PriGO8A cells at the concentrations used (Figure 5E).

A recent report indicated a role for the dopamine receptor D2 (DRD2) in glioblastoma growth (200). As this G protein-coupled receptor could be a potential source of G βγ for PREX1 activation, the effect of DRD2 inhibition with haloperidol was tested. Treatment of PriGO8A cells with 10μM haloperidol resulted in a significant decrease in motility (Figure 5D). Haloperidol did not affect the growth of PriGO8A cells at the concentrations used (Figure 5E).

PREX1 function in glioblastoma cells from additional patients. To assess the generalizability of the above findings, PREX1 function was assessed in glioblastoma cells from two additional patients, PriGO9A and PriGO7A. As mentioned above, PriGO8A, PriGO9A and PriGO7A cells all cluster with the "classical" molecular subtype (Kumar *et al., submitted for publication*), which was the subtype identified here as having generally higher levels of PREX1. These cells do differ in their PTEN expression level, which could potentially influence their ability to activate PREX1. PriGO8A cells lack any detectable expression of PTEN. PriGO9A cells show a faint PTEN band on Western blots (Figure 6A). Immunofluorescence showed that this is due to a small subset of cells that express PTEN (not shown). Thus, PriGO9A cells are likely a mixed culture of cells that are *PTEN*-null and cells that have lost a copy of *PTEN*. Knockdown of PREX1 decreased both

Figure 6: Effect of PREX1 inhibition on PriGO7A and PriGO9A cells. (A) PTEN levels in glioblastoma cells and human cortical tissue lysate were analysed by Western blotting. GAPDH was used as a loading control. (B and E) *In vitro* invasion as in Figure 4A was performed on PriGO9A and PriGO7A taken as an average of two independent experiments done in duplicate. (C and F) Cell motility of PriGO9A and PriGO7A cell cultures was assessed by time-lapse video microscopy as in Figure 4C three days after PREX1 knockdown by siRNA. (D and G) Cell motility of PriGO9A and PriGO7A cell cultures was assessed by time-lapse video microscopy as in Figure 4C 24 hours after treatment. Mean +/- SEM is shown; * $P<0.05$.

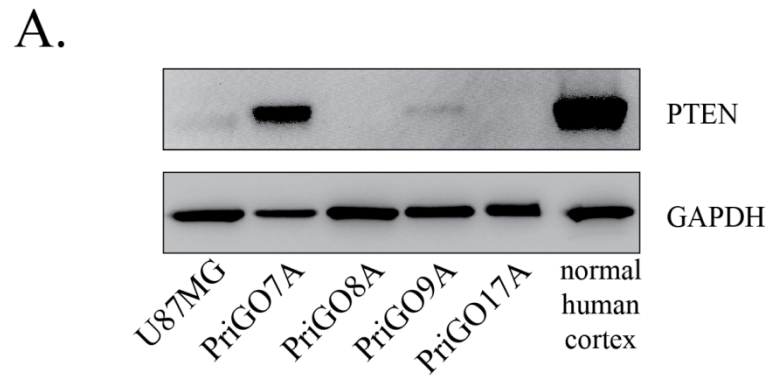
A.
PTEN
GAPDH
U87MG
PriGO7A
PriGO8A
PriGO9A
PriGO17A
normal human cortex

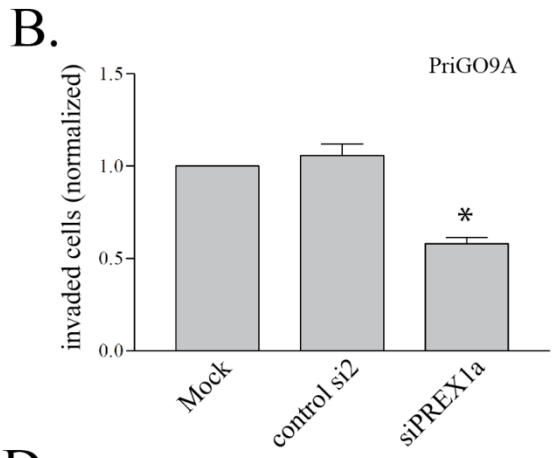
B.
PriGO9A
invaded cells (normalized)
1.5
1.0
0.5
0.0
*
Mock
control si2
siPREX1a

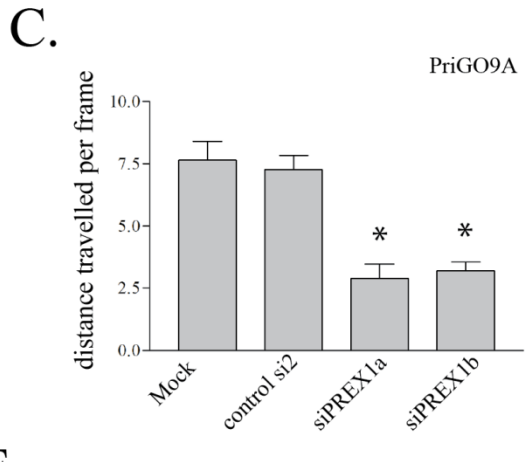
C.
PriGO9A
distance travelled per frame
10.0
7.5
5.0
2.5
0.0
*
*
Mock
control si2
siPREX1a
siPREX1b

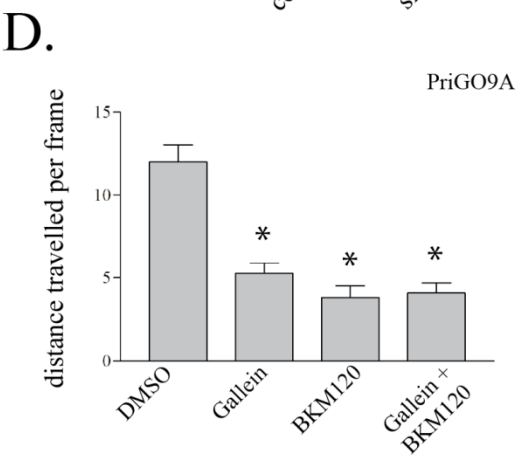
D.
PriGO9A
distance travelled per frame
15
10
5
0
*
*
*
DMSO
Gallein
BKM120
Gallein + BKM120

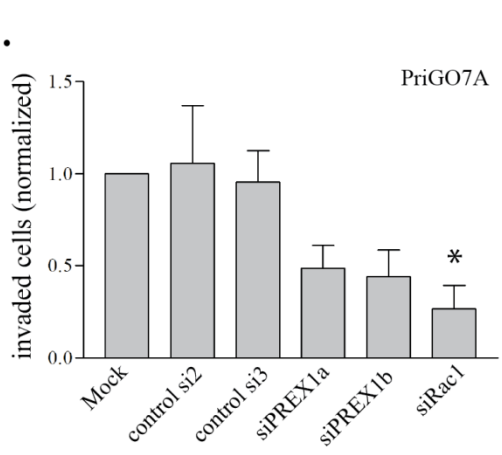
E.
PriGO7A
invaded cells (normalized)
1.5
1.0
0.5
0.0
*
Mock
control si2
control si3
siPREX1a
siPREX1b
siRac1

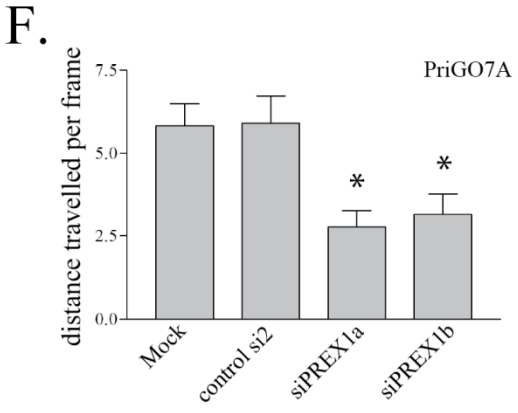
F.
PriGO7A
distance travelled per frame
7.5
5.0
2.5
0.0
*
*
Mock
control si2
siPREX1a
siPREX1b

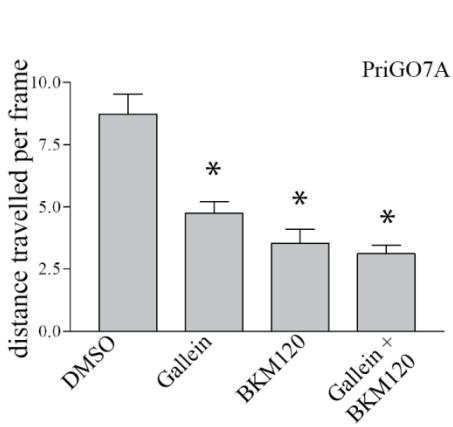
G.
PriGO7A
distance travelled per frame
10.0
7.5
5.0
2.5
0.0
*
*
*
DMSO
Gallein
BKM120
Gallein + BKM120

invasion and motility in PriGO9A cells, similar to what was seen in PriGO8A cells (Figure 6B and 6C). Blockade of PREX1 input signals with gallein and BKM120 also had similar effects in PriGO9A cells to those seen in PriGO8A cells (Figure 6E). Comparison of normal human brain tissue to PriGO7A lysates shows that this band is roughly half the intensity of that seen in normal brain (Figure 6A). Thus, PriGO7A cells likely have lost a copy of *PTEN*. Knockdown of PREX1 in these cells also inhibited invasion and motility, as did treatment with gallein and BKM120.

Signalling downstream of PREX1: Rac1 activation leads to the downstream activation of multiple kinase signalling pathways, either directly or indirectly (201). GTP-Rac directly binds to and activates PAK1, PAK2 and PAK3 kinases, which control multiple aspects of cell behaviour including F-actin polymerization (202). The activation of PAK1/2 by Rac can be monitored by the autophosphorylation of PAK1/2 on S144/S141 (203). Knockdown of PREX1, as well as treatment of cells with gallein, BKM120, and haloperidol all decreased PAK1/2 autophosphorylation (Figure 7A and 7B), demonstrating that PREX1 has a significant role in the activation of this pathway.

GTP-bound Cdc42 and Rac1 also have the potential to interact with the polarity protein Par6 to influence the activity of atypical PKC in polarity complexes (86, 87). Of the three Par6 isoforms, Par6A has the highest expression in normal brain and in glioblastoma, based on data in the Human Protein Atlas (204). A flag-tagged Par6A lentiviral expression vector (TFT-Par6) was constructed and transduced into PriGO8A and PriGO9A cells. Pull down experiments showed that Par6A associates with PKCι as expected and preferentially associates with Rac1 rather than

Figure 7: PREX1 signals through Rac1 to regulate PAK and PKCι activity. (A) Two days after PREX1 knockdown using siRNA phospho-PAK1/PAK2 levels were analysed by Western blotting and compared to total protein levels of PAK2. (B) PriGO8A cells were treated with DMSO, gallein, BMK120 and haloperidol as previously for 24 hours after which cell lysates were collected and phospho-PAK1/PAK2 levels were analysed by Western blotting. (C) PriGO8A (left) and PriGO9A (right) were transduced with triple-flag-tagged Par6A (TFT-Par6). Lysates were collected under non-denaturing conditions and immunoprecipitation was performed using anti-flag M2-conjugated magnetic beads. Bound proteins were eluted using triple-flag-peptide. (D to G) Phospho-PKCι (T555) levels were analysed by Western blot following expression of (D) TFT-Par6, (E and F) knockdown of Rac1 and (G) knockdown of PREX1.

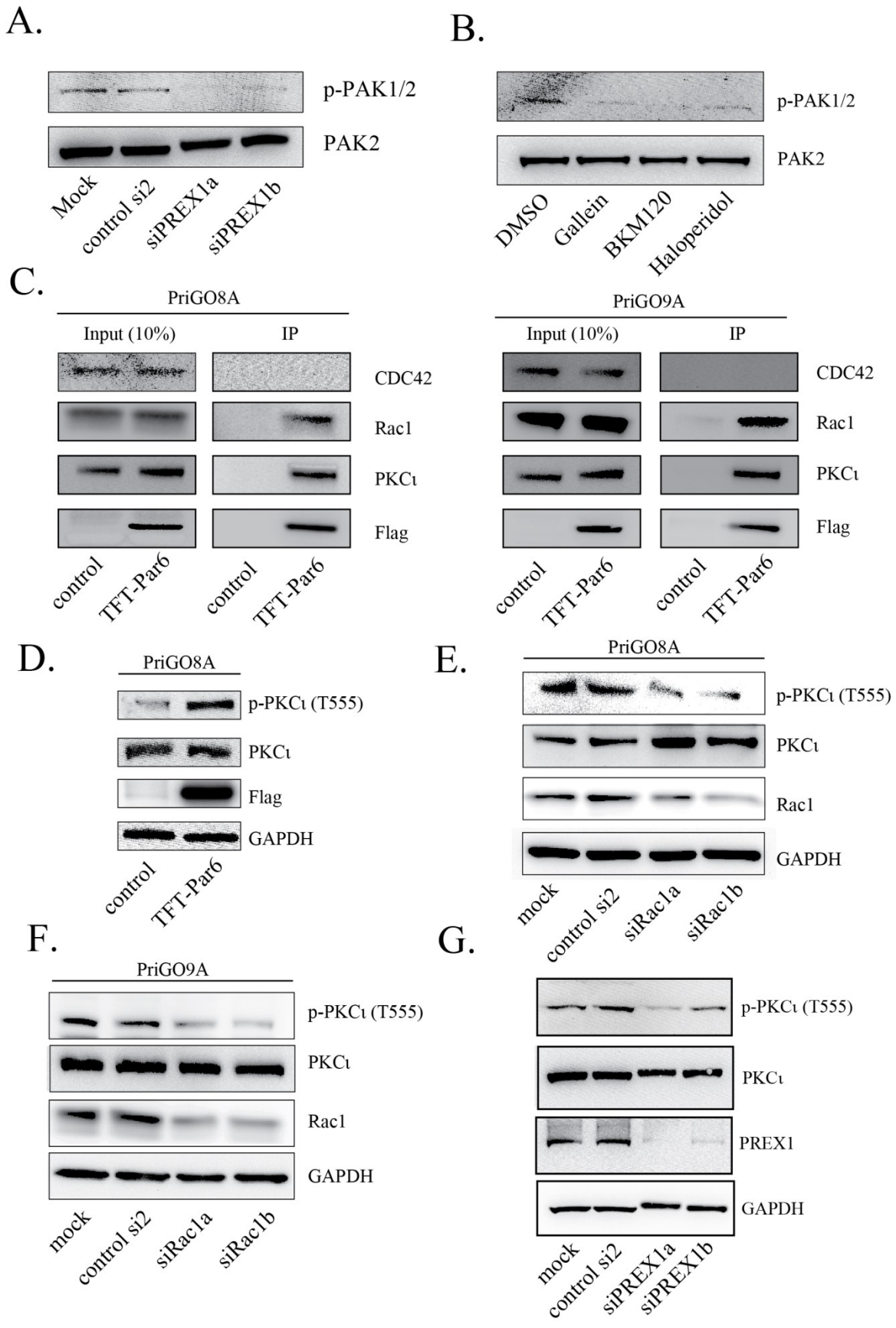
A.
p-PAK1/2
PAK2
Mock
control si2
siPREX1a
siPREX1b
B.
p-PAK1/2
PAK2
DMSO
Gallein
BKM120
Haloperidol
C.
PriGO8A
Input (10%)
IP
CDC42
Rac1
PKCι
Flag
control
TFT-Par6
control
TFT-Par6
PriGO9A
Input (10%)
IP
CDC42
Rac1
PKCι
Flag
control
TFT-Par6
control
TFT-Par6
D.
PriGO8A
p-PKCι (T555)
PKCι
Flag
GAPDH
control
TFT-Par6
E.
PriGO8A
p-PKCι (T555)
PKCι
Rac1
GAPDH
mock
control si2
siRac1a
siRac1b
F.
PriGO9A
p-PKCι (T555)
PKCι
Rac1
GAPDH
mock
control si2
siRac1a
siRac1b
G.
p-PKCι (T555)
PKCι
PREX1
GAPDH
mock
control si2
siPREX1a
siPREX1b

Cdc42, even though both are expressed in these cells (Figure 7C). Par6A itself functions as an activator of atypical PKC in these cells, as its overexpression increased phosphorylation of the atypical protein kinase C PKCι at Thr555 (Figure 7D). Phosphorylation at this site in the turn motif of PKCι stabilizes it in an active conformation (205). Knockdown of Rac1 in both PriGO8A and PriGO9A cells led to a reduction in PKCι Thr555 phosphorylation (Figure 7E). Knockdown of PREX1 also decreased in PKCι Thr555 phosphorylation (Figure 7F).

Discussion

PREX1 is expressed in glioblastoma: Our results demonstrate that PREX1 is commonly expressed at varying levels in glioblastoma clinical cases (Figure 3A, B) and in glioblastoma cell cultures isolated from clinical samples (Figure 1A). Data from the TCGA glioblastoma dataset demonstrates that PREX1 expression is elevated in the classical subtype of glioblastoma which correlates with elevated EGFR mRNA expression and pEGFR protein levels (Figure 3C). Microarray subtype analysis of PriGO cells complemented this observation: higher PREX1 expressing cells (PriGO 7A, 8A and 9A) group into the "classical" subtype and lower PREX1 expressing cells (PriGO17A) are a "mesenchymal" subtype (Kumar *et al., manuscript submitted*). The dramatic difference of PREX1 expression across cancer subtypes suggests that the mesenchymal subtype of glioblastoma might utilize different signalling pathways or molecules to promote migration and/ or Rac1 activation.

The variance of PREX1 expression in glioblastoma can also, in part, be explained by epigenetic regulation as treatment of the PriGO17A cells with a histone deacetylase inhibitor resulted in a modest increase of expression (Figure 1C). Studies in breast cancer support these findings since expression of PREX1 is enriched in the luminal subtype of breast cancer due to hypomethylation of its promoter region (163, 164).

Knockdown of PREX1 in multiple glioblastoma cell cultures from unique clinical cases resulted in decreased *in vitro* invasiveness (Figure 4A) and decreased motility (Figure 4C). These results support a pro-invasive role for PREX1, which has been previously reported in other cancers such as melanoma, breast, and prostate (159-162). Contrary to the role of PREX1 in cell proliferation in breast cancer (161, 162), knockdown of PREX1 in glioblastoma cell cultures did not decrease cell growth suggesting cell type specific functions (Figure 4B).

Estrogen receptor-α (ERα) is preferentially expressed in luminal subtypes of breast cancer, which is the subtype with the highest expression of PREX1 (161, 162, 206). Therefore, the isolated function of PREX1 on breast cancer proliferation may be explained by its potential to regulate ERα activity via Rac1/PAK1 (207-209).

PREX1 integrates GPCR βγ subunit signalling and PI3-kinase signalling to promote invasiveness in glioblastoma: Both the loss of *PTEN* and the direct activation of PI3-kinase have been shown to activate Rac1 to promote migration (57, 58). As expected, expression of PTEN in primary glioblastoma cell cultures resulted in decreased motility (Figure 5C). Mechanisms linking PI3-kinase pathway activation to Rac1 activation have been described but are either small in magnitude or not direct and involve intermediate transcriptional or post-translational events (152). Here, we demonstrate that PREX1 links PI3-kinase pathway activation to Rac1 activation promoting glioblastoma invasiveness (Figures 4 and 5).

PREX1 has previously been shown to be synergistically activated by binding of PIP3 and G-protein couple receptor βγ subunits (152). Individually, inhibition of Gβγ subunits using gallein and PIP3 using BKM120 resulted in decreased motility (Figure 5A) and Rac1 activity (Figure 7B) suggesting that inhibiting either activator is sufficient to inhibit PREX1. Combined inhibition did not have an additive effect on motility demonstrating the importance of the integration of both signalling pathways on PREX1 function (Figure 5A).

PREX1 function was assessed in glioblastoma cells from two additional patients from the classical subtype (PriGO9A and PriGO7A) with varying levels of PTEN expression (Figure 6). Similar effects on glioblastoma motility were observed as with the *PTEN*-null PriGO8A cells suggesting that the function of PREX1 in promoting glioblastoma invasion through increased motility can be generalized across multiple clinical samples, particularly those with the classical

molecular subtype expression patterns. This also demonstrates that the effect of PREX1 on motility is independent of whether cells have partially or fully compromised PTEN expression. This suggests that loss of one copy of *PTEN* is sufficient for activation of PREX1.

G-protein coupled neurotransmitter receptor signalling promotes glioblastoma motility: GPCRs have been shown to promote migration in many cancers but have been largely understudied in brain cancers (210). Over 90% of the known GPCRs are expressed in the brain demonstrating both the importance and diversity of GPCR-mediated signalling within the central nervous system (211). Neurotransmitter-induced GPCR signalling is likely sufficient to promote cellular motility. Ectopic expression of serotonin receptor 5HT7 in NIH3T3 fibroblasts promoted the activation of Rho GTPases RhoA and CDC42 but not Rac1 upon stimulation with a ligand (212). Additionally, treatment with serotonin in these cells promoted a change in morphology characteristic of motile cells (212). In the glioblastoma cell line U87MG, G-protein coupled receptor signalling pathways are important for glioblastoma cell line proliferation, particularly dopamine signalling through dopamine receptor D2 (200).

To investigate the role of GPCRs in glioblastoma motility we treated cells with haloperidol as a candidate approach based on *Li et al.,* 2014 (200). Haloperidol is a dopamine receptor antagonist, although at the concentration used in this study, there would also be inhibition of serotonin, histamine, acetylcholine receptor M1, and alpha adrenergic receptor signalling (213). Haloperidol treatment resulted in a decrease in motility (Figure 5D) and a corresponding decrease in Rac1 activity (Figure 7B). GPCRs signal through both α and βγ subunits (214). Our data, based on gallein inhibition, suggests that the βγ subunit is the important meditator of motility when activated in the presence of PREX1 (Figure 5A and Figure 7B).

PREX1 activates PAKs and PKCι via Rac1: Active, GTP-bound, Rac proteins promote motility by modulating actin cytoskeleton rearrangements though binding and activation of multiple kinases and proteins including the p21-activated kinase (PAK) family (215). We demonstrate that in glioblastoma, inhibition of the Rac-GEF PREX1 inhibits PAK activity as measured by autophosphorlyation levels of PAK1/PAK2 (Figure 7A). Treatment with gallein, BKM120, and haloperidol demonstrated a similar decrease of phospho-PAK levels attributing their effects on restricting glioblastoma motility to Rac1 activity (Figure 7B). Additionally, GTP-bound Cdc42 and Rac1 also have the potential to bind Par6 and influence the activity of atypical PKCs in polarity complexes (86, 87). Our data shows that Rac1 preferentially binds to Par6a to promote PKCι activity (Figure 7C-F). PREX1 is able to influence PKCι activity (Figure 7G), likely mediating the interaction of Rac1 with Par6. A study in lung cancer complements our finding that PKCι is activated through interaction with Par6; however, mechanisms influencing Par6/PKC binding were not demonstrated (216). PKCι has been previously shown to promote glioblastoma cell invasion (92, 93). Therefore, in glioblastoma cells, PREX1 promotes an invasive phenotype through activation of Rac1 and the resulting activation of PAK and PKCι.

In summary, our data demonstrates a novel context for *PTEN* loss and aberrant PI3-kinase signalling in glioblastoma whereby PREX1 integrates GPCR signalling via the βγ subunit and PI3-kinase pathway signalling to promote glioblastoma invasive behaviour.

Materials and methods

Antibodies and Reagents: PREX1 [D8O8D] rabbit monoclonal, PTEN [138G6] rabbit monoclonal, Phospho-PAK1 (Ser144)/ PAK2 (Ser141) rabbit polyclonal, PAK2 [3B5] mouse monoclonal were purchased from Cell signalling (Danvers, MA, USA). GAPDH [6C5] mouse monoclonal and CDC42 [M152] mouse monoclonal were purchased from Abcam (Cambridge, MA, USA). Phospho-PKCι (T555)/ PKCλ (T563) rabbit polyclonal was purchased from Invitrogen (Carlsbad, CA, USA) and PKCι mouse monoclonal from (BD Transduction Laboratories (Mississauga, ON, Canada). Rac1[23A8] mouse monoclonal, Anti-Flag M2 mouse monoclonal and Stem121 mouse monoclonal were purchased from Milipore (Temecula, CA, USA), Sigma-Aldrich (Oakville, ON, Canada) and Clontech (Mountain View, CA, USA), respectively.

Human brain, cerebral cortex Protein medley was purchased from Clontech (Mountain View, CA). The following inhibitors were used in the study: Gallein (Santa Cruz Biotechnology, CA, USA), BKM120 (Sigma-Aldrich, Oakville, ON, Canada), Haloperidol (Tocris Bioscience, Minneapolis, MN, USA) and Trichostatin A (Cayman chemical company, Ann Arbor, MI, USA).

Cell culture: Primary glioblastoma (PriGO) cultures were isolated following a protocol approved by the Ottawa Hospital Research Ethics Board as described previously (185) and were grown on laminin-coated plates in Neurobasal A medium supplemented with B27, N2, EGF and FGF2 at 37°C in 5% O_2/CO_2. Doxycycline inducible lentiviral vectors were used to express cDNA as described in (185).

Mouse intracranial xenografts: PriGO cell culture cells were established as xenografts in SCID/Beige mice (Charles River Laboratories, MA, USA) as previously (196) with $1x10^6$ cells in 10µL Neurobasal A medium injected by a Hamilton 700 series syringe (Reno, NV, USA) in a

stereotactic system intrastriatally. Mice were monitored for signs of morbidity or 6 months of intracranial growth prior to endpoint. Whole brains were harvested, formalin fixed and paraffin embedded.

RNAi mediated gene knockdown: RNA duplexes with the following sense strand sequences: Non-Targeting siRNA #2 and #3, siPrex1a (GAGAUGAGCUGCCCUGUGA), siPrex1b (GAAAGAAGAGUGUCAAAUC), siRac1a (UAAGGAGAUUGGUGCUGUA), siRac1b (UAAAGACACGAUCGAGAAA) were purchased from Dharmacon (Lafayette, CO, USA). RNA duplexes were incubated with PriGO cells at a concentration of 40nM in a mixture of Oligofectamine, Optimem and Neurobasal A medium. After 48 hour incubation, Neurobasal A media was replenished and cells were used for subsequent experiments.

In vitro invasion: After RNAi-mediated gene knockdown, PriGO cell cultures were counted and re-plated in the top compartment of 8μm Transwell inserts with Matrigel (Corning BioCoat, Corning, NY, USA) and in parallel in a 24 well plate with laminin directly added to the top and bottom compartments. 20-24 hours later, cells remaining in the top compartment were scraped off with a swab and invaded cells were fixed and stained using the Kwik Diff staining kit (ThermoElectron, Pittsburgh, PA, USA). Migrated cells were counted within 5 random fields at 40x magnification.

Cell counts: Cell counts following siRNA knockdowns were analyzed using the Invitrogen Countess instrument. Cell counts following inhibitor treatment were determined by crystal violet stain intensity at 570nm using the Multiskan Ascent plate reader with the Ascent Software program.

Videomicroscopy: Cells were directly plated on laminin coated Bioptechs delta-T dishes (Butler, PA, USA) in 1mL media. During image acquisition cells were maintained in sealed chambers at

37 degrees. Phase-contrast images were taken at 10 minute intervals for 1-1.3 hours using a 10x objective. Images were acquired using a ZiessAxiovert 200 M microscope equipped with a AxioCamHRm CCD camera (Zeiss, Göttingen, Germany). Motility was quantified using the MtrackJ plugin (217) in ImageJ software (National Institutes of Health, Bethesda, Maryland, USA) and scored as the average distance to point per cell per frame.

Immunohistochemistry: Glioblastoma tissue microarray consisting of 35 cores of brain tumor tissue (glioblastoma), 2 adjacent brain tissue and 3 normal brain tissue all as duplicate cores was purchased from US Biomax (GL805a F113, Rockville, MD, USA). Immunohistochemistry was done as described previously (196). Briefly, antigen retrieval was performed in citrate buffer (Vector, Burlingame, CA, USA) in a decloaking chamber (Biocare Medical, CA, USA). The DakoEnVision+ system HRP labeled polymer was used (Dako North America, Carpinteria, CA, USA) and sections were developed using DAB Peroxidase Substrate Kit (Vector, Burlingame, CA, USA) and counterstained with haematoxylin (Vector; Burlingame, CA, USA). Slides were digitized using the ScanScope CS2 (Aperio, CA, USA). The tissue microarray was scored independently by MD and JW and discrepancies were averaged. Signal intensity per core was scored as 0, 1, 2, or 3. Frequency of positive staining per core was scored as 0 – 0%, 1 – 0% to 33%, 2 – 33% to 66%, and 3 – 66% to 100% PREX1 positive cells over tumour cells.

Immunoprecipitation: PriGO cells transduced with triple-flag-tagged Par6 were scraped and collected in ice cold PBS buffer. Cells were then peletted and resuspended in 1 ml of lysis buffer (20 mM Tris-HCl, 150 mM NaCl, 1% Triton X-100, 20 mM NaF, 1 mM Na3VO4, 1mM glycerol-2-phosphate, 1 mM benzamidine, 1 mM β-mercaptoethanol, and 1 μg/ml each of leupeptin, pepstatin, and aprotinin at pH 7.5). Cells were passed once through a 27-gauge needle and centrifuged. Total protein amount was measured by BCA assay and equal amounts from the

two cell cultures were used. Cell lysates were incubated with anti-flag M2 magnetic beads (Sigma-Aldrich) for three hours with gentle rocking at 4°C. Beads were collected by magnetization and washed three times with lysis buffer. For elution, lysates were incubated with 200μg/mL triple flag peptide (Sigma-Aldrich) for three hours.

Statistical analyses: All statistical analyses were performed using SigmaPlot12 and Graphpad Prism software. Comparisons between two groups were performed using two-tailed t-tests with. Multiple group comparison to a single control was done using one-way ANOVA analysis with the Dunnett's Multiple Comparison post-hoc. Multiple group comparison was done using one-way ANOVA analysis with the Tukey's Multiple Comparison post-hoc. A p value less than 0.05 was considered significant.

Acknowledgements

This work was supported by a grant from the Canadian Institutes of Health Research (to IAJL) and funds from the Ottawa Regional Cancer Foundation and the Ottawa Hospital Foundation (to IAJL). IAJL is also supported by the J. Adrien and Eileen Leger Chair in Cancer Research at the Ottawa Hospital Research Institute. AG was supported by the Ontario Graduate Scholarship.

5. Discussion

In *Drosophila* loss of *Lgl* is sufficient to cause invasive neoplastic growth of brain tissue and thus is of particular interest to study in the context of brain cancer malignancy. Further study into the mechanisms controlling this phenotype revealed that, in *Drosophila* neural stem cells (neuroblasts), Lgl functions to maintain cell polarity through the coordination of asymmetric cell divisions (99, 100, 103). Lgl1 loss or inactivation by atypical protein kinase C (aPKC) promotes symmetric/self-renewal divisions leading to expansion of the neuroblast compartment (103). Thus, inhibition of Lgl in *Drosophila* results in undifferentiated and invasive growth with features that are also present in brain malignancies. The aim of this thesis was to investigate whether Lgl inactivation has a similar role in human glioblastoma. Primary glioblastoma cells, acquired directly from surgical samples, are the most clinically relevant model of glioblastoma, retaining both the genetic characteristic of the original patient tumour and the invasive potential of the original tumour (30, 32). Primary glioblastoma cells demonstrate the potential for distinct differentiation statuses. Primary glioblastoma cells express markers of neural stem cells and are able to differentiate along neuronal and astrocytic lineages (29-31). They, therefore, are an appropriate model to assess Lgl function in glioblastoma.

In glioblastoma, *PTEN* loss is the most common genetic alteration leading to activation of the PI3-kinase pathway. The PI3-kinase pathway activates multiple kinases including aPKCs (83, 84). In *Drosophila* and mammalian epithelial cells aPKC regulates Lgl activity by phosphorylation (104, 105). In addition to kinase activation through PDK1, PTEN loss has been shown to activated Rho GTPases Rac and CDC42 (57, 58). Rho GTPases Rac and CDC42 have two major roles in cells: 1) promoting motility via modulation of actin cytoskeleton dynamics

and 2) facilitating the establishment of the cell polarity complex containing Par6 and aPKC leading to aPKC activation (87, 139).

We hypothesised that in glioblastoma Lgl1 is inactivated through phosphorylation by PKCι as a consequence of PTEN loss. Inactivation of Lgl1 promotes glioblastoma malignancy through increased invasiveness and decreased differentiation recapitulating the characteristics of *Drosophila* brain tumour models. PREX1 links PTEN loss to activation of PKCι in glioblastoma.

5.1 Inactivation of Lgl1 restricts differentiation and promotes a more malignant phenotype

In humans, *Lgl1* is within a chromosomal locus that experiences allelic loss in Smith–Magenis syndrome (SMS) (218). SMS is complex neurobehavioral disorder marked by cognitive disability and congenital anomalies (218, 219). SMS has not been linked to increased susceptibility to neural malignancies (218, 219) suggesting that either single copy loss of *Lgl1* is not sufficient for neoplastic growth or there is a requirement for additional mutations. In the TCGA sequencing database Lgl1 is not lost or mutated suggesting alternate mechanisms of inactivation. I have demonstrated that in glioblastoma, the primary mechanism for Lgl inactivation is through phosphorylation by PKCι as a consequence of PTEN loss. Inactivation of Lgl1 resulting from PTEN loss demonstrates a similar phenotype to Lgl1 loss in *Drosophila* – inhibition of differentiation and increased invasiveness (Discussion Figure 1, data in Chapter 3). In mouse neural stem cells, knockout of *PTEN* alone does not affect differentiation potential but rather increased proliferation and long-term self-renewal (59). However, differentiation is supressed in mouse models of glioblastoma when *PTEN* is deleted in the presence of *P53* deletion (67). This suggests that in the context of cancer, PTEN loss is linked to

Figure 1: Summary model of thesis. Arrows show protein interaction/ activation events and dashed arrows show direct phosphorylation and dephosphorylation events.

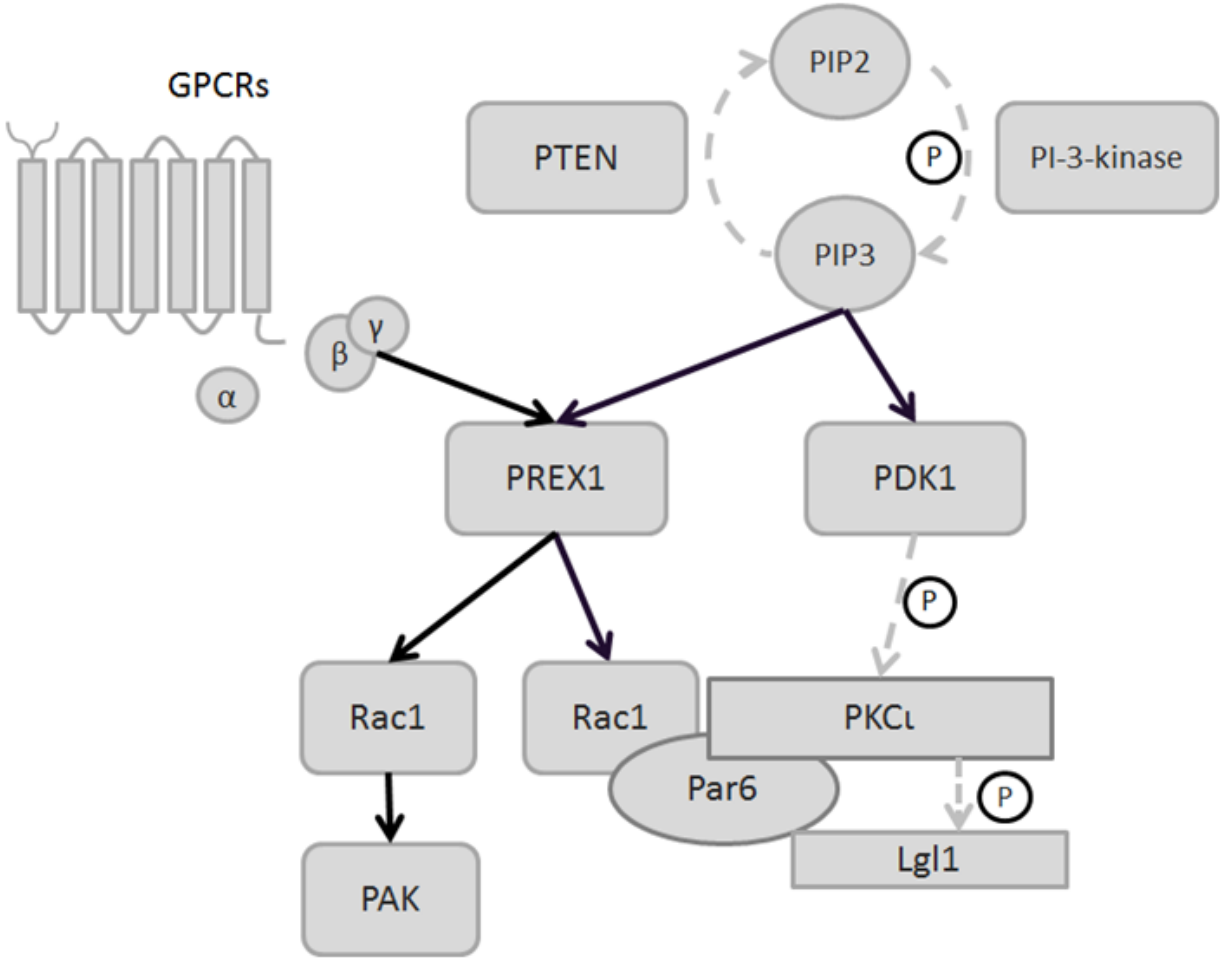
GPCRs
PIP2
PTEN
P
PI-3-kinase
PIP3
γ
β
α
PREX1
PDK1
P
Rac1
Rac1
PKCι
Par6
P
Lgl1
PAK

repression of differentiation which appears to be an important step in mouse models of gliomagenesis.

5.1.1 Role of Lgl1in glioblastoma differentiation

Few studies have investigated the mechanisms and phenotypes of primary glioblastoma differentiation. Treatment with serum promotes aberrant and non-specific increase of differentiation markers (29). The expression of lineage-specific markers following serum treatment correlates with decreased *in vitro* invasiveness and the formation of well-circumscribed non-invasive intracranial xenograft tumours suggesting that differentiation correlates with decreased invasiveness and malignancy (29, 36). A study by Rampazzo and colleagues (2013), demonstrated that Wnt or Numb induced inhibition of Notch signalling has the potential for neural-lineage differentiation of primary glioblastoma cells (35). In contrast to the results presented here, the mechanisms describing differentiation were not linked to genetic alterations or mutations in glioblastoma. However, Lgl has been shown to regulate the localization of Numb, a Notch antagonist (100). Thus, in the absence of exogenous Wnt, inactivation of Lgl may result in Numb mislocalization, Notch-pathway activation, and repression of differentiation, similarly to what is observed in $Lgl^{-/-}$ mice (98).

Markers of neuronal differentiation, particularly βIII-tubulin (TUJ1), have been investigated by histopathological analysis in brain cancers. In gliomas, TUJ1 expression increases with grade; however, it is detected mainly in borders of ischemic necrosis suggesting that expression is likely aberrant or due to stress conditions (220). In neuronal-type tumours such as medulloblastomas and retinoblastomas where differentiation status is assessed morphologically by neuritogenesis, expression of TUJ1 relates to a more differentiated and less malignant cancer (221).

The inactivation of Lgl in *Drosophila* is marked by both increased proliferation/ expansion of neuroblast numbers and increased invasiveness. In adult mammalian neural stem cells terminal differentiation is accompanied by a restriction of migratory ability and cell cycle exit (25). In chapter 2, the phenotype resulting from expression of active Lgl including differentiation, was investigated. In short-term culture, the expression of active Lgl did not affect proliferation. However, expression of active Lgl in mouse intracranial xenografts demonstrated a trend towards decreased proliferation suggesting that either differentiated cells have restricted long-term proliferative capacity or active Lgl has the capacity to inhibit proliferation in a context specific manner within the intracranial tumour microenvironment. A recent study in a glioblastoma cell line (lacking the differentiation potential of primary glioblastoma cell cultures) demonstrated that Lgl1 expression inhibited long-term *in vivo* tumour growth, and not in cell culture (222). Thus, active Lgl1 expression may function through both mechanisms to restrict proliferation *in vivo*.

5.1.2 Role of Lgl1 in glioblastoma invasiveness

A second phenotype of active Lgl in glioblastoma is decreased invasiveness through decreased motility. It is interesting to question whether Lgl-mediated differentiation is linked to its effect on motility. The effects of serum stated above combined with the fact that adult neural stem cells are migratory (along the rostral migratory stream) prior to differentiation in the olfactory bulb, suggests a possible link. However, in the U87MG cell line, which does not have differentiation potential, active Lgl expression inhibits migration, suggesting that a link between Lgl mediated differentiation and migration is either context specific or through indirect mechanisms. Lgl has been shown by many studies to directly bind non-muscle myosin IIA

(nmMIIA) (104, 118-120). Recently, two subsequent papers by Dahan and colleagues demonstrated that Lgl inhibition through either knockdown or phosphorylation by aPKC promoted nmMIIA assembly and motility (120, 121).

Invasion through the brain is a complex function driven by cellular attachment, contractile migration and degradation of matrix components (24). Of these steps, contractile (non-muscle myosin II mediated) migration is essential for invasion through the brain parenchyma (223). Compared to normal brain tissue, genetic mouse models of glioblastoma and primary glioblastoma xenograft tumours overexpress nmMIIA, which is thought to facilitate the high contractile requirements to pass through the small spaces in the tightly packed neuropil of the brain (170). In *Drosophila*, the invasive potential of $Lgl^{-/-}$ neuroblasts upon transplantation is mediated, in part, by matrix metalloproteinase activity (MMP) (224). MMPs promote tumour cell invasion by modulating the microenvironment through degradation of the surrounding extracellular matrix. In *Drosophila*, there are only two forms of MMPs: soluble MMP1 and membrane anchored MMP2. Secretion of MMP1 from $Lgl^{-/-}$ tumours facilitates metastasis to host ovaries (224). The assays used in Chapter 2 may not be sensitive enough to exclude the possibility of Lgl1 indirectly promoting the degradation of the extracellular matrix components. However, given the potent effect of Lgl1 on motility alone, this would likely be a minor contribution to its role in invasiveness. Additionally, in U87MG cells, active Lgl expression did not affect the amount or type of MMP secreted (data not shown). Therefore, the inhibition of nmMIIA by active Lgl1 is likely the major factor restricting motility. However, differentiation and other factors may contribute to the striking reduction of invasion *in vivo*.

5.2 The PI3-kinase pathway functions in a context of G protein–coupled receptor activity in order promote glioblastoma malignancy

Rac has been previously shown to facilitate the invasive behaviour of glioblastoma cell lines as well as primary glioblastoma cells (144, 145). PREX1 appears to be an important Rac activator to study in glioblastoma given the almost universal aberrant activation of PI3-kinase signalling in this cancer. U87MG cells, one of the more commonly used glioblastoma cell lines, do not express PREX1 and therefore are not a valid model to study Rac activation in glioblastoma. As demonstrated in Chapter 3, PREX1 is expressed across all primary glioblastoma cells tested as well as the majority of clinical glioblastoma samples. Knockdown of PREX1 in primary glioblastoma cells inhibits invasiveness through a reduction in motility proportional to that seen with knockdown of Rac1. This suggests that PREX1 is the principle Rac1 activating GEF in primary glioblastoma cultures and that upon depletion there doesn't appear to be compensation by other Rac GEFs. A study of PREX1 function in melanoma uncovered a similar finding that PREX1 has a significantly higher potential to promote invasive behaviour than Tiam1, a commonly studied Rac GEF (160). It would be important to investigate whether inhibition of PREX1 can also restrict glioblastoma invasiveness within the tumour microenvironment of the brain.

5.2.1 Role of PREX1 in activation of PKCι

There are two potential mechanisms leading to PKCι activation: 1) PDK1-mediated phosphorylation of the activation loop, and 2) specific protein interactions with GTP-bound Rac/CDC42 and Par6 (84, 87, 225). In primary glioblastoma cells, Par6 preferentially associated with Rac1 and these interactions modulated the activity of PKCι (phosphorylation at threonine 555 in the turn motif) (Discussion Figure 1, data in Chapter 3). PREX1 links the PI3-kinase

pathway to PKCι activity via Rac1 (Discussion Figure 1, data in Chapter 3). In lung cancer, the activation of PKCι facilitated by Par6 binding was also shown, without demonstrating direct interactions and cancer-specific mechanism (226). Taken together, in glioblastoma the loss of *PTEN* is sufficient to activate PKCι through both mechanisms in the presence of PREX1. In glioblastoma cell lines, PKCι promotes invasion through multiple mechanisms, including inactivation of Lgl1, and thus is an effector of PREX1 signalling promoting an invasive phenotype (92, 93, 185, 196). The highly invasive nature of glioblastoma can be explained, in part, through the direct link of *PTEN* loss to PKCι activation as well as activation of other Rac1 substrates including PAK.

Phosphorylation status of Lgl was assessed using the same conditions that modulated PKCι activity (not shown). Overexpression of Par6 did not increase the levels of phosphorylated Lgl suggesting that Lgl1 phosphorylation is maximal under the standard culture conditions. The levels of phosphorylated Lgl did not decrease upon PREX1 or Rac1 knockdown suggesting that isoform redundancy (PREX1/PREX2a and Rac1/Rac3) is sufficient to maintain functional levels of active PKCι, although further experiments knocking down both isoforms are required to confirm this.

5.2.2 PREX1 functions to link PI3-kinase pathway activation to G-protein couple receptor signalling in glioblastoma

Over 90% of the known GPCRs are expressed in the brain demonstrating the importance and diversity of GPCR-mediated signalling within the central nervous system (227). There are many GPCRs activated by neurotransmitters (i.e. dopamine, acetylcholine, serotonin, and glutamate). Glioblastoma cells may co-opt or even produce exogenous ligands to promote the invasive phenotype within the brain. A recent publication highlighted that multiple G-protein

coupled neurotransmitter receptor signalling pathways are important for glioblastoma cell line growth, particularly the dopamine pathway through DRD2 (200). In U87MG glioblastoma cells EGFR signalling converged with dopamine signalling via Gα subunit 2 to promote proliferation by activating the GTPase Rap1 and its effectors Ras and ERK (200). In primary glioblastoma cells, PI3-kinase signalling integrates with the Gβγ subunit to activate PREX1 and promote invasiveness through Rac1 (Discussion Figure 1, data in Chapter 3). This is a second pathway by which PI3-kinase and GPCR signalling converge to promote glioblastoma malignancy.

There are three major paradigms with tumour suppression genes: 1) two-hit where loss of one allele governs susceptibility and loss of both alleles is required for cancer (i.e. *Rb* in retinoblastoma), 2) haploinsufficiency (dosage levels) where the loss of one allele is sufficient to promote cancer (*P53*) and 3) quasi-haploinsufficiency where a threshold less than the loss of a complete allele is sufficient to promote cancer (i.e. *PTEN*) (228). In mouse genetic models, the impact of *PTEN* loss follows a step-wise, dose dependent function such that a 10% loss of PTEN expression is sufficient to promote Akt activation (229). In the context of glioblastoma motility and invasiveness the synergistic activation of PREX1 by GPCR βγ subunits and PIP3 could explain the sensitivity of glioblastoma to *PTEN* loss. Small changes in the concentration of PIP3 would have large effects on PREX1 with constitutive βγ subunit activity. In PriGO7A cells that express levels of PTEN indicative of single allelic loss, inhibition of PREX1 by knockdown, GPCR βγ subunit inhibitor gallein, and PI3-kinase inhibitor BKM120 resulted in decreased motility (Discussion Figure 1, data in Chapter 3). This suggests that in glioblastoma, loss of one copy of *PTEN* may be sufficient to drive the invasive phenotype through PREX1. The amount of PTEN expression required to inhibit this pathway could be assessed explicitly by varying the amount of doxycycline added to the inducible expression system.

An important question arising from this observation is how GPCR signalling is activated in glioblastoma. GPCR activating mutations have been described in thyroid-stimulating hormone receptor within cases of benign thyroid growths and thyroid carcinomas (230-233). Mutations in GPCRs and their subunits have been described in many cancers with particularly high incidence in growth hormone secreting pituitary tumours. These mutations are commonly associated with reducing the rate of GPCR subunit GTP-hydrolysis and therefore increasing duration of activity (234). Such mutations have not been described in glioblastoma and brain tumours suggesting alternate mechanisms of activation. Microarray data by Kumar *et al*., (*manuscript submitted*) demonstrated that in all tested PriGO cell cultures, the dopamine receptor is expressed. In this study, pharmacological inhibition with the GPCR antagonist haloperidol decreased PriGO cell motility, suggesting that the effects observed are through receptor-dependent activation of the G protein. It would be important to examine whether the reduction of motility is specifically a factor of dopamine receptor antagonism by limiting the concentration of haloperidol to inhibit only dopamine receptors or by specific receptor knockdown. In addition, given that no exogenous dopamine is added, it would be interesting to examine whether glioblastoma cells have the capacity to produce and secrete dopamine in an autocrine manner. Subsequent analysis of the PriGO microarray data revealed that tyrosine hydroxylase, the enzyme regulating the rate-limiting step of dopamine synthesis, is expressed in all PriGO cell cultures tested suggesting a capacity to synthesize dopamine. However, to formally test this, the presence of dopamine in cell-conditioned culture medium should be examined.

5.3 Restoration of PTEN expression as a therapeutic option for glioblastoma

Given the number and diversity of downstream effectors activated by *PTEN* loss, it would be very difficult to individually target them as a therapeutic option. Thus, expression of

PTEN may be the more effective option. Recently, a splice variant of PTEN, PTEN-long, has been described (235). The additional 173 N-terminal amino acids make PTEN-long membrane permeable and thus allow it to be secreted and taken up by cells (235). Recombinant PTEN-long is able to enter cells, antagonize the PI3-kinase pathway and exhibit its tumour suppressive function (235). The expression and tumour suppressive function of PTEN-long was confirmed by an independent group (236). A cell-based delivery of PTEN-long to the brain is an attractive approach. Neural stem cells, mesenchymal stem cells, and immune cells all demonstrate homing ability to glioblastoma tumour cells (237-241). Specifically, neural stem cells have been shown to hone to patient-derived orthotopic glioblastoma xenograft tumours and deliver pro-apoptotic molecules (242). The safety of cell-based delivery approaches as glioblastoma therapeutic strategies is currently being tested in Phase I clinical trials with neural stem cells expressing a prodrug converting enzyme (243).

5.4 Conclusions

In glioblastoma Lgl1 is inactivated through phosphorylation by PKCι as a consequence of *PTEN* loss. Inactivation of Lgl1 by phosphorylation inhibits differentiation towards a neuronal lineage and promotes invasiveness, recapitulating the characteristics of *Lgl1*$^{-/-}$ *Drosophila* brain tumour models. PREX1 links *PTEN* loss to activation of PKCι in glioblastoma by promoting Rac1 activity and complex formation with Par6. PREX1 is activated synergistically by GPCR βγ subunit and PIP3 binding demonstrating that, in glioblastoma, PI3-kinase activation requires the context of G protein–coupled receptor activity in order promote invasion.

References

1. Gonzalez, J, Gilbert, MR. 2005. Treatment of astrocytomas. Curr. Opin. Neurol. 18:632-638.

2. Smirniotopoulos, JG. 1999. The new WHO classification of brain tumors. Neuroimaging Clin. N. Am. 9:595-613.

3. Louis, DN, Ohgaki, H, Wiestler, OD, Cavenee, WK, Burger, PC, Jouvet, A, Scheithauer, BW, Kleihues, P. 2007. The 2007 WHO classification of tumours of the central nervous system. Acta Neuropathol. 114:97-109.

4. Miller, CR, Perry, A. 2007. Glioblastoma: morphologic and molecular genetic diversity. Arch. Pathol. Lab. Med. 131:397-406.

5. Alvarez-Buylla, A, Garcia-Verdugo, JM. 2002. Neurogenesis in adult subventricular zone. J. Neurosci. 22:629-634. doi: 22/3/629 [pii].

6. Jin, K, Minami, M, Lan, JQ, Mao, XO, Batteur, S, Simon, RP, Greenberg, DA. 2001. Neurogenesis in dentate subgranular zone and rostral subventricular zone after focal cerebral ischemia in the rat. Proc. Natl. Acad. Sci. U. S. A. 98:4710-4715. doi: 10.1073/pnas.081011098 [doi].

7. Llaguno, SA, Chen, J, Kwon, C, Jackson, EL, Li, Y, Burns, DK, Alvarez-Buylla, A, Parada, LF. 2009. Malignant astrocytomas originate from neural stem/progenitor cells in a somatic tumor suppressor mouse model. Cancer Cell. 15:45-56.

8. Holland, EC, Celestino, J, Dai, C, Schaefer, L, Sawaya, RE, Fuller, GN. 2000. Combined activation of Ras and Akt in neural progenitors induces glioblastoma formation in mice. Nat. Genet. 25:55-57.

9. Lindberg, N, Kastemar, M, Olofsson, T, Smits, A, Uhrbom, L. 2009. Oligodendrocyte progenitor cells can act as cell of origin for experimental glioma. Oncogene. 28:2266-2275.

10. Dai, C, Celestino, JC, Okada, Y, Louis, DN, Fuller, GN, Holland, EC. 2001. PDGF autocrine stimulation dedifferentiates cultured astrocytes and induces oligodendrogliomas and oligoastrocytomas from neural progenitors and astrocytes in vivo. Genes Dev. 15:1913-1925. doi: 10.1101/gad.903001 [doi].

11. Friedmann-Morvinski, D, Bushong, EA, Ke, E, Soda, Y, Marumoto, T, Singer, O, Ellisman, MH, Verma, IM. 2012. Dedifferentiation of neurons and astrocytes by oncogenes can induce gliomas in mice. Science. 338:1080-1084. doi: 10.1126/science.1226929 [doi].

12. Clarke, JL, Chang, SM. 2012. Neuroimaging: diagnosis and response assessment in glioblastoma. Cancer J. 18:26-31. doi: 10.1097/PPO.0b013e318244d7c8 [doi].

13. Stupp, R, Hegi, ME, Mason, WP, van den Bent, Martin J, Taphoorn, MJ, Janzer, RC, Ludwin, SK, Allgeier, A, Fisher, B, Belanger, K. 2009. Effects of radiotherapy with concomitant and adjuvant temozolomide versus radiotherapy alone on survival in glioblastoma in a randomised phase III study: 5-year analysis of the EORTC-NCIC trial. The Lancet Oncology. 10:459-466.

14. Malmström, A, Grønberg, BH, Marosi, C, Stupp, R, Frappaz, D, Schultz, H, Abacioglu, U, Tavelin, B, Lhermitte, B, Hegi, ME. 2012. Temozolomide versus standard 6-week radiotherapy versus hypofractionated radiotherapy in patients older than 60 years with glioblastoma: the Nordic randomised, phase 3 trial. The Lancet Oncology. 13:916-926.

15. Chamberlain, MC. 2011. Bevacizumab for the treatment of recurrent glioblastoma. Clinical Medicine Insights.Oncology. 5:117.

16. Sampson, JH. 2015. Alternating Electric Fields for the Treatment of Glioblastoma. Jama. 314:2511-2513.

17. Dandy, WE. 1928. Removal of right cerebral hemisphere for certain tumors with hemiplegia: Preliminary report. J. Am. Med. Assoc. 90:823-825.

18. Hou, LC, Veeravagu, A, Hsu, AR, Tse, VC. 2006. Recurrent glioblastoma multiforme: a review of natural history and management options. Neurosurgical Focus. 20:E3.

19. Hunter, S, Young, A, Olson, J, Brat, DJ, Bowers, G, Wilcox, JN, Jaye, D, Mendrinos, S, Neish, A. 2002. Differential Expression between Pilocytic and Anaplastic Astrocytomas: Identification of Apolipoprotein D as a Marker for Low-Grade, Non-Infiltrating Primary CNS Neoplasms. Journal of Neuropathology & Experimental Neurology. 61:275-281.

20. Kleihues, P, Cavenee, WK. 2000. Pathology and genetics of tumours of the nervous system. International Agency for Research on Cancer.

21. Scherer, H. 1938. Structural development in gliomas. The American Journal of Cancer. 34:333-351.

22. Cuddapah, VA, Robel, S, Watkins, S, Sontheimer, H. 2014. A neurocentric perspective on glioma invasion. Nature Reviews Neuroscience. 15:455-465.

23. Bellail, AC, Hunter, SB, Brat, DJ, Tan, C, Van Meir, EG. 2004. Microregional extracellular matrix heterogeneity in brain modulates glioma cell invasion. Int. J. Biochem. Cell Biol. 36:1046-1069.

24. Lefranc, F, Brotchi, J, Kiss, R. 2005. Possible future issues in the treatment of glioblastomas: special emphasis on cell migration and the resistance of migrating glioblastoma cells to apoptosis. J. Clin. Oncol. 23:2411-2422. doi: 23/10/2411 [pii].

25. Sun, W, Kim, H, Moon, Y. 2010. Control of neuronal migration through rostral migratory stream in mice. Anatomy & Cell Biology. 43:269-279.

26. Snapyan, M, Lemasson, M, Brill, MS, Blais, M, Massouh, M, Ninkovic, J, Gravel, C, Berthod, F, Gotz, M, Barker, PA, Parent, A, Saghatelyan, A. 2009. Vasculature guides migrating neuronal precursors in the adult mammalian forebrain via brain-derived neurotrophic factor signaling. J. Neurosci. 29:4172-4188. doi: 10.1523/JNEUROSCI.4956-08.2009 [doi].

27. Kakita, A, Zerlin, M, Takahashi, H, Goldman, JE. 2003. Some glial progenitors in the neonatal subventricular zone migrate through the corpus callosum to the contralateral cerebral hemisphere. J. Comp. Neurol. 458:381-388.

28. Tabar, V, Panagiotakos, G, Greenberg, ED, Chan, BK, Sadelain, M, Gutin, PH, Studer, L. 2005. Migration and differentiation of neural precursors derived from human embryonic stem cells in the rat brain. Nat. Biotechnol. 23:601-606.

29. Lee, J, Kotliarova, S, Kotliarov, Y, Li, A, Su, Q, Donin, NM, Pastorino, S, Purow, BW, Christopher, N, Zhang, W. 2006. Tumor stem cells derived from glioblastomas cultured in bFGF and EGF more closely mirror the phenotype and genotype of primary tumors than do serum-cultured cell lines. Cancer Cell. 9:391-403.

30. Al-Mayhani, TMF, Ball, SL, Zhao, J, Fawcett, J, Ichimura, K, Collins, PV, Watts, C. 2009. An efficient method for derivation and propagation of glioblastoma cell lines that conserves the molecular profile of their original tumours. J. Neurosci. Methods. 176:192-199.

31. Pollard, SM, Yoshikawa, K, Clarke, ID, Danovi, D, Stricker, S, Russell, R, Bayani, J, Head, R, Lee, M, Bernstein, M. 2009. Glioma stem cell lines expanded in adherent culture have tumor-specific phenotypes and are suitable for chemical and genetic screens. Cell Stem Cell. 4:568-580.

32. Wakimoto, H, Mohapatra, G, Kanai, R, Curry, WT,Jr, Yip, S, Nitta, M, Patel, AP, Barnard, ZR, Stemmer-Rachamimov, AO, Louis, DN, Martuza, RL, Rabkin, SD. 2012. Maintenance of primary tumor phenotype and genotype in glioblastoma stem cells. Neuro Oncol. 14:132-144. doi: 10.1093/neuonc/nor195 [doi].

33. Chen, R, Nishimura, MC, Bumbaca, SM, Kharbanda, S, Forrest, WF, Kasman, IM, Greve, JM, Soriano, RH, Gilmour, LL, Rivers, CS. 2010. A hierarchy of self-renewing tumor-initiating cell types in glioblastoma. Cancer Cell. 17:362-375.

34. Piccirillo, S, Reynolds, B, Zanetti, N, Lamorte, G, Binda, E, Broggi, G, Brem, H, Olivi, A, Dimeco, F, Vescovi, A. 2006. Bone morphogenetic proteins inhibit the tumorigenic potential of human brain tumour-initiating cells. Nature. 444:761-765.

35. Rampazzo, E, Persano, L, Pistollato, F, Moro, E, Frasson, C, Porazzi, P, Della Puppa, A, Bresolin, S, Battilana, G, Indraccolo, S. 2013. Wnt activation promotes neuronal differentiation of glioblastoma. Cell Death & Disease. 4:e500.

36. Sadahiro, H, Yoshikawa, K, Ideguchi, M, Kajiwara, K, Ishii, A, Ikeda, E, Owada, Y, Yasumoto, Y, Suzuki, M. 2014. Pathological features of highly invasive glioma stem cells in a mouse xenograft model. Brain Tumor Pathol. 31:77-84.

37. Holland, EC. 2001. Gliomagenesis: genetic alterations and mouse models. Nature Reviews Genetics. 2:120-129.

38. Verhaak, RG, Hoadley, KA, Purdom, E, Wang, V, Qi, Y, Wilkerson, MD, Miller, CR, Ding, L, Golub, T, Mesirov, JP. 2010. Integrated genomic analysis identifies clinically relevant subtypes of glioblastoma characterized by abnormalities in PDGFRA, IDH1, EGFR, and NF1. Cancer Cell. 17:98-110.

39. Brennan, CW, Verhaak, RG, McKenna, A, Campos, B, Noushmehr, H, Salama, SR, Zheng, S, Chakravarty, D, Sanborn, JZ, Berman, SH. 2013. The somatic genomic landscape of glioblastoma. Cell. 155:462-477.

40. Noushmehr, H, Weisenberger, DJ, Diefes, K, Phillips, HS, Pujara, K, Berman, BP, Pan, F, Pelloski, CE, Sulman, EP, Bhat, KP. 2010. Identification of a CpG island methylator phenotype that defines a distinct subgroup of glioma. Cancer Cell. 17:510-522.

41. Patel, AP, Tirosh, I, Trombetta, JJ, Shalek, AK, Gillespie, SM, Wakimoto, H, Cahill, DP, Nahed, BV, Curry, WT, Martuza, RL, Louis, DN, Rozenblatt-Rosen, O, Suva, ML, Regev, A, Bernstein, BE. 2014. Single-cell RNA-seq highlights intratumoral heterogeneity in primary glioblastoma. Science. 344:1396-1401. doi: 10.1126/science.1254257 [doi].

42. Ozawa, T, Riester, M, Cheng, Y, Huse, JT, Squatrito, M, Helmy, K, Charles, N, Michor, F, Holland, EC. 2014. Most human non-GCIMP glioblastoma subtypes evolve from a common proneural-like precursor glioma. Cancer Cell. 26:288-300.

43. Huse, JT, Brennan, C, Hambardzumyan, D, Wee, B, Pena, J, Rouhanifard, SH, Sohn-Lee, C, le Sage, C, Agami, R, Tuschl, T, Holland, EC. 2009. The PTEN-regulating microRNA miR-26a is amplified in high-grade glioma and facilitates gliomagenesis in vivo. Genes Dev. 23:1327-1337. doi: 10.1101/gad.1777409 [doi].

44. Meng, F, Henson, R, Wehbe–Janek, H, Ghoshal, K, Jacob, ST, Patel, T. 2007. MicroRNA-21 regulates expression of the PTEN tumor suppressor gene in human hepatocellular cancer. Gastroenterology. 133:647-658.

45. Vazquez, F, Ramaswamy, S, Nakamura, N, Sellers, WR. 2000. Phosphorylation of the PTEN tail regulates protein stability and function. Mol. Cell. Biol. 20:5010-5018.

46. Li, J, Yen, C, Liaw, D, Podsypanina, K, Bose, S, Wang, SI, Puc, J, Miliaresis, C, Rodgers, L, McCombie, R, Bigner, SH, Giovanella, BC, Ittmann, M, Tycko, B, Hibshoosh, H, Wigler, MH, Parsons, R. 1997. PTEN, a putative protein tyrosine phosphatase gene mutated in human brain, breast, and prostate cancer. Science. 275:1943-1947.

47. Wang, SI, Puc, J, Li, J, Bruce, JN, Cairns, P, Sidransky, D, Parsons, R. 1997. Somatic mutations of PTEN in glioblastoma multiforme. Cancer Res. 57:4183-4186.

48. Cristofano, AD, Pesce, B, Cordon-Cardo, C, Pandolfi, PP. 1998. Pten is essential for embryonic development and tumour suppression. Nat. Genet. 19:348-355.

49. Liaw, D, Marsh, DJ, Li, J, Dahia, PL, Wang, SI, Zheng, Z, Bose, S, Call, KM, Tsou, HC, Peacoke, M. 1997. Germline mutations of the PTEN gene in Cowden disease, an inherited breast and thyroid cancer syndrome. Nat. Genet. 16:64-67.

50. Suzuki, A, de la Pompa, José Luis, Stambolic, V, Elia, AJ, Sasaki, T, del Barco Barrantes, I, Ho, A, Wakeham, A, Khoo, W, Fukumoto, M. 1998. High cancer susceptibility and embryonic lethality associated with mutation of the PTEN tumor suppressor gene in mice. Current Biology. 8:1169-1178.

51. Myers, MP, Stolarov, JP, Eng, C, Li, J, Wang, SI, Wigler, MH, Parsons, R, Tonks, NK. 1997. P-TEN, the tumor suppressor from human chromosome 10q23, is a dual-specificity phosphatase. Proc. Natl. Acad. Sci. U. S. A. 94:9052-9057.

52. Maehama, T, Dixon, JE. 1998. The tumor suppressor, PTEN/MMAC1, dephosphorylates the lipid second messenger, phosphatidylinositol 3, 4, 5-trisphosphate. J. Biol. Chem. 273:13375-13378.

53. Myers, MP, Pass, I, Batty, IH, Van der Kaay, J, Stolarov, JP, Hemmings, BA, Wigler, MH, Downes, CP, Tonks, NK. 1998. The lipid phosphatase activity of PTEN is critical for its tumor supressor function. Proc. Natl. Acad. Sci. U. S. A. 95:13513-13518.

54. Stambolic, V, Suzuki, A, De La Pompa, José Luis, Brothers, GM, Mirtsos, C, Sasaki, T, Ruland, J, Penninger, JM, Siderovski, DP, Mak, TW. 1998. Negative regulation of PKB/Akt-dependent cell survival by the tumor suppressor PTEN. Cell. 95:29-39.

55. Haas-Kogan, D, Shalev, N, Wong, M, Mills, G, Yount, G, Stokoe, D. 1998. Protein kinase B (PKB/Akt) activity is elevated in glioblastoma cells due to mutation of the tumor suppressor PTEN/MMAC. Current Biology. 8:1195-S1.

56. Vanhaesebroeck, B, Alessi, DR. 2000. The PI3K-PDK1 connection: more than just a road to PKB. Biochem. J. 346 Pt 3:561-576.

57. Liliental, J, Moon, SY, Lesche, R, Mamillapalli, R, Li, D, Zheng, Y, Sun, H, Wu, H. 2000. Genetic deletion of the Pten tumor suppressor gene promotes cell motility by activation of Rac1 and Cdc42 GTPases. Current Biology. 10:401-404.

58. Keely, PJ, Westwick, JK, Whitehead, IP, Der, CJ, Parise, LV. 1997. Cdc42 and Rac1 induce integrin-mediated cell motility and invasiveness through PI (3) K. Nature. 390:632-636.

59. Groszer, M, Erickson, R, Scripture-Adams, DD, Lesche, R, Trumpp, A, Zack, JA, Kornblum, HI, Liu, X, Wu, H. 2001. Negative regulation of neural stem/progenitor cell proliferation by the Pten tumor suppressor gene in vivo. Science. 294:2186-2189. doi: 10.1126/science.1065518 [doi].

60. Li, L, Liu, F, Salmonsen, RA, Turner, TK, Litofsky, NS, Di Cristofano, A, Pandolfi, PP, Jones, SN, Recht, LD, Ross, AH. 2002. PTEN in neural precursor cells: regulation of migration, apoptosis, and proliferation. Molecular and Cellular Neuroscience. 20:21-29.

61. Groszer, M, Erickson, R, Scripture-Adams, DD, Dougherty, JD, Le Belle, J, Zack, JA, Geschwind, DH, Liu, X, Kornblum, HI, Wu, H. 2006. PTEN negatively regulates neural stem cell self-renewal by modulating G0-G1 cell cycle entry. Proc. Natl. Acad. Sci. U. S. A. 103:111-116. doi: 0509939103 [pii].

62. Gregorian, C, Nakashima, J, Le Belle, J, Ohab, J, Kim, R, Liu, A, Smith, KB, Groszer, M, Garcia, AD, Sofroniew, MV, Carmichael, ST, Kornblum, HI, Liu, X, Wu, H. 2009. Pten deletion in adult neural stem/progenitor cells enhances constitutive neurogenesis. J. Neurosci. 29:1874-1886. doi: 10.1523/JNEUROSCI.3095-08.2009 [doi].

63. Backman, SA, Stambolic, V, Suzuki, A, Haight, J, Elia, A, Pretorius, J, Tsao, M, Shannon, P, Bolon, B, Ivy, GO. 2001. Deletion of Pten in mouse brain causes seizures, ataxia and defects in soma size resembling Lhermitte-Duclos disease. Nat. Genet. 29:396-403.

64. Fraser, MM, Zhu, X, Kwon, CH, Uhlmann, EJ, Gutmann, DH, Baker, SJ. 2004. Pten loss causes hypertrophy and increased proliferation of astrocytes in vivo. Cancer Res. 64:7773-7779. doi: 64/21/7773 [pii].

65. Wang, S, Gao, J, Lei, Q, Rozengurt, N, Pritchard, C, Jiao, J, Thomas, GV, Li, G, Roy-Burman, P, Nelson, PS. 2003. Prostate-specific deletion of the murine Pten tumor suppressor gene leads to metastatic prostate cancer. Cancer Cell. 4:209-221.

66. Stambolic, V, Tsao, MS, Macpherson, D, Suzuki, A, Chapman, WB, Mak, TW. 2000. High incidence of breast and endometrial neoplasia resembling human Cowden syndrome in pten+/- mice. Cancer Res. 60:3605-3611.

67. Zheng, H, Ying, H, Yan, H, Kimmelman, AC, Hiller, DJ, Chen, A, Perry, SR, Tonon, G, Chu, GC, Ding, Z. 2008. p53 and Pten control neural and glioma stem/progenitor cell renewal and differentiation. Nature. 455:1129-1133.

68. Li, L, Dutra, A, Pak, E, Labrie, JE,3rd, Gerstein, RM, Pandolfi, PP, Recht, LD, Ross, AH. 2009. EGFRvIII expression and PTEN loss synergistically induce chromosomal instability and glial tumors. Neuro Oncol. 11:9-21. doi: 10.1215/15228517-2008-081 [doi].

69. Li, DM, Sun, H. 1998. PTEN/MMAC1/TEP1 suppresses the tumorigenicity and induces G1 cell cycle arrest in human glioblastoma cells. Proc. Natl. Acad. Sci. U. S. A. 95:15406-15411.

70. Cheney, IW, Johnson, DE, Vaillancourt, MT, Avanzini, J, Morimoto, A, Demers, GW, Wills, KN, Shabram, PW, Bolen, JB, Tavtigian, SV, Bookstein, R. 1998. Suppression of tumorigenicity of glioblastoma cells by adenovirus-mediated MMAC1/PTEN gene transfer. Cancer Res. 58:2331-2334.

71. Tamura, M, Gu, J, Takino, T, Yamada, KM. 1999. Tumor suppressor PTEN inhibition of cell invasion, migration, and growth: differential involvement of focal adhesion kinase and p130Cas. Cancer Res. 59:442-449.

72. Park, MJ, Kim, MS, Park, IC, Kang, HS, Yoo, H, Park, SH, Rhee, CH, Hong, SI, Lee, SH. 2002. PTEN suppresses hyaluronic acid-induced matrix metalloproteinase-9 expression in U87MG glioblastoma cells through focal adhesion kinase dephosphorylation. Cancer Res. 62:6318-6322.

73. Cheng, R, Ma, R, Wang, Z, Yang, S, Lin, X, Rong, H, Ma, Y. 2011. PTEN status is related to cell proliferation and self-renewal independent of CD133 phenotype in the glioma-initiating cells. Mol. Cell. Biochem. 349:149-157.

74. Wendel, H, de Stanchina, E, Fridman, JS, Malina, A, Ray, S, Kogan, S, Cordon-Cardo, C, Pelletier, J, Lowe, SW. 2004. Survival signalling by Akt and eIF4E in oncogenesis and cancer therapy. Nature. 428:332-337.

75. Shin, I, Yakes, FM, Rojo, F, Shin, N, Bakin, AV, Baselga, J, Arteaga, CL. 2002. PKB/Akt mediates cell-cycle progression by phosphorylation of p27Kip1 at threonine 157 and modulation of its cellular localization. Nat. Med. 8:1145-1152.

76. Brunet, A, Bonni, A, Zigmond, MJ, Lin, MZ, Juo, P, Hu, LS, Anderson, MJ, Arden, KC, Blenis, J, Greenberg, ME. 1999. Akt promotes cell survival by phosphorylating and inhibiting a Forkhead transcription factor. Cell. 96:857-868.

77. Datta, SR, Dudek, H, Tao, X, Masters, S, Fu, H, Gotoh, Y, Greenberg, ME. 1997. Akt phosphorylation of BAD couples survival signals to the cell-intrinsic death machinery. Cell. 91:231-241.

78. Cardone, MH, Roy, N, Stennicke, HR, Salvesen, GS, Franke, TF, Stanbridge, E, Frisch, S, Reed, JC. 1998. Regulation of cell death protease caspase-9 by phosphorylation. Science. 282:1318-1321.

79. Gallia, GL, Tyler, BM, Hann, CL, Siu, IM, Giranda, VL, Vescovi, AL, Brem, H, Riggins, GJ. 2009. Inhibition of Akt inhibits growth of glioblastoma and glioblastoma stem-like cells. Mol. Cancer. Ther. 8:386-393. doi: 10.1158/1535-7163.MCT-08-0680 [doi].

80. Koul, D, Shen, R, Bergh, S, Sheng, X, Shishodia, S, Lafortune, TA, Lu, Y, de Groot, JF, Mills, GB, Yung, WK. 2006. Inhibition of Akt survival pathway by a small-molecule inhibitor in human glioblastoma. Mol. Cancer. Ther. 5:637-644. doi: 5/3/637 [pii].

81. Fan, Q, Knight, ZA, Goldenberg, DD, Yu, W, Mostov, KE, Stokoe, D, Shokat, KM, Weiss, WA. 2006. A dual PI3 kinase/mTOR inhibitor reveals emergent efficacy in glioma. Cancer Cell. 9:341-349.

82. Cloughesy, TF, Yoshimoto, K, Nghiemphu, P, Brown, K, Dang, J, Zhu, S, Hsueh, T, Chen, Y, Wang, W, Youngkin, D. 2008. Antitumor activity of rapamycin in a Phase I trial for patients with recurrent PTEN-deficient glioblastoma. PLoS Med. 5:e8.

83. Le Good, JA, Ziegler, WH, Parekh, DB, Alessi, DR, Cohen, P, Parker, PJ. 1998. Protein kinase C isotypes controlled by phosphoinositide 3-kinase through the protein kinase PDK1. Science. 281:2042-2045.

84. Balendran, A, Biondi, RM, Cheung, PC, Casamayor, A, Deak, M, Alessi, DR. 2000. A 3-phosphoinositide-dependent protein kinase-1 (PDK1) docking site is required for the phosphorylation of protein kinase Czeta (PKCzeta) and PKC-related kinase 2 by PDK1. J. Biol. Chem. 275:20806-20813. doi: 10.1074/jbc.M000421200 [doi].

85. Rosse, C, Linch, M, Kermorgant, S, Cameron, AJ, Boeckeler, K, Parker, PJ. 2010. PKC and the control of localized signal dynamics. Nature Reviews Molecular Cell Biology. 11:103-112.

86. Lin, D, Edwards, AS, Fawcett, JP, Mbamalu, G, Scott, JD, Pawson, T. 2000. A mammalian PAR-3–PAR-6 complex implicated in Cdc42/Rac1 and aPKC signalling and cell polarity. Nat. Cell Biol. 2:540-547.

87. Noda, Y, Takeya, R, Ohno, S, Naito, S, Ito, T, Sumimoto, H. 2001. Human homologues of the Caenorhabditis elegans cell polarity protein PAR6 as an adaptor that links the small GTPases Rac and Cdc42 to atypical protein kinase C. Genes to Cells. 6:107-119.

88. Justilien, V, Fields, AP. 2009. Ect2 links the PKCι–Par6α complex to Rac1 activation and cellular transformation. Oncogene. 28:3597-3607.

89. Kovac, J, Oster, H, Leitges, M. 2007. Expression of the atypical protein kinase C (aPKC) isoforms ι/λ and ζ during mouse embryogenesis. Gene Expression Patterns. 7:187-196.

90. Murray, NR, Kalari, KR, Fields, AP. 2011. Protein kinase Cι expression and oncogenic signaling mechanisms in cancer. J. Cell. Physiol. 226:879-887.

91. Baldwin, R, Garratt-Lalonde, M, Parolin, D, Krzyzanowski, P, Andrade, M, Lorimer, I. 2006. Protection of glioblastoma cells from cisplatin cytotoxicity via protein kinase Cι-mediated attenuation of p38 MAP kinase signaling. Oncogene. 25:2909-2919.

92. Baldwin, R, Parolin, D, Lorimer, I. 2008. Regulation of glioblastoma cell invasion by PKCι and RhoB. Oncogene. 27:3587-3595.

93. Baldwin, RM, Barrett, GM, Parolin, DA, Gillies, JK, Paget, JA, Lavictoire, SJ, Gray, DA, Lorimer, IA. 2010. Coordination of glioblastoma cell motility by PKCι. Molecular Cancer. 9:1.

94. Restall, IJ, Paget, JA, Daneshmand, M, Amin, MS, Islam, S, Lorimer, IA. 2011. Repression of cancer cell senescence by PKCι. Cancer Res. 71:1224-1224.

95. Restall, IJ, Parolin, DA, Daneshmand, M, Hanson, JE, Simard, MA, Fitzpatrick, ME, Kumar, R, Lavictoire, SJ, Lorimer, IA. 2015. PKCι depletion initiates mitotic slippage-induced senescence in glioblastoma. Cell Cycle. 14:2938-2948.

96. Gateff, E. 1978. Malignant neoplasms of genetic origin in Drosophila melanogaster. Science. 200:1448-1459.

97. Woodhouse, E, Hersperger, E, Shearn, A. 1998. Growth, metastasis, and invasiveness of Drosophila tumors caused by mutations in specific tumor suppressor genes. Dev. Genes Evol. 207:542-550.

98. Klezovitch, O, Fernandez, TE, Tapscott, SJ, Vasioukhin, V. 2004. Loss of cell polarity causes severe brain dysplasia in Lgl1 knockout mice. Genes Dev. 18:559-571. doi: 10.1101/gad.1178004 [doi].

99. Ohshiro, T, Yagami, T, Zhang, C, Matsuzaki, F. 2000. Role of cortical tumour-suppressor proteins in asymmetric division of Drosophila neuroblast. Nature. 408:593-596.

100. Albertson, R, Doe, CQ. 2003. Dlg, Scrib and Lgl regulate neuroblast cell size and mitotic spindle asymmetry. Nat. Cell Biol. 5:166-170.

101. Wang, W, Liu, W, Wang, Y, Zhou, L, Tang, X, Luo, H. 2011. Notch signaling regulates neuroepithelial stem cell maintenance and neuroblast formation in Drosophila optic lobe development. Dev. Biol. 350:414-428.

102. Doe, CQ. 2008. Neural stem cells: balancing self-renewal with differentiation. Development. 135:1575-1587. doi: 10.1242/dev.014977 [doi].

103. Lee, C, Robinson, KJ, Doe, CQ. 2006. Lgl, Pins and aPKC regulate neuroblast self-renewal versus differentiation. Nature. 439:594-598.

104. Betschinger, J, Eisenhaber, F, Knoblich, JA. 2005. Phosphorylation-induced autoinhibition regulates the cytoskeletal protein Lethal (2) giant larvae. Current Biology. 15:276-282.

105. Yamanaka, T, Horikoshi, Y, Sugiyama, Y, Ishiyama, C, Suzuki, A, Hirose, T, Iwamatsu, A, Shinohara, A, Ohno, S. 2003. Mammalian Lgl forms a protein complex with PAR-6 and aPKC independently of PAR-3 to regulate epithelial cell polarity. Current Biology. 13:734-743.

106. Rolls, MM, Albertson, R, Shih, HP, Lee, CY, Doe, CQ. 2003. Drosophila aPKC regulates cell polarity and cell proliferation in neuroblasts and epithelia. J. Cell Biol. 163:1089-1098. doi: 10.1083/jcb.200306079 [doi].

107. Lin, D, Edwards, AS, Fawcett, JP, Mbamalu, G, Scott, JD, Pawson, T. 2000. A mammalian PAR-3–PAR-6 complex implicated in Cdc42/Rac1 and aPKC signalling and cell polarity. Nat. Cell Biol. 2:540-547.

108. Wirtz-Peitz, F, Nishimura, T, Knoblich, JA. 2008. Linking cell cycle to asymmetric division: Aurora-A phosphorylates the Par complex to regulate Numb localization. Cell. 135:161-173.

109. Graybill, C, Wee, B, Atwood, SX, Prehoda, KE. 2012. Partitioning-defective protein 6 (Par-6) activates atypical protein kinase C (aPKC) by pseudosubstrate displacement. J. Biol. Chem. 287:21003-21011. doi: 10.1074/jbc.M112.360495 [doi].

110. Yamanaka, T, Horikoshi, Y, Izumi, N, Suzuki, A, Mizuno, K, Ohno, S. 2006. Lgl mediates apical domain disassembly by suppressing the PAR-3-aPKC-PAR-6 complex to orient apical membrane polarity. J. Cell. Sci. 119:2107-2118. doi: jcs.02938 [pii].

111. Hutterer, A, Betschinger, J, Petronczki, M, Knoblich, JA. 2004. Sequential roles of Cdc42, Par-6, aPKC, and Lgl in the establishment of epithelial polarity during Drosophila embryogenesis. Developmental Cell. 6:845-854.

112. Russ, A, Louderbough, JM, Zarnescu, D, Schroeder, JA. 2012. Hugl1 and Hugl2 in mammary epithelial cells: polarity, proliferation, and differentiation. PloS One. 7:e47734.

113. Musch, A, Cohen, D, Yeaman, C, Nelson, WJ, Rodriguez-Boulan, E, Brennwald, PJ. 2002. Mammalian homolog of Drosophila tumor suppressor lethal (2) giant larvae interacts with basolateral exocytic machinery in Madin-Darby canine kidney cells. Mol. Biol. Cell. 13:158-168. doi: 10.1091/mbc.01-10-0496 [doi].

114. Jewell, JL, Oh, E, Thurmond, DC. 2010. Exocytosis mechanisms underlying insulin release and glucose uptake: conserved roles for Munc18c and syntaxin 4. Am. J. Physiol. Regul. Integr. Comp. Physiol. 298:R517-31. doi: 10.1152/ajpregu.00597.2009 [doi].

115. Washbourne, P, Thompson, PM, Carta, M, Costa, ET, Mathews, JR, Lopez-Benditó, G, Molnár, Z, Becher, MW, Valenzuela, CF, Partridge, LD. 2002. Genetic ablation of the t-SNARE SNAP-25 distinguishes mechanisms of neuroexocytosis. Nat. Neurosci. 5:19-26.

116. Miyata, T, Ohnishi, H, Suzuki, J, Yoshikumi, Y, Ohno, H, Mashima, H, Yasuda, H, Ishijima, T, Osawa, H, Satoh, K. 2004. Involvement of syntaxin 4 in the transport of membrane-type 1 matrix metalloproteinase to the plasma membrane in human gastric epithelial cells. Biochem. Biophys. Res. Commun. 323:118-124.

117. Williams, KC, McNeilly, RE, Coppolino, MG. 2014. SNAP23, Syntaxin4, and vesicle-associated membrane protein 7 (VAMP7) mediate trafficking of membrane type 1-matrix metalloproteinase (MT1-MMP) during invadopodium formation and tumor cell invasion. Mol. Biol. Cell. 25:2061-2070. doi: 10.1091/mbc.E13-10-0582 [doi].

118. Strand, D, Unger, S, Corvi, R, Hartenstein, K, Schenkel, H, Kalmes, A, Merdes, G, Neumann, B, Krieg-Schneider, F, Coy, JF. 1995. A human homologue of the Drosophila tumour suppressor gene l(2)gl maps to 17p11.2-12 and codes for a cytoskeletal protein that associates with nonmuscle myosin II heavy chain. Oncogene. 11:291-301.

119. Kalmes, A, Merdes, G, Neumann, B, Strand, D, Mechler, BM. 1996. A serine-kinase associated with the p127-l(2)gl tumour suppressor of Drosophila may regulate the binding of p127 to nonmuscle myosin II heavy chain and the attachment of p127 to the plasma membrane. J. Cell. Sci. 109 (Pt 6):1359-1368.

120. Dahan, I, Yearim, A, Touboul, Y, Ravid, S. 2012. The tumor suppressor Lgl1 regulates NMII-A cellular distribution and focal adhesion morphology to optimize cell migration. Mol. Biol. Cell. 23:591-601. doi: 10.1091/mbc.E11-01-0015 [doi].

121. Dahan, I, Petrov, D, Cohen-Kfir, E, Ravid, S. 2014. The tumor suppressor Lgl1 forms discrete complexes with NMII-A and Par6alpha-aPKCzeta that are affected by Lgl1 phosphorylation. J. Cell. Sci. 127:295-304. doi: 10.1242/jcs.127357 [doi].

122. Bilder, D, Li, M, Perrimon, N. 2000. Cooperative regulation of cell polarity and growth by Drosophila tumor suppressors. Science. 289:113-116. doi: 8658 [pii].

123. Zhan, L, Rosenberg, A, Bergami, KC, Yu, M, Xuan, Z, Jaffe, AB, Allred, C, Muthuswamy, SK. 2008. Deregulation of scribble promotes mammary tumorigenesis and reveals a role for cell polarity in carcinoma. Cell. 135:865-878.

124. Yates, LL, Schnatwinkel, C, Hazelwood, L, Chessum, L, Paudyal, A, Hilton, H, Romero, MR, Wilde, J, Bogani, D, Sanderson, J. 2013. Scribble is required for normal epithelial cell–cell contacts and lumen morphogenesis in the mammalian lung. Dev. Biol. 373:267-280.

125. Dow, LE, Brumby, AM, Muratore, R, Coombe, ML, Sedelies, KA, Trapani, JA, Russell, SM, Richardson, HE, Humbert, PO. 2003. hScrib is a functional homologue of the Drosophila tumour suppressor Scribble. Oncogene. 22:9225-9230.

126. Mathew, D, Gramates, LS, Packard, M, Thomas, U, Bilder, D, Perrimon, N, Gorczyca, M, Budnik, V. 2002. Recruitment of scribble to the synaptic scaffolding complex requires GUK-holder, a novel DLG binding protein. Current Biology. 12:531-539.

127. Kallay, LM, McNickle, A, Brennwald, PJ, Hubbard, AL, Braiterman, LT. 2006. Scribble associates with two polarity proteins, Lgl2 and Vangl2, via distinct molecular domains. J. Cell. Biochem. 99:647-664.

128. Zhu, J, Shang, Y, Wan, Q, Xia, Y, Chen, J, Du, Q, Zhang, M. 2014. Phosphorylation-dependent interaction between tumor suppressors Dlg and Lgl. Cell Res. 24:451-463.

129. Humbert, P, Russell, S, Richardson, H. 2003. Dlg, Scribble and Lgl in cell polarity, cell proliferation and cancer. Bioessays. 25:542-553.

130. Gardiol, D, Zacchi, A, Petrera, F, Stanta, G, Banks, L. 2006. Human discs large and scrib are localized at the same regions in colon mucosa and changes in their expression patterns are correlated with loss of tissue architecture during malignant progression. International Journal of Cancer. 119:1285-1290.

131. Lin, H, Steller, MA, Aish, L, Hanada, T, Chishti, AH. 2004. Differential expression of human Dlg in cervical intraepithelial neoplasias. Gynecol. Oncol. 93:422-428.

132. Grifoni, D, Garoia, F, Schimanski, CC, Schmitz, G, Laurenti, E, Galle, PR, Pession, A, Cavicchi, S, Strand, D. 2004. The human protein Hugl-1 substitutes for Drosophila lethal giant larvae tumour suppressor function in vivo. Oncogene. 23:8688-8694.

133. Jang, TJ. 2010. Lethal Giant Larvae2 Expression Is Reduced or Localized at Cytoplasm in Colon Adenomas and Adenocarcinomas. Korean Journal of Pathology. 44:488-492.

134. Heidel, FH, Bullinger, L, Arreba-Tutusaus, P, Wang, Z, Gaebel, J, Hirt, C, Niederwieser, D, Lane, SW, Dohner, K, Vasioukhin, V, Fischer, T, Armstrong, SA. 2013. The cell fate determinant Llgl1 influences HSC fitness and prognosis in AML. J. Exp. Med. 210:15-22. doi: 10.1084/jem.20120596 [doi].

135. Beekman, R, Valkhof, MG, Sanders, MA, van Strien, PM, Haanstra, JR, Broeders, L, Geertsma-Kleinekoort, WM, Veerman, AJ, Valk, PJ, Verhaak, RG, Lowenberg, B, Touw, IP. 2012. Sequential gain of mutations in severe congenital neutropenia progressing to acute myeloid leukemia. Blood. 119:5071-5077. doi: 10.1182/blood-2012-01-406116 [doi].

136. Kuphal, S, Wallner, S, Schimanski, C, Bataille, F, Hofer, P, Strand, S, Strand, D, Bosserhoff, A. 2006. Expression of Hugl-1 is strongly reduced in malignant melanoma. Oncogene. 25:103-110.

137. Kashyap, A, Zimmerman, T, Ergül, N, Bosserhoff, A, Hartman, U, Alla, V, Bataille, F, Galle, P, Strand, S, Strand, D. 2013. The human Lgl polarity gene, Hugl-2, induces MET and suppresses Snail tumorigenesis. Oncogene. 32:1396-1407.

138. Boguski, MS, McCormick, F. 1993. Proteins regulating Ras and its relatives. Nature. 366:643-654. doi: 10.1038/366643a0 [doi].

139. Symons, M. 1996. Rho family GTPases: the cytoskeleton and beyond. Trends Biochem. Sci. 21:178-181.

140. Haataja, L, Groffen, J, Heisterkamp, N. 1997. Characterization of RAC3, a novel member of the Rho family. J. Biol. Chem. 272:20384-20388.

141. Malosio, ML, Gilardelli, D, Paris, S, Albertinazzi, C, de Curtis, I. 1997. Differential expression of distinct members of Rho family GTP-binding proteins during neuronal development: identification of Rac1B, a new neural-specific member of the family. J. Neurosci. 17:6717-6728.

142. Sander, EE, van Delft, S, ten Klooster, JP, Reid, T, van der Kammen, RA, Michiels, F, Collard, JG. 1998. Matrix-dependent Tiam1/Rac signaling in epithelial cells promotes either cell-cell adhesion or cell migration and is regulated by phosphatidylinositol 3-kinase. J. Cell Biol. 143:1385-1398.

143. Parri, M, Chiarugi, P. 2010. Rac and Rho GTPases in cancer cell motility control. Cell Commun Signal. 8:10.1186.

144. Chan, AY, Coniglio, SJ, Chuang, Y, Michaelson, D, Knaus, UG, Philips, MR, Symons, M. 2005. Roles of the Rac1 and Rac3 GTPases in human tumor cell invasion. Oncogene. 24:7821-7829.

145. Kwiatkowska, A, Didier, S, Fortin, S, Chuang, Y, White, T, Berens, ME, Rushing, E, Eschbacher, J, Tran, NL, Chan, A. 2012. The small GTPase RhoG mediates glioblastoma cell invasion. Molecular Cancer. 11:1.

146. Ruiz-Ontañon, P, Orgaz, JL, Aldaz, B, Elosegui-Artola, A, Martino, J, Berciano, MT, Montero, JA, Grande, L, Nogueira, L, Diaz-Moralli, S. 2013. Cellular Plasticity Confers Migratory and Invasive Advantages to a Population of Glioblastoma-Initiating Cells that Infiltrate Peritumoral Tissue. Stem Cells. 31:1075-1085.

147. Anand-Apte, B, Zetter, BR, Viswanathan, A, Qiu, R, Chen, J, Ruggieri, R, Symons, M. 1997. Platelet-derived growth factor and fibronectin-stimulated migration are differentially regulated by the Rac and extracellular signal-regulated kinase pathways. J. Biol. Chem. 272:30688-30692.

148. Salhia, B, Tran, NL, Chan, A, Wolf, A, Nakada, M, Rutka, F, Ennis, M, McDonough, WS, Berens, ME, Symons, M. 2008. The guanine nucleotide exchange factors trio, Ect2, and Vav3 mediate the invasive behavior of glioblastoma. The American Journal of Pathology. 173:1828-1838.

149. Feng, H, Hu, B, Vuori, K, Sarkaria, JN, Furnari, FB, Cavenee, WK, Cheng, S. 2014. EGFRvIII stimulates glioma growth and invasion through PKA-dependent serine phosphorylation of Dock180. Oncogene. 33:2504-2512.

150. Tamas, P, Solti, Z, Bauer, P, Illes, A, Sipeki, S, Bauer, A, Farago, A, Downward, J, Buday, L. 2003. Mechanism of epidermal growth factor regulation of Vav2, a guanine nucleotide exchange factor for Rac. J. Biol. Chem. 278:5163-5171. doi: 10.1074/jbc.M207555200 [doi].

151. Han, J, Luby-Phelps, K, Das, B, Shu, X, Xia, Y, Mosteller, RD, Krishna, UM, Falck, JR, White, MA, Broek, D. 1998. Role of substrates and products of PI 3-kinase in regulating activation of Rac-related guanosine triphosphatases by Vav. Science. 279:558-560.

152. Welch, HC, Coadwell, WJ, Ellson, CD, Ferguson, GJ, Andrews, SR, Erdjument-Bromage, H, Tempst, P, Hawkins, PT, Stephens, LR. 2002. P-Rex1, a PtdIns (3, 4, 5) P 3-and Gβγ-regulated guanine-nucleotide exchange factor for Rac. Cell. 108:809-821.

153. Welch, HC, Condliffe, AM, Milne, LJ, Ferguson, GJ, Hill, K, Webb, LM, Okkenhaug, K, Coadwell, WJ, Andrews, SR, Thelen, M. 2005. P-Rex1 regulates neutrophil function. Current Biology. 15:1867-1873.

154. Dong, X, Mo, Z, Bokoch, G, Guo, C, Li, Z, Wu, D. 2005. P-Rex1 is a primary Rac2 guanine nucleotide exchange factor in mouse neutrophils. Current Biology. 15:1874-1879.

155. Yoshizawa, M, Kawauchi, T, Sone, M, Nishimura, YV, Terao, M, Chihama, K, Nabeshima, Y, Hoshino, M. 2005. Involvement of a Rac activator,P-Rex1, in neurotrophin-derived signaling and neuronal migration. J. Neurosci. 25:4406-4419. doi: 25/17/4406 [pii].

156. Rosenfeldt, H, Vázquez-Prado, J, Gutkind, JS. 2004. P-REX2, a novel PI-3-kinase sensitive Rac exchange factor. FEBS Lett. 572:167-171.

157. Donald, S, Hill, K, Lecureuil, C, Barnouin, R, Krugmann, S, Coadwell, WJ, Andrews, SR, Walker, SA, Hawkins, PT, Stephens, LR. 2004. P-Rex2, a new guanine-nucleotide exchange factor for Rac. FEBS Lett. 572:172-176.

158. Donald, S, Humby, T, Fyfe, I, Segonds-Pichon, A, Walker, SA, Andrews, SR, Coadwell, WJ, Emson, P, Wilkinson, LS, Welch, HC. 2008. P-Rex2 regulates Purkinje cell dendrite morphology and motor coordination. Proc. Natl. Acad. Sci. U. S. A. 105:4483-4488. doi: 10.1073/pnas.0712324105 [doi].

159. Qin, J, Xie, Y, Wang, B, Hoshino, M, Wolff, DW, Zhao, J, Scofield, MA, Dowd, FJ, Lin, M, Tu, Y. 2009. Upregulation of PIP3-dependent Rac exchanger 1 (P-Rex1) promotes prostate cancer metastasis. Oncogene. 28:1853-1863.

160. Lindsay, CR, Lawn, S, Campbell, AD, Faller, WJ, Rambow, F, Mort, RL, Timpson, P, Li, A, Cammareri, P, Ridgway, RA. 2011. P-Rex1 is required for efficient melanoblast migration and melanoma metastasis. Nature Communications. 2:555.

161. Sosa, MS, Lopez-Haber, C, Yang, C, Wang, H, Lemmon, MA, Busillo, JM, Luo, J, Benovic, JL, Klein-Szanto, A, Yagi, H. 2010. Identification of the Rac-GEF P-Rex1 as an essential mediator of ErbB signaling in breast cancer. Mol. Cell. 40:877-892.

162. Montero, JC, Seoane, S, Ocaña, A, Pandiella, A. 2011. P-Rex1 participates in Neuregulin-ErbB signal transduction and its expression correlates with patient outcome in breast cancer. Oncogene. 30:1059-1071.

163. Wong, CY, Wuriyanghan, H, Xie, Y, Lin, MF, Abel, PW, Tu, Y. 2011. Epigenetic regulation of phosphatidylinositol 3,4,5-triphosphate-dependent Rac exchanger 1 gene expression in prostate cancer cells. J. Biol. Chem. 286:25813-25822. doi: 10.1074/jbc.M110.211292 [doi].

164. Barrio-Real, L, Benedetti, LG, Engel, N, Tu, Y, Cho, S, Sukumar, S, Kazanietz, MG. 2014. Subtype-specific overexpression of the Rac-GEF P-REX1 in breast cancer is associated with

promoter hypomethylation. Breast Cancer Res. 16:441-014-0441-7. doi: 10.1186/s13058-014-0441-7 [doi].

165. Fine, B, Hodakoski, C, Koujak, S, Su, T, Saal, LH, Maurer, M, Hopkins, B, Keniry, M, Sulis, ML, Mense, S, Hibshoosh, H, Parsons, R. 2009. Activation of the PI3K pathway in cancer through inhibition of PTEN by exchange factor P-REX2a. Science. 325:1261-1265. doi: 10.1126/science.1173569 [doi].

166. Mense, SM, Barrows, D, Hodakoski, C, Steinbach, N, Schoenfeld, D, Su, W, Hopkins, BD, Su, T, Fine, B, Hibshoosh, H, Parsons, R. 2015. PTEN inhibits PREX2-catalyzed activation of RAC1 to restrain tumor cell invasion. Sci. Signal. 8:ra32. doi: 10.1126/scisignal.2005840 [doi].

167. Stupp, R, Mason, WP, Van Den Bent, Martin J, Weller, M, Fisher, B, Taphoorn, MJ, Belanger, K, Brandes, AA, Marosi, C, Bogdahn, U. 2005. Radiotherapy plus concomitant and adjuvant temozolomide for glioblastoma. N. Engl. J. Med. 352:987-996.

168. Singh, SK, Hawkins, C, Clarke, ID, Squire, JA, Bayani, J, Hide, T, Henkelman, RM, Cusimano, MD, Dirks, PB. 2004. Identification of human brain tumour initiating cells. Nature. 432:396-401.

169. Venere, M, Fine, HA, Dirks, PB, Rich, JN. 2011. Cancer stem cells in gliomas: identifying and understanding the apex cell in cancer's hierarchy. Glia. 59:1148-1154.

170. Muñoz, DM, Guha, A. 2011. Mouse models to interrogate the implications of the differentiation status in the ontogeny of gliomas. Oncotarget. 2:590-598.

171. Bao, S, Wu, Q, McLendon, RE, Hao, Y, Shi, Q, Hjelmeland, AB, Dewhirst, MW, Bigner, DD, Rich, JN. 2006. Glioma stem cells promote radioresistance by preferential activation of the DNA damage response. Nature. 444:756-760.

172. Chen, J, Li, Y, Yu, T, McKay, RM, Burns, DK, Kernie, SG, Parada, LF. 2012. A restricted cell population propagates glioblastoma growth after chemotherapy. Nature. 488:522-526.

173. Weber, GL, Parat, M, Binder, ZA, Gallia, GL, Riggins, GJ. 2011. Abrogation of PIK3CA or PIK3R1 reduces proliferation, migration, and invasion in glioblastoma multiforme cells. Oncotarget. 2:833-849.

174. Fields, AP, Regala, RP. 2007. Protein kinase Cι: human oncogene, prognostic marker and therapeutic target. Pharmacological Research. 55:487-497.

175. Paget, J, Restall, I, Daneshmand, M, Mersereau, J, Simard, M, Parolin, D, Lavictoire, S, Amin, M, Islam, S, Lorimer, I. 2012. Repression of cancer cell senescence by PKCι. Oncogene. 31:3584-3596.

176. Knoblich, JA. 2010. Asymmetric cell division: recent developments and their implications for tumour biology. Nature Reviews Molecular Cell Biology. 11:849-860.

177. Plant, PJ, Fawcett, JP, Lin, DC, Holdorf, AD, Binns, K, Kulkarni, S, Pawson, T. 2003. A polarity complex of mPar-6 and atypical PKC binds, phosphorylates and regulates mammalian Lgl. Nat. Cell Biol. 5:301-308.

178. Schimanski, CC, Schmitz, G, Kashyap, A, Bosserhoff, AK, Bataille, F, Schäfer, SC, Lehr, HA, Berger, MR, Galle, PR, Strand, S. 2005. Reduced expression of Hugl-1, the human homologue of Drosophila tumour suppressor gene lgl, contributes to progression of colorectal cancer. Oncogene. 24:3100-3109.

179. Ishii, N, Maier, D, Merlo, A, Tada, M, Sawamura, Y, Diserens, A, Meir, EG. 1999. Frequent Co-Alterations of TP53, p16/CDKN2A, p14ARF, PTEN Tumor Suppressor Genes in Human Glioma Cell Lines. Brain Pathology. 9:469-479.

180. Rafalski, VA, Brunet, A. 2011. Energy metabolism in adult neural stem cell fate. Prog. Neurobiol. 93:182-203.

181. Leontieva, OV, Natarajan, V, Demidenko, ZN, Burdelya, LG, Gudkov, AV, Blagosklonny, MV. 2012. Hypoxia suppresses conversion from proliferative arrest to cellular senescence. Proc. Natl. Acad. Sci. U. S. A. 109:13314-13318. doi: 10.1073/pnas.1205690109 [doi].

182. Higgins, DM, Wang, R, Milligan, B, Schroeder, M, Carlson, B, Pokorny, J, Cheshier, SH, Meyer, FB, Weissman, IL, Sarkaria, JN, Henley, JR. 2013. Brain tumor stem cell multipotency correlates with nanog expression and extent of passaging in human glioblastoma xenografts. Oncotarget. 4:792-801. doi: 1059 [pii].

183. Hill, R, Wu, H. 2009. PTEN, stem cells, and cancer stem cells. J. Biol. Chem. 284:11755-11759. doi: 10.1074/jbc.R800071200 [doi].

184. Wiederschain, D, Susan, W, Chen, L, Loo, A, Yang, G, Huang, A, Chen, Y, Caponigro, G, Yao, Y, Lengauer, C. 2009. Single-vector inducible lentiviral RNAi system for oncology target validation. Cell Cycle. 8:498-504.

185. Gont, A, Hanson, JE, Lavictoire, SJ, Parolin, DA, Daneshmand, M, Restall, IJ, Soucie, M, Nicholas, G, Woulfe, J, Kassam, A, Da Silva, VF, Lorimer, IA. 2013. PTEN loss represses glioblastoma tumor initiating cell differentiation via inactivation of Lgl1. Oncotarget. 4:1266-1279. doi: 1164 [pii].

186. Killela, PJ, Pirozzi, CJ, Reitman, ZJ, Jones, S, Rasheed, BA, Lipp, E, Friedman, H, Friedman, AH, He, Y, McLendon, RE, Bigner, DD, Yan, H. 2014. The genetic landscape of anaplastic astrocytoma. Oncotarget. 5:1452-1457. doi: 1505 [pii].

187. Kelly, S, Bliss, TM, Shah, AK, Sun, GH, Ma, M, Foo, WC, Masel, J, Yenari, MA, Weissman, IL, Uchida, N, Palmer, T, Steinberg, GK. 2004. Transplanted human fetal neural stem cells survive, migrate, and differentiate in ischemic rat cerebral cortex. Proc. Natl. Acad. Sci. U. S. A. 101:11839-11844. doi: 10.1073/pnas.0404474101 [doi].

188. Brown, JP, Couillard-Després, S, Cooper-Kuhn, CM, Winkler, J, Aigner, L, Kuhn, HG. 2003. Transient expression of doublecortin during adult neurogenesis. J. Comp. Neurol. 467:1-10.

189. Kashyap, A, Zimmerman, T, Ergül, N, Bosserhoff, A, Hartman, U, Alla, V, Bataille, F, Galle, P, Strand, S, Strand, D. 2013. The human Lgl polarity gene, Hugl-2, induces MET and suppresses Snail tumorigenesis. Oncogene. 32:1396-1407.

190. Barkho, BZ, Zhao, X. 2011. Adult neural stem cells: response to stroke injury and potential for therapeutic applications. Curr. Stem Cell. Res. Ther. 6:327-338. doi: BSP/CSCRT/E-Pub/00090 [pii].

191. Goldstein, B, Macara, IG. 2007. The PAR proteins: fundamental players in animal cell polarization. Developmental Cell. 13:609-622.

192. Gupta, PB, Fillmore, CM, Jiang, G, Shapira, SD, Tao, K, Kuperwasser, C, Lander, ES. 2011. Stochastic state transitions give rise to phenotypic equilibrium in populations of cancer cells. Cell. 146:633-644.

193. Yamanaka, T, Tosaki, A, Kurosawa, M, Akimoto, K, Hirose, T, Ohno, S, Hattori, N, Nukina, N. 2013. Loss of aPKCλ in Differentiated Neurons Disrupts the Polarity Complex but Does Not Induce Obvious Neuronal Loss or Disorientation in Mouse Brains. PloS One. 8:e84036.

194. Higgins, DM, Wang, R, Milligan, B, Schroeder, M, Carlson, B, Pokorny, J, Cheshier, SH, Meyer, FB, Weissman, IL, Sarkaria, JN, Henley, JR. 2013. Brain tumor stem cell multipotency correlates with nanog expression and extent of passaging in human glioblastoma xenografts. Oncotarget. 4:792-801. doi: 1059 [pii].

195. Meijering, E, Dzyubachyk, O, Smal, I. 2012. Methods for cell and particle tracking. Meth. Enzymol. 504:183-200.

196. Gont, A, Hanson, JE, Lavictoire, SJ, Daneshmand, M, Nicholas, G, Woulfe, J, Kassam, A, Da Silva, VF, Lorimer, IA. 2014. Inhibition of glioblastoma malignancy by Lgl1. Oncotarget. 5:11541-11551. doi: 2580 [pii].

197. Cerami, E, Gao, J, Dogrusoz, U, Gross, BE, Sumer, SO, Aksoy, BA, Jacobsen, A, Byrne, CJ, Heuer, ML, Larsson, E, Antipin, Y, Reva, B, Goldberg, AP, Sander, C, Schultz, N. 2012. The cBio cancer genomics portal: an open platform for exploring multidimensional cancer genomics data. Cancer. Discov. 2:401-404. doi: 10.1158/2159-8290.CD-12-0095 [doi].

198. Lehmann, DM, Seneviratne, AM, Smrcka, AV. 2008. Small molecule disruption of G protein beta gamma subunit signaling inhibits neutrophil chemotaxis and inflammation. Mol. Pharmacol. 73:410-418. doi: mol.107.041780 [pii].

199. Burger, MT, Pecchi, S, Wagman, A, Ni, Z, Knapp, M, Hendrickson, T, Atallah, G, Pfister, K, Zhang, Y, Bartulis, S. 2011. Identification of NVP-BKM120 as a potent, selective, orally bioavailable class I PI3 kinase inhibitor for treating cancer. ACS Medicinal Chemistry Letters. 2:774-779.

200. Li, J, Zhu, S, Kozono, D, Ng, K, Futalan, D, Shen, Y, Akers, JC, Steed, T, Kushwaha, D, Schlabach, M. 2014. Genome-wide shRNA screen revealed integrated mitogenic signaling between dopamine receptor D2 (DRD2) and epidermal growth factor receptor (EGFR) in glioblastoma. Oncotarget. 5:882-893.

201. Bustelo, XR, Sauzeau, V, Berenjeno, IM. 2007. GTP-binding proteins of the Rho/Rac family: Regulation, effectors and functions in vivo. Bioessays. 29:356-370.

202. Baker, NM, Yee Chow, H, Chernoff, J, Der, CJ. 2014. Molecular pathways: targeting RAC-p21-activated serine-threonine kinase signaling in RAS-driven cancers. Clin. Cancer Res. 20:4740-4746. doi: 10.1158/1078-0432.CCR-13-1727 [doi].

203. Chong, C, Tan, L, Lim, L, Manser, E. 2001. The mechanism of PAK activation. Autophosphorylation events in both regulatory and kinase domains control activity. J. Biol. Chem. 276:17347-17353. doi: 10.1074/jbc.M009316200 [doi].

204. Uhlen, M, Fagerberg, L, Hallstrom, BM, Lindskog, C, Oksvold, P, Mardinoglu, A, Sivertsson, A, Kampf, C, Sjostedt, E, Asplund, A, Olsson, I, Edlund, K, Lundberg, E, Navani, S, Szigyarto, CA, Odeberg, J, Djureinovic, D, Takanen, JO, Hober, S, Alm, T, Edqvist, PH, Berling, H, Tegel, H, Mulder, J, Rockberg, J, Nilsson, P, Schwenk, JM, Hamsten, M, von Feilitzen, K, Forsberg, M, Persson, L, Johansson, F, Zwahlen, M, von Heijne, G, Nielsen, J, Ponten, F. 2015. Proteomics. Tissue-based map of the human proteome. Science. 347:1260419. doi: 10.1126/science.1260419 [doi].

205. Messerschmidt, A, Macieira, S, Velarde, M, Bädeker, M, Benda, C, Jestel, A, Brandstetter, H, Neuefeind, T, Blaesse, M. 2005. Crystal structure of the catalytic domain of human atypical protein kinase C-iota reveals interaction mode of phosphorylation site in turn motif. J. Mol. Biol. 352:918-931.

206. Perou, CM, Sørlie, T, Eisen, MB, van de Rijn, M, Jeffrey, SS, Rees, CA, Pollack, JR, Ross, DT, Johnsen, H, Akslen, LA. 2000. Molecular portraits of human breast tumours. Nature. 406:747-752.

207. Su, LF, Knoblauch, R, Garabedian, MJ. 2001. Rho GTPases as modulators of the estrogen receptor transcriptional response. J. Biol. Chem. 276:3231-3237. doi: 10.1074/jbc.M005547200 [doi].

208. Rosenblatt, AE, Garcia, MI, Lyons, L, Xie, Y, Maiorino, C, Desire, L, Slingerland, J, Burnstein, KL. 2011. Inhibition of the Rho GTPase, Rac1, decreases estrogen receptor levels and is a novel therapeutic strategy in breast cancer. Endocr. Relat. Cancer. 18:207-219. doi: 10.1677/ERC-10-0049 [doi].

209. Rayala, SK, Molli, PR, Kumar, R. 2006. Nuclear p21-activated kinase 1 in breast cancer packs off tamoxifen sensitivity. Cancer Res. 66:5985-5988. doi: 66/12/5985 [pii].

210. Cotton, M, Claing, A. 2009. G protein-coupled receptors stimulation and the control of cell migration. Cell. Signal. 21:1045-1053.

211. Vassilatis, DK, Hohmann, JG, Zeng, H, Li, F, Ranchalis, JE, Mortrud, MT, Brown, A, Rodriguez, SS, Weller, JR, Wright, AC, Bergmann, JE, Gaitanaris, GA. 2003. The G protein-coupled receptor repertoires of human and mouse. Proc. Natl. Acad. Sci. U. S. A. 100:4903-4908. doi: 10.1073/pnas.0230374100 [doi].

212. Kvachnina, E, Liu, G, Dityatev, A, Renner, U, Dumuis, A, Richter, DW, Dityateva, G, Schachner, M, Voyno-Yasenetskaya, TA, Ponimaskin, EG. 2005. 5-HT7 receptor is coupled to G alpha subunits of heterotrimeric G12-protein to regulate gene transcription and neuronal morphology. J. Neurosci. 25:7821-7830. doi: 25/34/7821 [pii].

213. Kroeze, WK, Hufeisen, SJ, Popadak, BA, Renock, SM, Steinberg, S, Ernsberger, P, Jayathilake, K, Meltzer, HY, Roth, BL. 2003. H1-histamine receptor affinity predicts short-term weight gain for typical and atypical antipsychotic drugs. Neuropsychopharmacology. 28:519-526.

214. Hamm, HE. 1998. The many faces of G protein signaling. J. Biol. Chem. 273:669-672.

215. Dráber, P, Sulimenko, V, Dráberová, E. 2014. Cytoskeleton in mast cell signaling. Deciphering New Molecular Mechanisms of Mast Cell Activation. 34.

216. Frederick, L, Matthews, J, Jamieson, L, Justilien, V, Thompson, EA, Radisky, DC, Fields, A. 2008. Matrix metalloproteinase-10 is a critical effector of protein kinase Cι-Par6α-mediated lung cancer. Oncogene. 27:4841-4853.

217. Meijering, E. 2006. MTrackJ: A Java program for manual object tracking. University Medical Center Rotterdam,[Online].Available: Http://Www.Imagescience.Org/Meijering/Software/Mtrackj.[Accessed 17 July 2013]. .

218. Lucas, RE, Vlangos, CN, Das, P, Patel, PI, Elsea, SH. 2001. Genomic organisation of the∼ 1. 5 Mb Smith-Magenis syndrome critical interval: Transcription map, genomic contig, and candidate gene analysis. European Journal of Human Genetics. 9:892-902.

219. Elsea, SH, Girirajan, S. 2008. Smith–Magenis syndrome. European Journal of Human Genetics. 16:412-421.

220. Katsetos, CD, Del Valle, L, Geddes, JF, Assimakopoulou, M, Legido, A, Boyd, JC, Balin, B, Parikh, NA, Maraziotis, T, de Chadarevian, J. 2001. Aberrant localization of the neuronal class III β-tubulin in astrocytomas: a marker for anaplastic potential. Arch. Pathol. Lab. Med. 125:613-624.

221. Katsetos, CD, Herman, MM, Mörk, SJ. 2003. Class III β-tubulin in human development and cancer. Cell Motil. Cytoskeleton. 55:77-96.

222. Liu, X, Lu, D, Ma, P, Liu, H, Cao, Y, Sang, B, Zhu, X, Shi, Q, Hu, J, Yu, R. 2015. Hugl-1 inhibits glioma cell growth in intracranial model. J. Neurooncol. 125:113-121.

223. Beadle, C, Assanah, MC, Monzo, P, Vallee, R, Rosenfeld, SS, Canoll, P. 2008. The role of myosin II in glioma invasion of the brain. Mol. Biol. Cell. 19:3357-3368. doi: 10.1091/mbc.E08-03-0319 [doi].

224. Beaucher, M, Hersperger, E, Page-McCaw, A, Shearn, A. 2007. Metastatic ability of Drosophila tumors depends on MMP activity. Dev. Biol. 303:625-634.

225. Qiu, R, Abo, A, Martin, GS. 2000. A human homolog of the C. elegans polarity determinant Par-6 links Rac and Cdc42 to PKCζ signaling and cell transformation. Current Biology. 10:697-707.

226. Frederick, L, Matthews, J, Jamieson, L, Justilien, V, Thompson, EA, Radisky, DC, Fields, A. 2008. Matrix metalloproteinase-10 is a critical effector of protein kinase Cι-Par6α-mediated lung cancer. Oncogene. 27:4841-4853.

227. Vassilatis, DK, Hohmann, JG, Zeng, H, Li, F, Ranchalis, JE, Mortrud, MT, Brown, A, Rodriguez, SS, Weller, JR, Wright, AC, Bergmann, JE, Gaitanaris, GA. 2003. The G protein-coupled receptor repertoires of human and mouse. Proc. Natl. Acad. Sci. U. S. A. 100:4903-4908. doi: 10.1073/pnas.0230374100 [doi].

228. Berger, AH, Knudson, AG, Pandolfi, PP. 2011. A continuum model for tumour suppression. Nature. 476:163-169.

229. Trotman, LC, Niki, M, Dotan, ZA, Koutcher, JA, Di Cristofano, A, Xiao, A, Khoo, AS, Roy-Burman, P, Greenberg, NM, Van Dyke, T. 2003. Pten dose dictates cancer progression in the prostate. PLoS Biol. 1:e59.

230. Russo, D, Tumino, S, Arturi, F, Vigneri, P, Grasso, G, Pontecorvi, A, Filetti, S, Belfiore, A. 1997. Detection of an Activating Mutation of the Thyrotropin Receptor in a Case of an Autonomously Hyperfunctioning Thyroid Insular Carcinoma 1. The Journal of Clinical Endocrinology & Metabolism. 82:735-738.

231. Holzapfel, H, Führer, D, Wonerow, P, Weinland, G, Scherbaum, WA, Paschke, R. 1997. Identification of Constitutively Activating Somatic Thyrotropin Receptor Mutations in a Subset of Toxic Multinodular Goiters 1. The Journal of Clinical Endocrinology & Metabolism. 82:4229-4233.

232. Parma, J, Duprez, L, Van Sande, J, Cochaux, P, Gervy, C, Mockel, J, Dumont, J, Vassart, G. 1993. Somatic mutations in the thyrotropin receptor gene cause hyperfunctioning thyroid adenomas. Nature. 365:649-651.

233. Führer, D, Holzapfel, H, Wonerow, P, Scherbaum, WA, Paschke, R. 1997. Somatic Mutations in the Thyrotropin Receptor Gene and Not in the Gsα Protein Gene in 31 Toxic Thyroid Nodules 1. The Journal of Clinical Endocrinology & Metabolism. 82:3885-3891.

234. Tao, Y. 2008. Constitutive activation of G protein-coupled receptors and diseases: insights into mechanisms of activation and therapeutics. Pharmacol. Ther. 120:129-148.

235. Hopkins, BD, Fine, B, Steinbach, N, Dendy, M, Rapp, Z, Shaw, J, Pappas, K, Yu, JS, Hodakoski, C, Mense, S, Klein, J, Pegno, S, Sulis, ML, Goldstein, H, Amendolara, B, Lei, L, Maurer, M, Bruce, J, Canoll, P, Hibshoosh, H, Parsons, R. 2013. A secreted PTEN phosphatase that enters cells to alter signaling and survival. Science. 341:399-402. doi: 10.1126/science.1234907 [doi].

236. Wang, H, Zhang, P, Lin, C, Yu, Q, Wu, J, Wang, L, Cui, Y, Wang, K, Gao, Z, Li, H. 2015. Relevance and Therapeutic Possibility of PTEN-Long in Renal Cell Carcinoma. PloS One. 10:e114250.

237. Aboody, KS, Brown, A, Rainov, NG, Bower, KA, Liu, S, Yang, W, Small, JE, Herrlinger, U, Ourednik, V, Black, PM, Breakefield, XO, Snyder, EY. 2000. Neural stem cells display extensive tropism for pathology in adult brain: evidence from intracranial gliomas. Proc. Natl. Acad. Sci. U. S. A. 97:12846-12851. doi: 10.1073/pnas.97.23.12846 [doi].

238. Sasportas, LS, Kasmieh, R, Wakimoto, H, Hingtgen, S, van de Water, JA, Mohapatra, G, Figueiredo, JL, Martuza, RL, Weissleder, R, Shah, K. 2009. Assessment of therapeutic efficacy and fate of engineered human mesenchymal stem cells for cancer therapy. Proc. Natl. Acad. Sci. U. S. A. 106:4822-4827. doi: 10.1073/pnas.0806647106 [doi].

239. Lamfers, M, Idema, S, van Milligen, F, Schouten, T, van der Valk, P, Vandertop, P, Dirven, C, Noske, D. 2009. Homing properties of adipose-derived stem cells to intracerebral glioma and the effects of adenovirus infection. Cancer Lett. 274:78-87.

240. Hussain, SF, Yang, D, Suki, D, Aldape, K, Grimm, E, Heimberger, AB. 2006. The role of human glioma-infiltrating microglia/macrophages in mediating antitumor immune responses. Neuro Oncol. 8:261-279. doi: 15228517-2006-008 [pii].

241. Valable, S, Barbier, EL, Bernaudin, M, Roussel, S, Segebarth, C, Petit, E, Rémy, C. 2008. In vivo MRI tracking of exogenous monocytes/macrophages targeting brain tumors in a rat model of glioma. Neuroimage. 40:973-983.

242. Bagó, JR, Alfonso-Pecchio, A, Okolie, O, Dumitru, R, Rinkenbaugh, A, Baldwin, AS, Miller, CR, Magness, ST, Hingtgen, SD. 2016. Therapeutically engineered induced neural stem cells are tumour-homing and inhibit progression of glioblastoma. Nature Communications. 7:.

243. Aboody, KS, Najbauer, J, Metz, MZ, D'Apuzzo, M, Gutova, M, Annala, AJ, Synold, TW, Couture, LA, Blanchard, S, Moats, RA, Garcia, E, Aramburo, S, Valenzuela, VV, Frank, RT, Barish, ME, Brown, CE, Kim, SU, Badie, B, Portnow, J. 2013. Neural stem cell-mediated

enzyme/prodrug therapy for glioma: preclinical studies. Sci. Transl. Med. 5:184ra59. doi: 10.1126/scitranslmed.3005365 [doi].

Curriculum vitae

Educational Background:

Thesis submitted April 2016	PhD Biochemistry Department of Biochemistry, Faculty of Medicine, University of Ottawa Thesis title: Inactivation of Lgl1 in glioblastoma Supervisor: Dr. Ian Lorimer
2011	B.Sc., Honours in Biopharmaceutical Science. *Magna cum laude*. Faculty of Science, University of Ottawa

Honours, Scholarships and Awards:

March 2016	Faculty nomination for the CIHR national poster presentation Canadian Student Health Research Forum, Winnipeg, MB, Canada
Sept. 2015 – Sept. 2016	Ontario Graduate Scholarship University of Ottawa, Ottawa, ON, Canada
Sept. 2014 – Sept. 2015	Ontario Graduate Scholarship University of Ottawa, Ottawa, ON, Canada
Sept. 2011 – Sept. 2013	Queen Elizabeth II - Graduate Scholarship in Science and Technology University of Ottawa, Ottawa, ON, Canada
June 2013	Phil Gold Scientist-in-training Award Montreal International Symposium on Angiogenesis and Metastasis, Montreal, QC, Canada
Jan. – April 2013	The Dean's Scholarship University of Ottawa, Ottawa, ON, Canada
May 2012	Faculty of Medicine Poster Prize University of Ottawa, Ottawa, ON, Canada
Jan. – April 2009	Biopharmaceutical Science Director Scholarship University of Ottawa, Ottawa, ON, Canada

Research Experience:

Sept. 2011 – Present **PhD student**
Faculty of Medicine, University of Ottawa
Supervisor: Dr. Ian Lorimer (Ottawa Hospital Research Institute, University of Ottawa)

- Uncovered novel molecular mechanisms driving glioblastoma malignancy downstream of *PTEN* loss by genetic manipulations and use of pharmacological inhibitors on glioblastoma patient-derived cell cultures
- Assessed glioblastoma cell motility *in vitro* using videomicroscopy and microporous chamber inserts
- Developed orthotropic xenograft mouse models of human glioblastoma to study molecular mechanisms driving invasion and restricting differentiation using immunohistochemistry techniques
- Established and implemented project directions, experimental design, and manuscript preparation

April 2011 – Sept. 2011 **Summer student research assistant**
Ottawa Hospital Research Institute
Supervisor: Dr. Ian Lorimer (Ottawa Hospital Research Institute, University of Ottawa)

- Developed lentiviral vectors for inducible and constitutive expression of Lgl1
- Investigated the role of Lgl1 on glioblastoma proliferation and senescence
- Examined the subcellular localization of Lgl1 by confocal microscopy in glioblastoma cells

Sept. 2010 – April 2011 **Undergraduate thesis student**
Faculty of Science, University of Ottawa
Supervisor: Dr. Ian Lorimer (Ottawa Hospital Research Institute, University of Ottawa)

- Performed site-directed mutagenesis to create a non-phosphorylatable mutant of Lgl1 to investigate effect of phosphorylation by PKCι
- Investigated the role of tumor suppressor Lgl1 in glioblastoma proliferation

May 2010 – Sept. 2010 **Summer student research assistant**
Ottawa Hospital Research Institute
Supervisor: Dr. Ian Lorimer (Ottawa Hospital Research Institute, University of Ottawa)

- Investigated the role of PKCι in sensitization of glioblastoma to chemotherapeutics using the MTT assay

Publications and Presentations:
Publications:

Alexander Gont, Manijeh Daneshmand, John Woulfe, Sylvie J Lavictoire, and Ian AJ Lorimer. *PREX1 integrates G Protein-Coupled Receptor and Phosphoinositide 3-Kinase signaling to promote glioblastoma invasion*. Manuscript submitted (2016).

Ritesh Kumar, Alexander Gont, Theodore J Perkins, Jennifer E L Hanson, and Ian AJ Lorimer. *Induction of senescence in primary glioblastoma cells by serum and TGFβ*. Manuscript submitted (2016).

Alexander Gont, Jennifer E L Hanson, Sylvie J Lavictoire, Manijeh Daneshmand, Garth Nicholas, John Woulfe, Amin Kassam, Vasco F Da Silva and Ian AJ Lorimer. *Inhibition of glioblastoma malignancy by* Lgl1. Oncotarget 5.22 (2014): 11541-11551.

Alexander Gont, Jennifer E L Hanson, Sylvie J Lavictoire, Doris A E Parolin, Manijeh Daneshmand, Ian J Restall, Mathieu Soucie, Garth Nicholas, John Woulfe, Amin Kassam, Vasco F Da Silva and Ian AJ Lorimer. *PTEN loss represses glioblastoma tumor initiating cell differentiation via inactivation of Lgl1*. Oncotarget 4.8 (2013): 1266-1279.

Selected conference presentations:

Alexander Gont, Manijeh Daneshmand, John Woulfe, Ian A Lorimer. *PREX1 integrates G Protein-Coupled Receptor and Phosphoinositide 3-Kinase signaling to promote glioblastoma invasion*. [Abstract accepted for poster presentation] In: 24th Biennial Congress of the European Association for Cancer Research. 09-July-2016; Manchester, UK.

Alexander Gont, Manijeh Daneshmand, John Woulfe, Ian A Lorimer. *PREX1 integrates G Protein-Coupled Receptor and Phosphoinositide 3-Kinase signaling to promote glioblastoma invasion*. [Abstract accepted for poster presentation] In: Canadian Student Health Research Forum 2016. 08-June-2016; Winnipeg, MB, CAN.

Alexander Gont and Ian AJ Lorimer. *Investigating the role of P-rex1 in glioblastoma*. [poster presentation] In: Proceedings of the Ottawa Hospital Research Institute 2015 Research Day. 18-Nov-2015; Ottawa, ON, CAN.

Alexander Gont, Jennifer E L Hanson, Sylvie J Lavictoire, Garth Nicholas, John Woulfe, Amin Kassam, Vasco F Da Silva and Ian AJ Lorimer. *PTEN represses glioblastoma tumor initiating cell differentiation via the polarity proteins aPKC and Lgl*. [poster presentation] In: Proceedings of the Ottawa Hospital Research Institute 2014 Research Day. 13-Nov-2014; Ottawa, ON, CAN.
Alexander Gont, Jennifer E L Hanson, Sylvie J Lavictoire, Garth Nicholas, John Woulfe, Amin Kassam, Vasco F Da Silva and Ian AJ Lorimer. *PTEN represses glioblastoma tumor initiating cell differentiation via the polarity proteins aPKC and Lgl* [poster presentation]. In: Proceedings of the Cold Spring Harbor conference on PTEN Pathways & Targets. 2014 March 25-28; New York, NY, USA

Alexander Gont. *Investigating the role of tumour suppressor Lgl1 in glioblastoma tumour initiating cells*. [oral presentation] In: Proceedings of the Ottawa Hospital Research Institute 2013 Research Day. 14-Nov-2013; Ottawa, ON, CAN.

Alexander Gont, Jennifer E L Hanson, Sylvie J Lavictoire, Mathieu Soucie, Doris A E Parolin, Garth Nicholas, John Woulfe, Amin Kassam, Vasco F Da Silva and Ian AJ Lorimer. *Inactivation of the tumour suppressor Lgl in glioblastoma by PTEN loss: effects on tumour initiating cell differentiation*. [poster presentation] In: Proceedings of the Montreal International Symposium on Angiogenesis and Metastasis meeting. 2013 June 12-14; Montreal, QC, CAN.

Alexander Gont, Ian J Restall, Jennifer E L Hanson, Sylvie J Lavictoire, Mathieu Soucie, Garth Nicholas, John Woulfe, Amin Kassam, Vasco F Da Silva and Ian AJ Lorimer. *Inactivation of the tumor suppressor Lgl via PTEN loss promotes the invasiveness of glioblastoma multiforme*. [poster presentation]. In: Proceedings of the 104th Annual Meeting of the American Association for Cancer Research; 2013 Apr 6-10; Washington, DC.,USA: AACR; 2013. Abstract nr 1968.

Alexander Gont and Ian AJ Lorimer. *Inactivation of tumor suppressor lethal giant larvae via PTEN loss promotes the invasiveness of glioblastoma multiforme*. [poster presentation] In: Proceedings of the Ottawa Hospital Research Institute 2012 Research Day. 15-Nov-2012; Ottawa, ON, CAN.

Alexander Gont and Ian AJ Lorimer. *Investigating the role of tumour suppressor lethal giant larvae in glioblastoma*. [poster presentation] In: Proceedings of the Ottawa Hospital Research Institute 2011 Research Day. 10-Nov-2011; Ottawa, ON, CAN.